Final Report 2007

On the Design of Interconnections for the SIS300 Synchrotron

Project FAIR

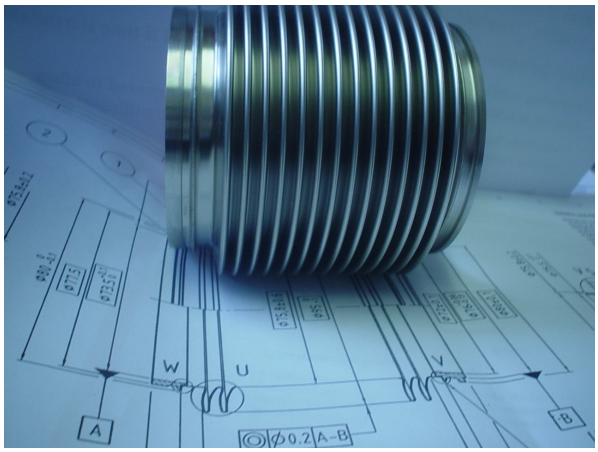

Błażej Skoczeń
Adam Wróblewski

Cracow University of Technology (CUT), Cracow, Poland
31-155 Kraków, ul. Warszawska 24
Centre for Particle Accelerators Design at CUT
31-864 Kraków, Jana Pawła II 37 Ave.

December 2007

Contents

1 Introduction

The SIS300 synchrotron is planned to be installed on top of SIS100, as the second stage of two-stage facility. The first stage will have acceleration and compression functions, whereas the second stage - apart from acceleration - will have stretching function. The general topology of SIS300 is to a large extent determined by the topology of SIS100 since both of them will be contained in the same tunnel. The injection into SIS300 will be done from SIS100 by means of special vertical transfer line. The design injection energy has been set to 1.5 GeV and the beam emittance will be of 10x4 π mm mrad. SIS300 will be equipped with type cos(θ) bending superconducting magnets that will develop the maximum field of 4.5 T. The maximum field gradient for quadrupoles will be of 45 T/m. The synchrotron magnetic structure will be based on modern FODO lattice comprising 14 half-cells per arc. The magnets will be operated in high energy mode with the ramping rate of 1T/s for dipoles and 10 T/s^2 for quadrupoles as well as static stretcher mode (without ramping). The change of modes will take place from cycle to cycle. The maximum rigidity of SIS300 in high energy mode will be of 300 Tm and up to 100 Tm in the stretcher mode. Apart from main magnets the synchrotron will be equipped with a correction scheme based on dipole orbit correctors (steerers), chromaticity and extraction sextupoles as well as error correction multipoles.

The present report is dedicated to the analysis of topology of SIS300, design and optimisation of the interconnections and verification of local and global stability of the pressurized synchrotron. As the document has been stretched over the period since November 2006, the lattice of the synchrotron evolved in the mean time from doublet to FODO version. This evolution led to major change in machine optics and definition of new topology including main and corrector magnets. As a result of this modification new interconnection types appeared and the final version of lattice has been subdivided in the present report into the so-called assemblies in order to highlight the most characteristic portions of the machine. The report addresses mainly the standard arc of the synchrotron. However, the structure of magnet-to-magnet interconnections, including some of the components can be easily transferred to the arc extremities. The report starts with a typical layout of single interconnection, which constitutes a basis for development of specific interconnection types by modifying the basic components. This interconnection pattern contains 7 channels: beam vacuum interconnect, 4 channels containing the superconducting bus-bars and 2 helium flow channels. For such configuration components of the compensation system as well as the structure of the superconducting bus-bar connections has been developed. Furthermore, the local and the semi-global analysis of stability under the pressure loads has been carried out. The analysis is aimed at ensuring that the synchrotron remains stable during the cool-down, warm-up and operation of the facility. Moreover, the elements of the compensation system (expansion bellows) were optimised with respect to their performance, including stability and reliability. The semi-global stability analysis takes into account a compensation element (expansion bellows) in its environment, that means adjacent portions of the bus-bar and the helium flow channels. The analysis is aimed at determining the conditions of stable operation of the interconnects and safe distance between the magnets. If the magnet-to-magnet slot exceeds the safe distance (cf. stability diagrams) special measures have to be

implemented in order to avoid system instability. These measures include cross-links between the interconnection channels in order to eliminate possible transverse motion under the pressure loads. Global stability verification is based on the so-called eigenvalue analysis that results in determination of the eigenvalues and eigenvectors corresponding to the critical levels of inner pressure and forms of instability of the synchrotron as a whole. This analysis is fundamental for the correct operation of beam transport system and is strongly coupled with the alignment of the machine. If the critical (instability) pressure for such cryogenic machine is too low a transverse motion of the magnets with respect to the cryostats may occur during the cool-down or warm-up of the synchrotron. As strong transverse motion may lead to a permanent misalignment of the magnets, it is of primary importance to assure the correctness of design from this point of view. In the past many cryogenic machines suffered from this particular problem.

Final version of the synchrotron optics includes main magnets (dipoles and quadrupoles), orbit correctors (steerers) as well as higher order correctors (chromaticity and extraction sextupoles, error correction multipoles). The synchrotron topology has been classified by subdividing the machine arc into the assemblies (from A to E) and defining specific components like connection cryostats (do not contain magnets) or arc ends equipped with the cold-warm transitions (CWT). All the nonstandard components generate specific types of interconnects that have to be correctly designed. Moreover, the standard and the nonstandard components have different lengths and their support inside the continuous cryostat has to be set in such a way so as to reduce the vertical sagitta (due to their own weight). For this reason an optimisation of the system of supports inside the cryostat for each single cold mass component has been carried out. The system of inner supports (composite columns) is cross-checked with the system of outer supports (jacks) in order to minimise deformation of the cold mass and the cryostat. Finally, a finite element analysis of the synchrotron under its own weight, pressure loads and possible misalignment pattern has been carried out. The aim of this analysis is to verify maximum deformation across the interconnections, magnet extremities and inner supports. This analysis is precise and close to the real behaviour of magnets and their interconnections. Similar analysis has been carried out for smaller components like cold-warm transitions (CWT) in order to assure their correct performance during the machine operation. Only with all above mentioned verifications the overall topology of SIS300 arc can be accepted as safe from the structural point of view.

2 Optimum design of SIS300 magnet to magnet interconnections

2.1 Introduction

The magnet-to-magnet interconnections play an important role in the accelerator design because of the following reasons:

- they provide connections of all the vital systems of the accelerator,
- in the beam transport system they constitute drift spaces, therefore, their length has to be minimized,
- interconnections contribute to the alignment of the magnets,
- interconnections are the last system to be assembled in-situ.

The following main functions of the interconnections shall be accounted for:

- continuity of the beam transport system,
- continuity of the beam and insulation vacuum,
- continuity of the electrical powering system,
- continuity of the helium supply system (cryogenics),
- continuity of thermal shielding,
- compensation for thermal contraction of adjacent components,
- transverse flexibility for magnet alignment.

The architecture of SIS300 interconnections is composed of 7 magnet-to-magnet connections:

1. beam vacuum interconnect
2. 4 channels containing the main bus-bar splices
3. 2 helium flow channels

Under the assumption that the beam transport system is not equipped with the beam screen the beam vacuum interconnect carries a single expansion joint, called beam vacuum bellows. The main feature of this expansion joint is related to the fact that in the operational conditions the bellows stays in the insulation vacuum and contains the beam vacuum. Therefore, the expansion joint is loaded exclusively due to the thermal contraction (expansion) of the adjacent components. However, the incidental conditions (special cases) have to be taken into account. They correspond to the situation when either the beam vacuum or the insulation vacuum are broken. In these cases the bellows is subjected to inner or outer pressure of 1 bar. Both cases are taken into account in the process of bellows optimization.

The beam vacuum interconnect is surrounded by 4 channels that carry the main bus-bars and their connections. In order to provide the interconnections with the compensation capacity, each channel is equipped with an identical expansion bellows. As the cold mass will be pressurized, a maximum of 2 MPa inner pressure has been assumed in the analysis. This yields a multiply structure of the expansion joints (number of plies 3-4). As the bellows in the bus-bar channels will coexist with the connection box containing splices of the superconducting bus-bars, they have to be optimised from the point of view of their length and outside diameter. Due to the fact that inner pressure may lead to a semi-global instability of the interconnect, stiffness of all the components separating the bellows from

the magnets including the magnet heads has to be taken into account. Due to their peripheral location these bellows have to provide more transverse flexibility than the beam vacuum bellows.

Finally, the magnet-to-magnet interconnections are equipped with two additional peripheral channels, called helium flow channels. Here also a maximum operational pressure of 2 MPa has been assumed. Because of their peripheral location the helium flow interconnects have to be equipped with compensation elements allowing for a significant transverse motion of adjacent magnets. Therefore, the helium flow channels may be equipped either with expansion joints of sufficient length or with double bellows universal joints. As the cost of double bellows universal joint is significantly higher than the cost of a single bellows and for stability reasons the solution with standard single bellows is recommended. The following architecture of compensation system for the SIS300 synchrotron is recommended (Table 2.1):

Interconnect	**Type of expansion joint**	**Option**
Beam vacuum (1)	Single ply thin-walled stainless steel bellows with type-U convolutions	Single ply thin-walled stainless steel nested bellows
Bus-bar interconnects (4)	Multi-ply stainless steel bellows with type-U convolutions	
Helium flow interconnects (2)	Multi-ply stainless steel bellows with type-U convolutions	Double bellows universal joints based on multi-ply stainless steel make

Table 2.1 Types of expansion joints for the SIS300 interconnections

It is worth pointing out that in the absence of the beam screen, one single bellows for the beam vacuum interconnect is sufficient (unless there is a need to decouple mechanically the beam pipe with respect to the cold mass).
General parameters defined in the design of expansion bellows for subsequent lines are listed in Table 2.2.

Interconnect	**ID [mm]**	**N° plies**	**Inner Pressure**	**Outer Pressure**	**Minimum lifetime**	**Extension/ compression**	**Offset [mm]**
Beam vac.	100	1	0	0	500 cycles	+5/-5	4
Bus-bar	70	3-4	2 MPa	0	500 cycles	+5/-5	8
Helium flow	70	3-4	2 MPa	0	500 cycles	+5/-5	10

Table 2.2 Main parameters of the bellows expansion joints for the SIS300 interconnections

2.2 Parametric optimisation

The parametric optimization is carried out by using the code BELOPT. The main objective of the optimisation is to reduce the bellows stiffness as much as possible since the bellows provide a mechanical decoupling between the neighbouring objects (cryomagnets). Usually the available space constitutes one of the serious limitations (constraints) for every expansion joint (the requirement of maximum magnetic length of accelerator). Thus, we are searching for minimum axial and transverse stiffness under the geometrical, stress, stability and fatigue constraints – everything in the framework

of the previously apportioned reliability. The relevant formulation of the optimisation problem is given below:

- Minimise the objective function:

$$F_{ax}(\underline{x}_{bl}) = \frac{\mu}{C_f}\left(E_T d_m \left(\frac{t_p}{w}\right)^3 \left(\frac{n_p}{n_c}\right)\right)$$

- equality constraints:

inner diameter	$D_{in} = const$

- inequality constraints:

bellows convoluted length	$L_{bl} \le L_{\max}$
outer diameter	$D_{out} \le D_{\max}$
bellows maxi compression	$\Delta_{bl-} \ge \Delta_{\min}$
cost function	$Q_{bl} \le Q_{0bl}$
probability of failure	$P(\underline{x})\big\|_{\Omega_{bl}} \le p_{0bl}$
membrane stress	$P[S_1 > S_{ad}] \le p_{2bl}$
membrane stress	$P[S_2 > S_{ad}] \le p_{2bl}$
membrane & bending stress	$P[S_3 + S_4 > S_{34}] \le p_{2bl}$
fatigue life	$P[N_f(S_t) < N_{f0}] \le p_{3bl}$
column buckling	$P[P_{col} < P_1] \le p_{4bl}$
in-plane squirm	$P[P_{inp} < P_2] \le p_{4bl}$

- random design variables:

$$\underline{x_{bl}} \rightarrow (n_c, n_p, t_p, q, w, \Delta_+ / \Delta_-)$$

Here Δ_+ / Δ_- denote the repartition of the axial offset between compression and tension and S_t stands for the EJMA equivalent stress.

The above shown general formulation can be simplified to a deterministic form, if the reliability aspect plays a less important role:

- Minimise the objective function:

$$F_{ax}(\underline{x}_{bl})$$

- inequality constraints:

bellows convoluted length	$L_{\max} - L_{bl} \ge 0$
inner diameter	$D_{in} - D_{\min} \ge 0$
outer diameter	$D_{\max} - D_{out} \ge 0$
bellows maxi compression	$\Delta_{bl-} - \Delta_{\min} \ge 0$
cost function	$Q_{0bl} - Q_{bl} \ge 0$
membrane stress	$S_{ad} - S_1 \ge 0$
membrane stress	$S_{ad} - S_2 \ge 0$

membrane & bending stress	$S_{34} - (S_3 + S_4) \geq 0$
fatigue life	$N_f(S_t) - N_{f0} \geq 0$
column buckling	$P_{col} - P_1 \geq 0$
in-plane squirm	$P_{inp} - P_2 \geq 0$

- design variables:

$$\underline{x_{bl}} \rightarrow \left(n_c, n_p, t_p, q, w, \zeta\right)$$

where $\zeta = \Delta_+ / \Delta_-$. Here, for simplicity, all the constraints were expressed as inequalities. It is convenient to introduce a unified notation (changing the direction of inequalities):

- Minimise the objective function:

$$F(\underline{x}) = g_0(\underline{x})$$

- under the inequality constraints:

$$f_k = g_k(\underline{x}) \leq 0 \quad ; \quad k = 1,...,m$$

- and with the design vector:

$$\underline{x} \rightarrow \left(x_i \geq 0; i = 1,n\right)$$

In this particular case the number of inequalities is *m*=11 and the number of variables is *n*=6.

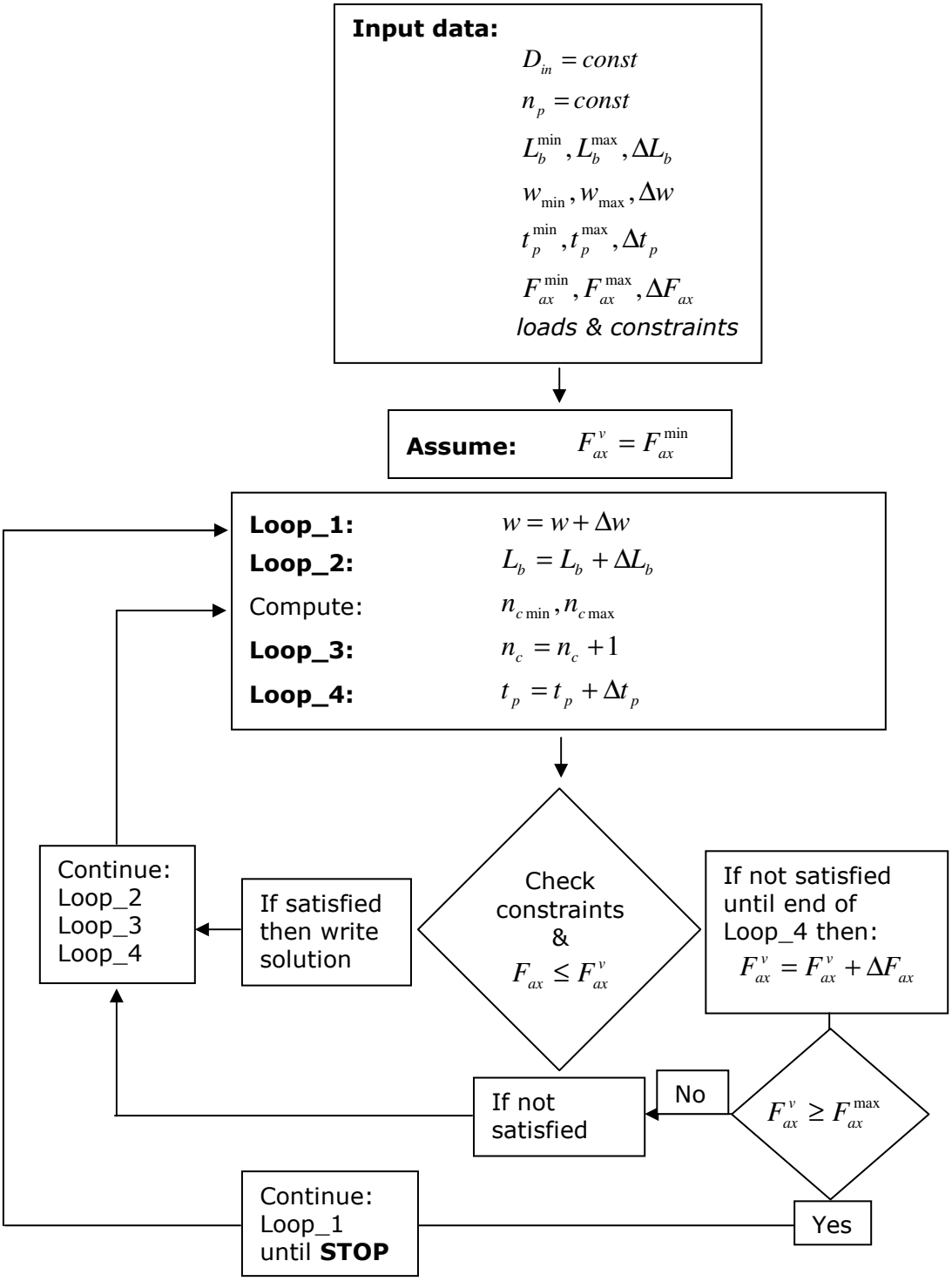

Fig. 2.1: Algorithm for optimisation of the bellows expansion joints

With this formulation a Lagrange function can be constructed:

$$L(\underline{x}, \underline{\lambda}) = g_0(\underline{x}) + \sum_{k=1}^{m} \lambda_k g_k(\underline{x})$$

Finally, based on the Kuhn-Tucker theorem, a typical minmax problem is solved: point of global minimum $(\underline{\hat{x}}, \underline{\hat{\lambda}})$ is attained if the following inequality is satisfied:

$$L(\underline{\hat{x}}, \underline{\lambda}) \leq L(\underline{\hat{x}}, \underline{\hat{\lambda}}) \leq L(\underline{x}, \underline{\hat{\lambda}})$$

which is equivalent to determining the saddle point of Lagrange function *L*. This can be done by using different methods of non-linear programming. A method that is particularly well adapted to the case under consideration is the geometric programming.

A simplified parametric way of solving the problem is based on the algorithm shown in Fig. 2.1. Here the number of design variables was reduced to 4:

$$\underline{x_{bl}} \rightarrow (n_c, t_p, q, w)$$

The number of plies n_p is assumed at the beginning of the procedure and the parameter $\zeta = \Delta_+ / \Delta_-$ is recomputed from the admissible compression Δ_{bl-} (inequality constraint). The algorithm is searching for all the solutions, for which the axial stiffness is smaller than a check value:

$$F_{ax} \leq F_{ax}^{v}$$

arbitrarily chosen at the beginning of the process. The local minimum solutions are collected (see Fig.2.2) and a global minimum is chosen for a given number of plies.

The operation can be repeated for different number of plies and, finally, a global minimum is found. A corresponding Fortran code of optimization of the expansion joints for cryogenic applications has been developed.

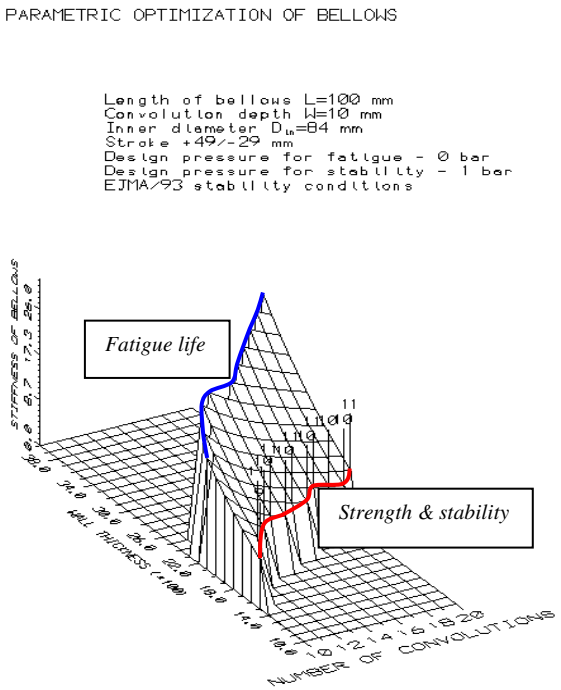

Fig. 2.2: The local minimum solutions in the optimization procedure

The advantage of the above presented algorithm of sweeping the objective function in the optimisation domain consists mainly in the possibility of finding always the global minimum without the additional cost of checking the necessary and sufficient conditions.

2.3 Parameters of the expansion bellows

As a result of the optimization process the following parameters of the SIS300 expansion bellows were obtained (Tables 2.3, 2.4, 2.5):

Inner dia.	***Outer dia.***	***Nbr of convolutions***	***Pitch***	***Nbr of plies***	***Nom. thick. of ply***	***Maxi. static compression /maxi offset***	***Design pres.***	***Axial rate***
mm	mm		mm		mm	mm	MPa	N/mm
100	120	19	5.3	1	0.2	31/11	0.1	~ 10
-.5/+.5	-1/+0		-.1/+.1		-0/+.01			

Table 2.3 Parameters of the SIS300 beam vacuum interconnect expansion bellows
(cf. Annex 1)

Inner dia.	***Outer dia.***	***Nbr of convolutions***	***Pitch***	***Nbr of plies***	***Nom. thick. of ply***	***Maxi. static compression /maxi offset***	***Design pres.***	***Axial rate***
mm	mm		mm		mm	mm	MPa	N/mm
70	82.8	16	5.0	4	0.2	18/7.5	2.0	~ 155
-0/+.5	-.5/+.5		-.1/+.1		-0/+.02			

Table 2.4 Parameters of the SIS300 bus-bar interconnect expansion bellows
(cf. Annex 2)

Inner dia.	***Outer dia.***	***Nbr of convolutions***	***Pitch***	***Nbr of plies***	***Nom. thick. of ply***	***Maxi. static compression /maxi offset***	***Design pres.***	***Axial rate***
mm	mm		mm		mm	mm	MPa	N/mm
70	84.9	20	4.75	3	0.3	19.5/11	2.0	~ 179
-0/+.5	-.5/+.5		-.1/+.1		-0/+.03			

Table 2.5 Parameters of the SIS300 He flow interconnect expansion bellows
(cf. Annex 3)

2.4 Quality of the materials

The material properties will be specified in a dedicated document (Technical Specification). However, a general description and some important details are listed in the present chapter. The current description is related to type Cr Ni 17 13 Mo stainless steel for the production of sheet steel or tubing for flexible expansion joints (bellows etc.). The chemical composition of the material is

presented in Table 2.6. The structure of the alloy after full quenching shall be completely austenitic. In accordance with the standard ASTM E112-96, grain size ≤ 40 μm shall be accepted. The relative magnetic permeability after full quenching and at room temperature shall be lower than or equal to 1.005 for fields of over 80 000 A/m (equivalent to 1000 Oe). The amount and definition of inclusions shall meet the standard ASTM E45-97e1, method D. The class of inclusions shall be at most 1. The tolerance for acceptance may be a half-class above the set limit to the extent of 2% of the fields counted.

The required mechanical properties at RT and at 4.2 K are specified in Tables 2.7 and 2.8.

Components	**Content %**	**Tolerances Above maximum and Below minimum**
Cr	16 - 18.5	0.20
Ni	11 - 14	0.15
C	0.030 max.	0.005
Si	1 max.	0.05
Mn	2 max.	0.04
Mo	2 – 2.5	0.10
*N	0.050 max.	0.01
*P	0.030 max.	0.005
*S	0.010 max.	0.001
Fe	Remaining	
Cobalt shall be present only as a trace or to a maximum proportion of 0.22%, including measuring tolerance.		

Table 2.6 Chemical composition of the 316L stainless steel for expansion bellows (* denotes a specific requirement)

Tensile strength	R_m min.	600 N/mm^2
Yield stress	R_p 0.2% min.	225 N/mm^2
Elongation at break	A_5 min.	35%
Brinell hardness	HB max.	180

Table 2.7 The required mechanical properties at room temperature

Impact strength	KCV min.	80 J/cm^2

Table 2.8 The required mechanical properties at 4.2 K

2.5 Magnet to magnet distance

It is proposed to apply similar configuration of bus-bar interconnects like in the LHC.

Each bus-bar interconnect is stretched between the magnet head nozzles and contains a chamber for bus-bar splices (connection box) and an expansion joint. Also, it is recommended to guide the bus-bars in the nozzles in order to keep their position in the channels for soldering process. To this end installation of a guide (spider) on the lyra side of the interconnect is recommended. On the other hand,

installation of a spacer on the connection side of the interconnect should be anticipated. Its function is again related to the correct positioning of the bus-bar extremities for soldering. Finally, given the space needed for connection box, expansion bellows and nozzles containing the spacers a total length of around 480 mm is needed for the bus-bar interconnects.

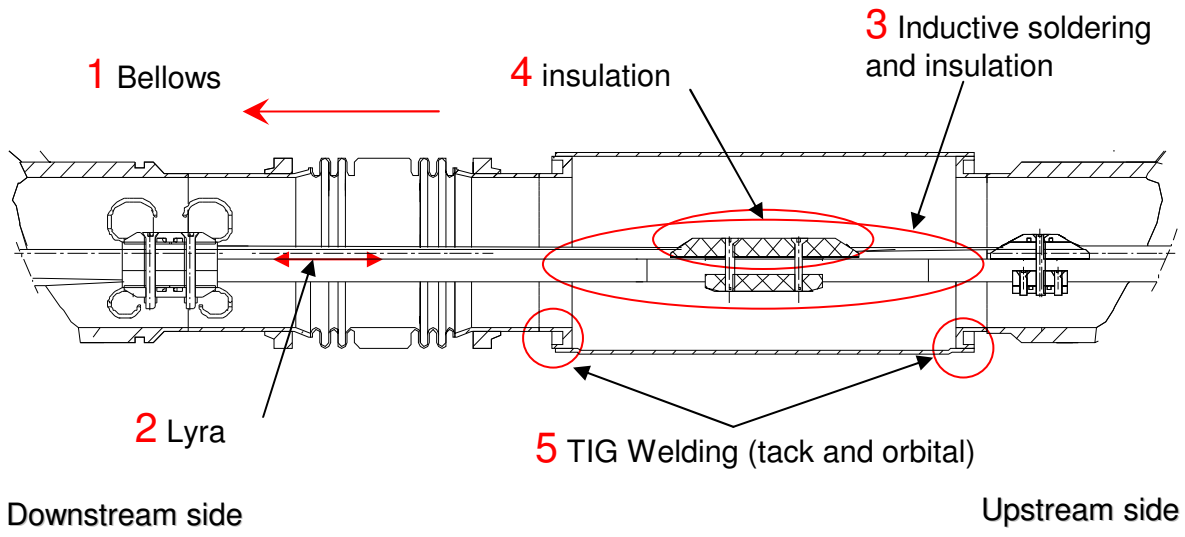

Fig. 2.3 Recommended configuration of the magnet-to-magnet bus-bar interconnect

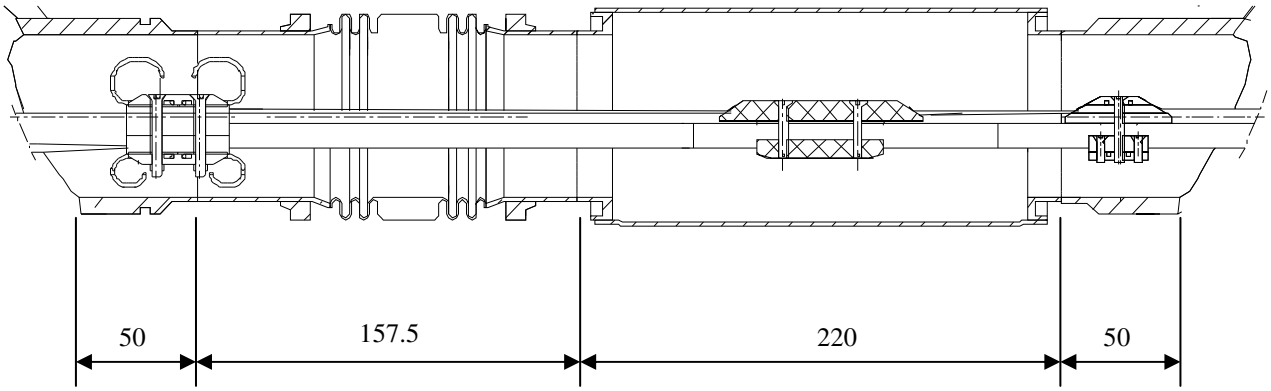

Fig. 2.4 Minimum magnet-to-magnet distance

A general view of the SIS300 interconnections containing the position of the expansion bellows and the space for bus-bar connections is shown in Fig. 2.5.

2.6 Conclusions

The following recommendations are made:

1. In the beam vacuum interconnects a central expansion joint is sufficient both for compensation of the thermal contraction and for the alignment issues.

2. Installation of single compact expansion joint for the helium flow interconnects is proposed. This expansion joint has enhanced capacity for transverse compensation because of peripheral location of these interconnects.
3. Similar configuration of the bus-bar interconnects like in the LHC is highly recommended. The interconnects shall comprise connection boxes, compact expansion joints and bus-bar spacers (spiders + spacers).
4. All possible data for the expansion joints obtained from the optimisation process are contained in the Annexes 1,2,3. Analysis of the plastic strain fields evolution under cyclic loads is presented in Annex 4.
5. The minimum magnet-to-magnet distance for the bus-bar interconnects is equal to around **480 mm**.

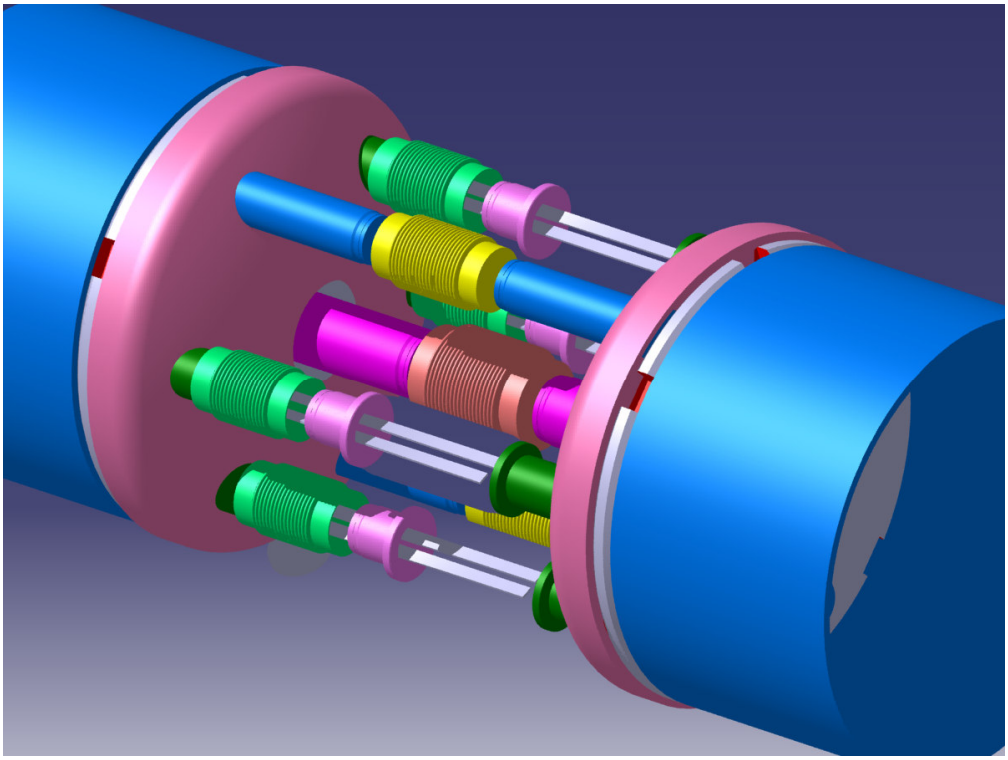

Fig. 2.5 General configuration of the SIS300 interconnections

3 Structural stability of SIS300 interconnections in the regular cell

3.1 Introduction

SIS300 regular cell in the arcs contains main quadrupole, main dipole and the corrector magnets (closed orbit correctors, chromaticity sextupoles and other multipole correctors). In the present document the semi-global stability of the magnet-to-magnet interconnect is addressed. As a second step the global stability of single regular cell or a sequence of cells is analysed. The global stability analysis shall help to solve the problem of support the cold-mass in the continuous cryostat in order to achieve stable conditions of operation of the ring. The analysis of semi-global stability is based on the eigenvalue problem for interconnects containing the bellows expansion joints. The experience shows that this problem has been misunderstood in the past and provoked a number of catastrophic events (Fig. 3.1).

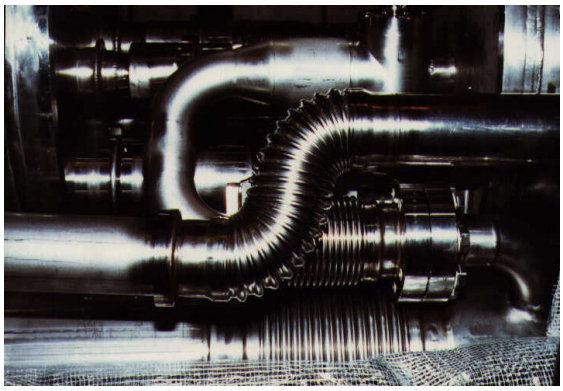

Fig. 3.1 Instability of interconnect containing the expansion bellows

Analysis of global stability is also based on the eigenvalue problem defined for a set of rigid components connected by the elasto-plastic interconnects and supported inside the cryostat in elastic manner. The way of supporting the cold mass in the continuous cryostat and the stiffness of supports has a fundamental importance for the transverse motion of the magnets during the cool-down or warm-up as well as during the alignment of the synchrotron. It is worth pointing out that the stiffness of cold-mass supports is in contradiction with the heat loads transferred via the supports to the cold-mass, therefore a thermo-mechanical optimization is needed.

3.2 Semi-global stability of SIS300 interconnections

The most critical interconnections of SIS300 from the point of view of local stability are the bus-bar channels and the helium flow interconnects.

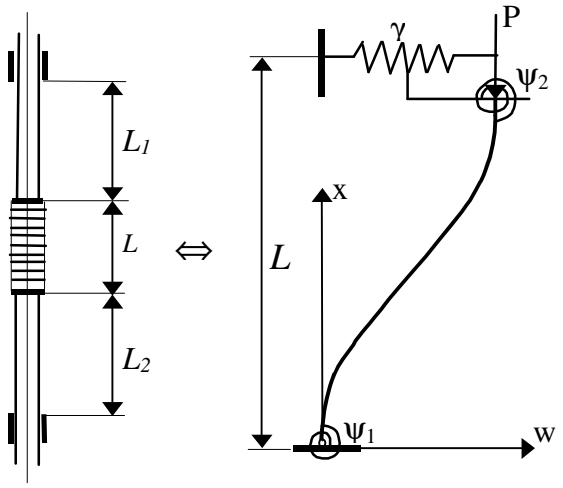

Fig. 3.2 Elastically supported column – model of the interconnections

The bus-bar and the helium flow interconnections are susceptible to buckling since they are subjected to the same design pressure as the cold mass. Also, the layout of the interconnections is such that the bellows expansion joints are situated close to the cold mass head and the portion of the interconnect on the opposite side of bellows is rather long (Fig. 3.3). This induces a weak support of the expansion joints on one side. For this particular reason, a more precise analysis of the mechanical stability of the SIS300 interconnections is needed.

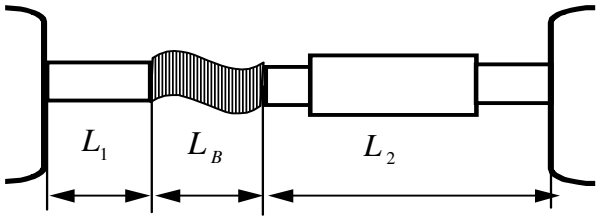

Fig. 3.3 Layout of the bus-bar and helium flow interconnections

The mathematical model used in this analysis is based on the equivalent column concept (Fig. 3.2). The bellows expansion joint is modelled as a flexible and elastically supported column. The parameters of the elastic support are evaluated as a function of L_1/L_B ; L_2/L_B for each interconnect separately. Finally, a stability diagram is plotted and the so-called critical length $(L_1+L_2)_{cr}$ is evaluated. It corresponds to such a sum of guidance distances on both sides of the bellows expansion joint that provokes a radical change of instability mode and a dramatic reduction of the critical buckling pressure (Fig. 3.4). Thus, each interconnect shall (approximately) satisfy the following criterion:

$$L_1 + L_2 \leq 0.5 (L_1 + L_2)_{cr}$$

which is equivalent to an approximate safety factor of 2 with respect to the critical guiding distance. In addition, a safety factor of 5.88 (required by EJMA) is imposed on the critical pressure itself. Thus, the domain of safe operation of interconnect is limited by a pair of values (L_{safe}, P_{safe}) as shown in Fig. 3.4 (box with texture).

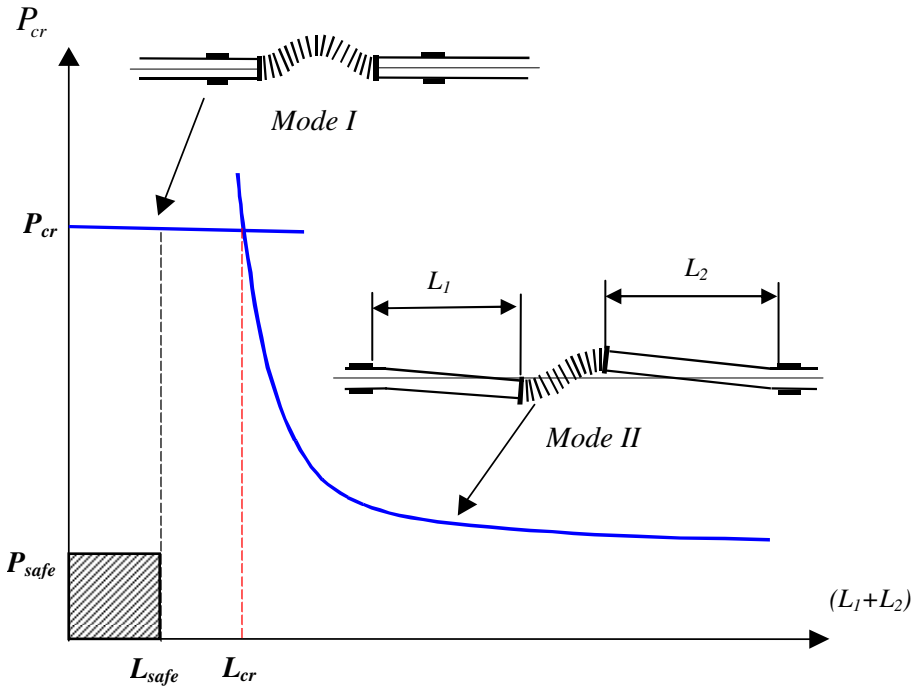

Fig. 3.4 Stability diagram for the magnet-to-magnet interconnections

The corresponding diagrams have been prepared for both pressurized types of interconnections: bus-bar interconnects (Annex I) and helium flow interconnects (Annex II). In both diagrams the critical pressure is shown as a function of the mean bellows to support distance $0.5(L_1 + L_2)$.

3.3 Phase transformation in the material of expansion bellows

The Fe-Cr-Ni stainless steels are commonly used to manufacture components of superconducting magnets and cryogenic transfer lines since they retain their ductility at low temperatures and are paramagnetic. The nitrogen-strengthened stainless steels of series 300 belong to the group of metastable austenitic alloys. Under certain conditions the steels undergo martensitic transformation at cryogenic temperatures that leads to a considerable evolution of material properties and to a ferromagnetic behaviour. The martensitic transformations are induced mainly by the plastic strain fields and amplified by the high magnetic fields. The stainless steels of series 300 show at room temperature a classical γ-phase of face centred cubic austenite (FCC). This phase may transform either to α' phase of body centred tetragonal ferrite (BCT) or to a hexagonal ε phase. The most often occurring γ-α' transformation leads to formation of the martensite dispersed in the surrounding austenite matrix. In the course of the strain-induced transformation the martensite platelets modify the FCC lattice leading to local distortions. The volume fraction of the martensite (ξ) depends on the chemical composition, temperature, stress state, plastic strains and exposure to a magnetic field.

The most suitable alloy for low temperature applications in corrugated thin-walled bellows is 316L stainless steel. The chemical composition that assures stable behaviour of the steel under high inelastic strains has been presented in Chapter 2. Fig. 3.5 illustrates the behaviour of stainless steel,

including hardening due to the phase transformation. The numerical simulation has been cross-checked with the experimental data.

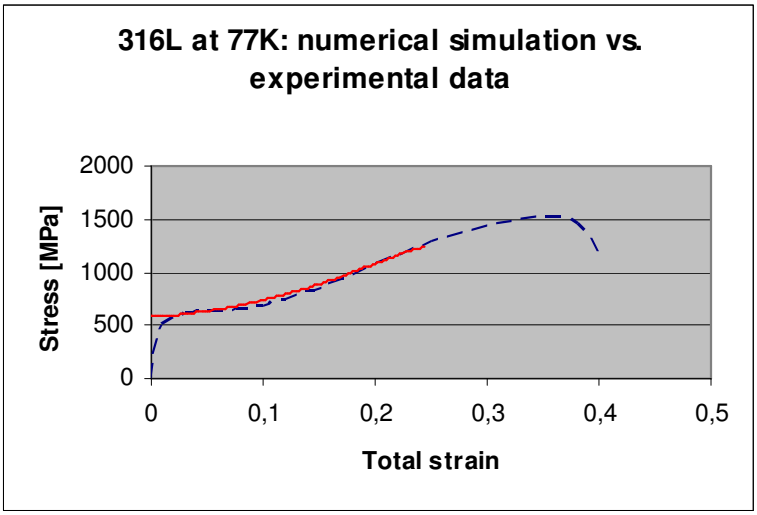

Fig.3.5 Numerical simulation versus experimental data for 316L at 77K

The expansion bellows of SIS300 were subjected to tension/compression according to the predicted motion based on the new design of magnets (longer version) and FODO lattice.

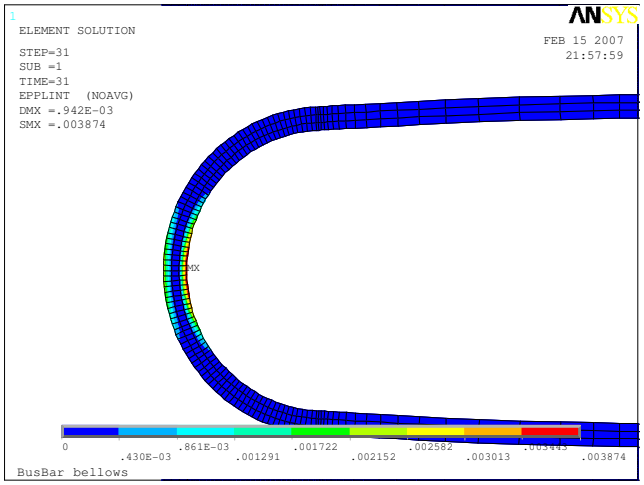

Fig. 3.6 Analysis of plastic strain fields in the bellows convolutions

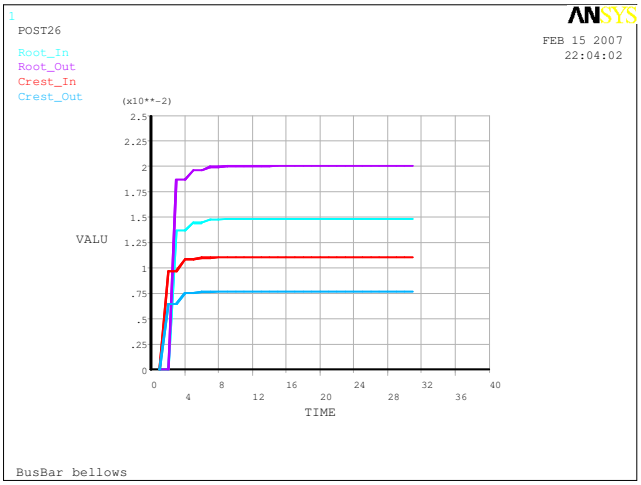

Fig. 3.7 Plastic shakedown in the bellows convolutions

The inelastic strain fields accumulated in the bellows convolutions are shown in Fig. 3.6. The fields are highly localized at root and at crest of the convolutions. This is also the localization where the phase transformation will take place. As the constitutive model accounts for the hardening due to the phase transformation (Fig. 3.5) there is a considerable difference in material response between the classical bilinear model (without phase transformation) and the model with the phase transformation process. A single cycle of loading – unloading and reverse loading is shown in Fig. 3.8 for both versions of the material model: classical versus phase transformation model. The plastic strains are accumulated from cycle to cycle and reach – after N_ξ cycles the phase transformation threshold p_ξ. From this moment on each subsequent cycle induces additional increment of α' phase and increases the magnetic permeability with respect to the initial value of (1.005).

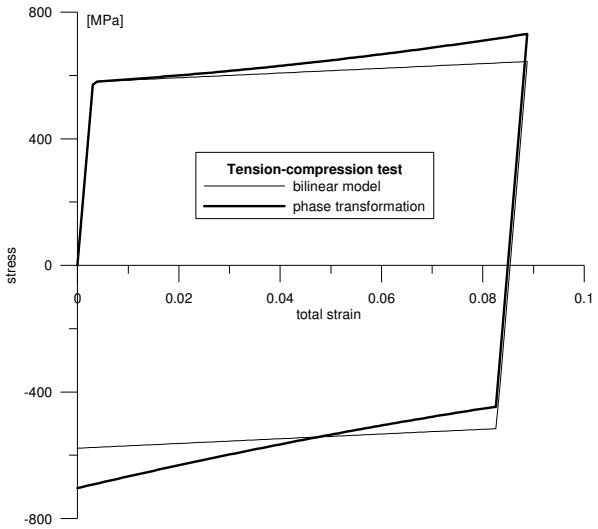

Fig. 3.8 One loading – unloading – reverse loading cycle for expansion bellows

As different materials have different sensitivity to the plastic strain induced phase transformation at cryogenic temperatures, a comparison between the behaviour of 304 L stainless steel (upper left) and

316L stainless steel (upper right) after 20 complete cycles imposed on the bellows convolutions is shown in Fig. 3.9. Bottom plot in Fig. 3.9 shows the accumulation of α' phase in the case of 304L, whereas the same test for 316L shows no visible traces of phase transformation (the threshold p_ξ was not reached). Stainless steel 304L has much lower threshold value p_ξ and much higher saturation level ξ_L , which implies more intensive phase transformation than in the case of 316L (special low temperature grade). Finally, the plot showing the increase of ferromagnetic α' content against the number of cycles for 316 L stainless steel is shown in Fig. 3.10.

The analysis shows that the threshold value N_ξ is reached after 45 cycles of cool-down and warm-up. Afterwards, the α' content increases linearly to reach after subsequent 30 cycles the highest measured value for this stainless steel grade equal to 0.3. Thus, in total some 75 cycles are needed in order to transform 30% of initial austenitic structure to a mixture of 70% of γ-phase and 30% of α'-phase.

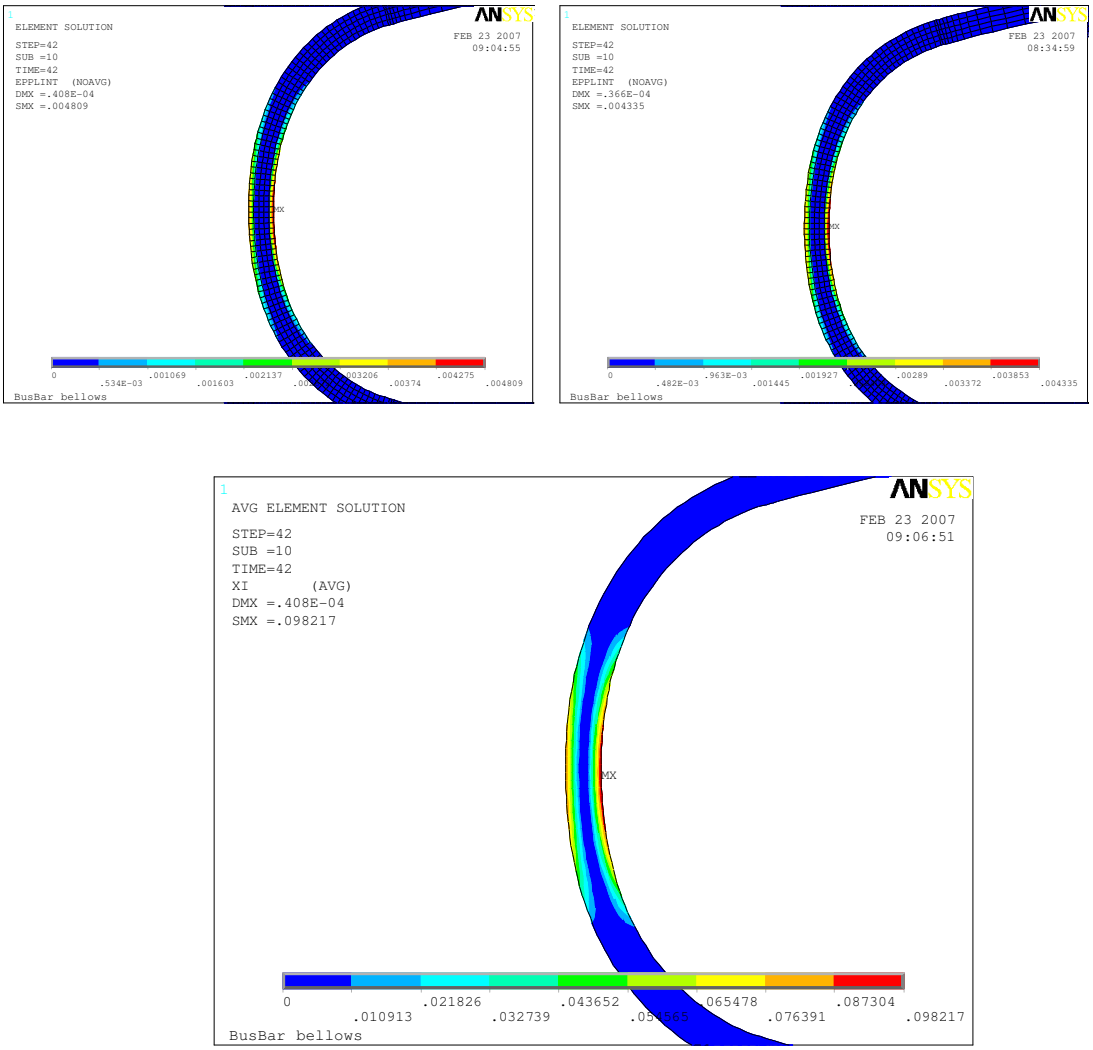

Fig. 3.9 Comparison between grades 304 L and 316L stainless steel

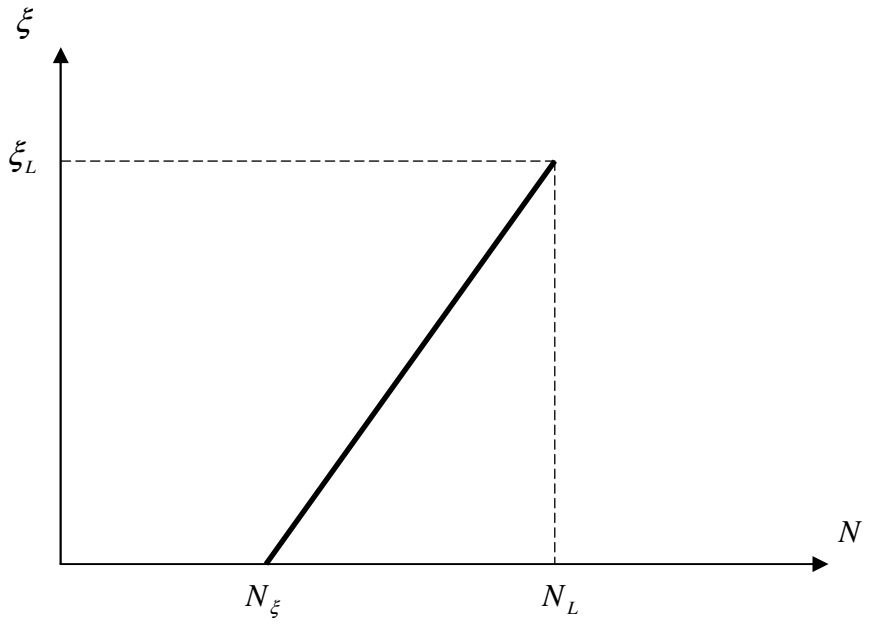

Fig. 3.10 Increase of the α' content as a function of the number of cycles

3.4 Cold-warm transition: preliminary analysis

A parametric FE model of the cold-warm transition has been built (cf. Appendix 3). The model is axisymmetric and composed of the beam tube, thermal shield and vacuum vessel. A similar design like for SIS100 has been adopted. The parameters used for the analysis (emissivities, temperature boundary conditions, geometry) have been assumed in a preliminary way (iteration 0). The analysis has been carried out by using the solid conduction and radiation features. The results are presented in Annex 3.3 in terms of temperature and thermal gradient distributions.

3.5 Conclusions

1. Semi-global stability analysis leads to the conclusion that the bellows-to-support distance for all the pressurized interconnects, specified in Chapter 2, stays within the safe limits (domain of safe operation). The corresponding stability diagrams are presented in Annexes 3.1 and 3.2. Here, the wall thickness of the tubes linking the bellows with the magnets has been assumed equal to 2 mm.
2. Analysis of the phase transformation process in the convolutions of bus-bar bellows shows that the threshold value in terms of the accumulated plastic strains (p=0.09) has been reached within 45 cycles of cool-down and warm-up. Additional 30 cycles bring the bellows material (316L stainless steel) close to the maximum measured value of α'-phase content equal to 30%.
3. The phase transformation process takes place locally in the bellows convolution (at root and at crest) and leads to enhanced magnetic permeability.

4. From the point of view of the interconnections it is recommended not to exceed 75 complete cycles of cool-down and warm-up in the life-time of the accelerator.
5. The temperature distribution in the cold-warm transition designed for SIS300 (preliminary design) is shown in Annex 3.3.

Annex 3.1: Stability diagram for SIS300 bus-bar interconnections

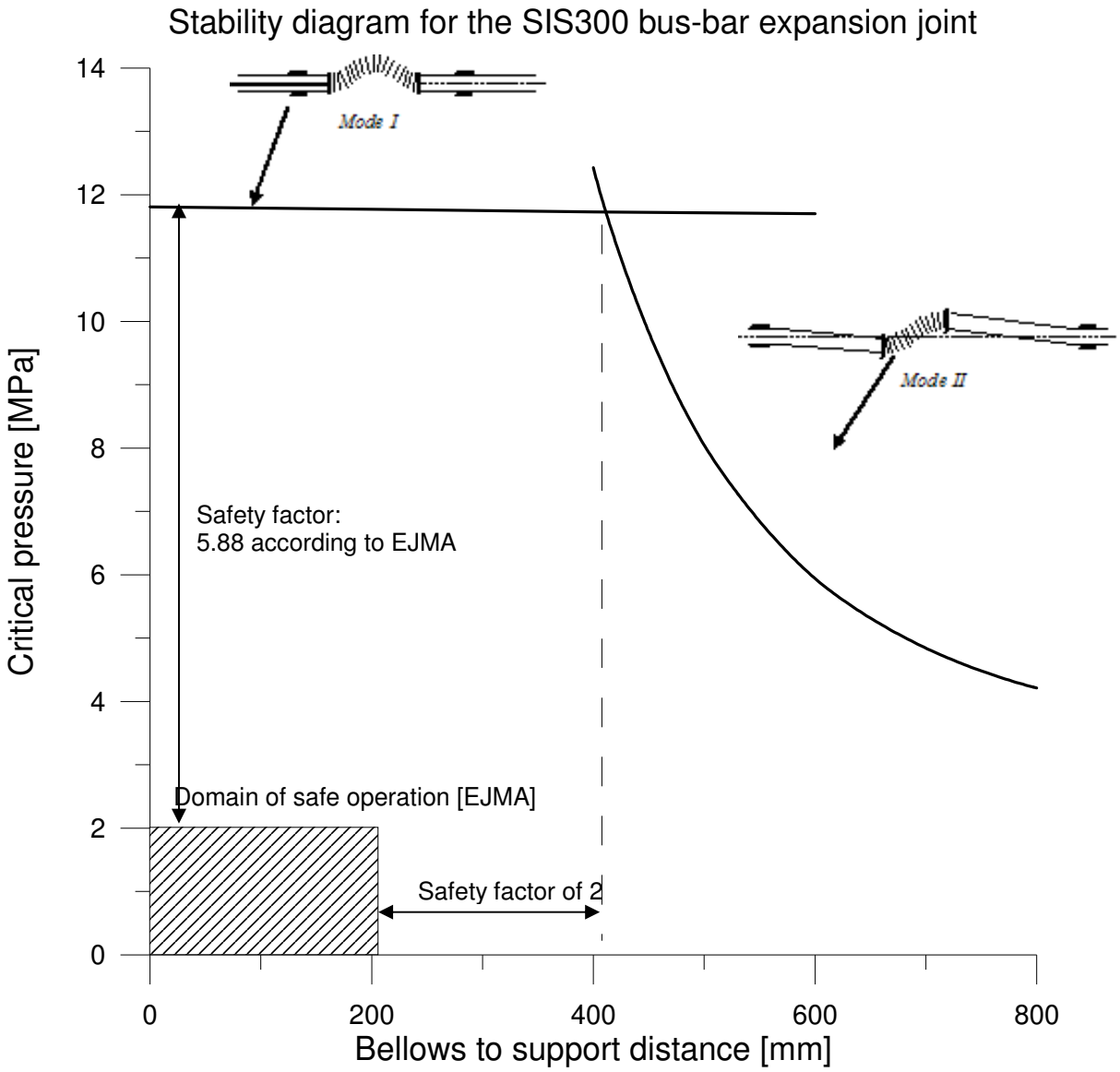

Annex 3.2: Stability diagram for SIS300 helium flow interconnections

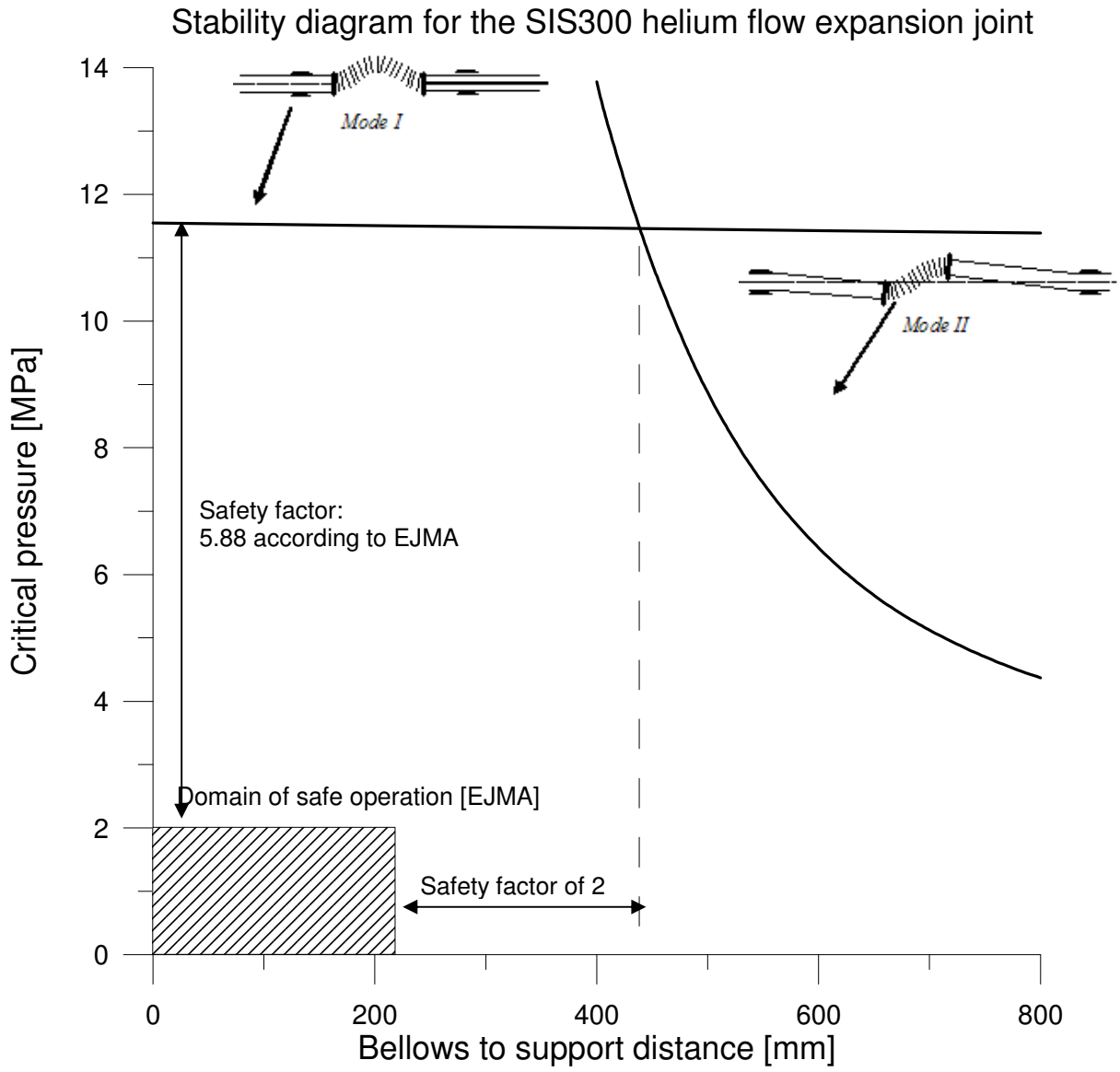

Annex 3.3: Temperature and axial thermal gradient distribution in CWT

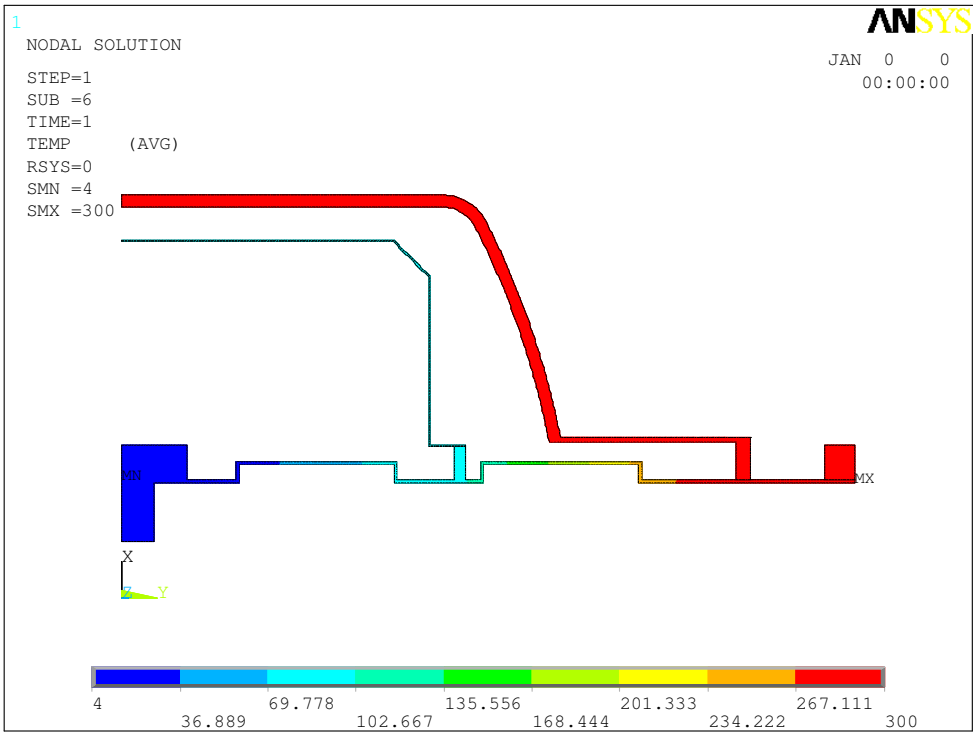

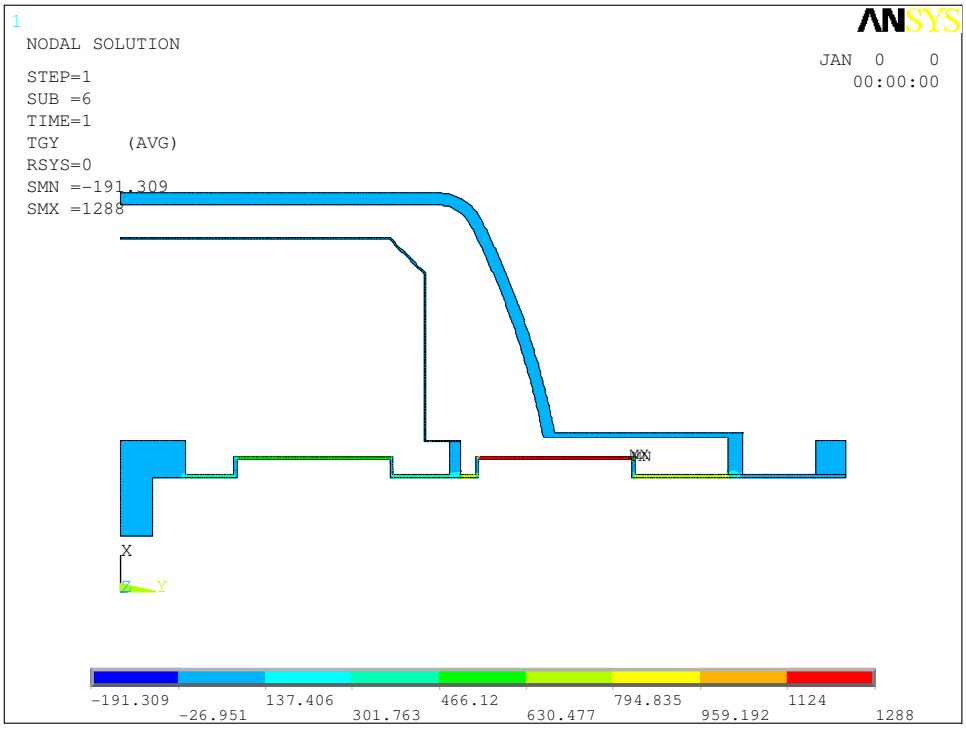

4 Global structural stability of magnets and interconnections in the SIS300 regular cell

4.1 Current version of lattice

According to the current version of lattice, the SIS300 regular cell in the arcs is based on the FODO principle. Each main dipole magnet is flanked by main quadrupole, as indicated in Fig. 4.1. In the present document the global structural stability of the SIS300 magnets and interconnections is addressed. In addition, analysis of sensitivity of interconnections with respect to imperfections is carried out. Investigation of global stability comprises analysis of single regular cell and a sequence of cells. It shall help to solve the problem of how to support the cold-mass in the continuous cryostat in order to achieve stable conditions of operation of the ring.

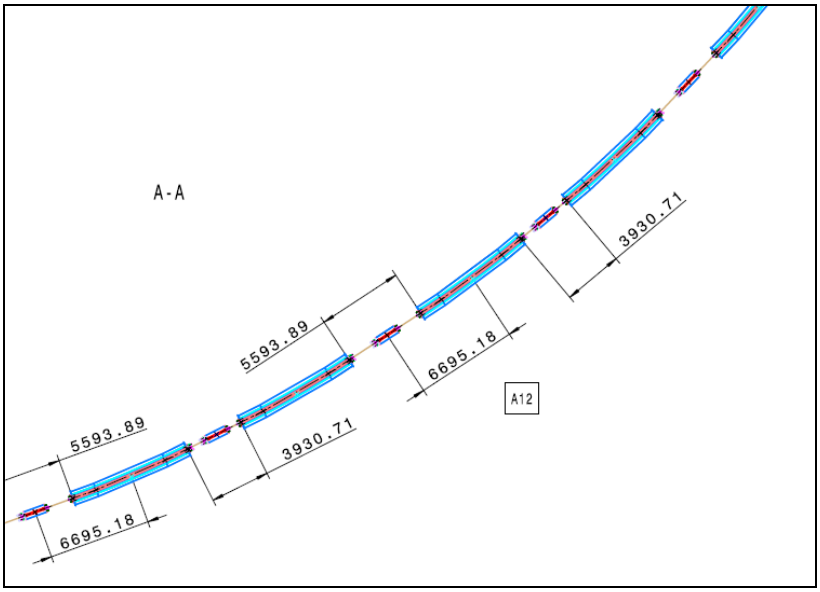

Fig. 4.1 SIS300 FODO lattice

Global stability analysis is also based on the eigenvalue problem defined for a set of rigid components connected by means of elasto-plastic interconnects and supported inside the cryostat in elastic manner. The way of supporting the cold mass in the continuous cryostat and the stiffness of supports has fundamental importance for the transverse motion of magnets during cool-down or warm-up as well as during the alignment of the synchrotron. It is worth pointing out that the enhanced stiffness of cold-mass supports is in contradiction with the heat loads transferred via the supports to the cold-mass. Therefore, a thermo-mechanical optimization is needed.

4.2 Global stability of the SIS300 regular cell (formulation)

The regular cell is composed of ~8 m long dipole and ~2 m long quadrupole. As the slot length between the dipoles amounts to either ~3.93 m or ~5.6 m, and given the length of the quadrupole, the average length of interconnect is equal to either ~1 m or ~1.8 m, respectively. Given the stiffness of the interconnections and the way the magnets are supported in the continuous

cryostat, the whole structure forms a combination of stiff components elastically supported (Winkler's foundation), as shown in Fig. 4.2.

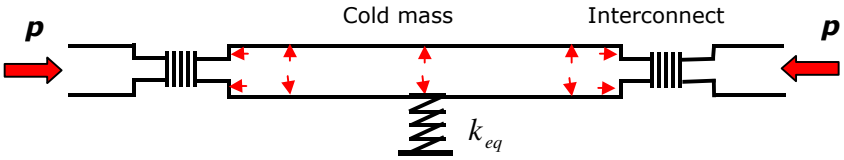

Fig. 4.2 Cold mass elastically supported in the cryostat

The cold mass constitutes a system of mechanically decoupled pressure vessels separated by means of the interconnections (mechanical compensation system: expansion joints). The magnets are supported inside the continuous vacuum vessel in elastic way. The support is symbolically illustrated in Fig. 4.2 by the elastic spring k_{eq}. Thus, all the magnets together form an elastically supported discontinuous system of pressure vessels subjected to thermo-mechanical and pressure loads (Fig. 4.3).

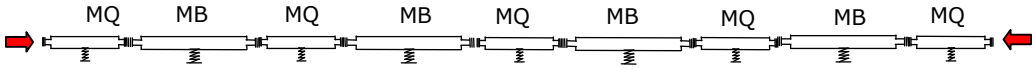

Fig. 4.3 Elastically supported discontinuous system (FODO lattice)

Such a system is susceptible to buckling when pressurised to its corresponding critical pressure. In order to evaluate the critical pressure, a simplified analytical model of SIS300 arc has been developed.

The model is based on the assumption of infinite rigidity of the cold mass when compared to the stiffness of interconnections and of the elastic supports. Consequently, it is assumed that the entire energy of deformation is concentrated in the interconnections (bellows expansion joints) and in the foundation. In order to account for the combined contribution of the supports and the cryostat, the elastic (Winkler's type) foundation was introduced. The stiffness of the elastic foundation is equivalent in terms of the elastic strain energy to the sum of all the components that deform under pressure loads. As the interconnections deform in an inelastic way the total dissipation of energy is concentrated there. However, for the sake of simplicity, during the first step of analysis the behaviour of interconnections will have a quasi-elastic representation.

The elastic multi-link model consisting of n segments and laying on the above defined elastic foundation leads to the following general set of equations:

$$P = \frac{\frac{c}{L_D} B_1 + \frac{kL_D^{\,2}}{3} C_1}{A_1} = \frac{L}{M} \qquad (4.1)$$

$$A_1 = A_1(\delta_i); B_1 = B_1(\delta_i); C_1 = C_1(\delta_i)$$

where:

- c, k denote the elastic equivalent stiffness of the interconnections and the elastic foundation, respectively,
- L_D denotes the length of dipole magnet MB. The length of main quadrupole is approximately quarter that of main dipole,
- P stands for the global axial force,
- δ_i are the transverse horizontal displacements of extremities of the consecutive magnets.

Here P plays a role of the hypothetical axial load (equivalent with respect to pressure acting on the active section of all the expansion joints in the interconnections) which is obtained from the equivalence of work of external loads on the corresponding displacements and the increase of internal elastic energy of the system (see Timoshenko et al., 1961). The load P needs to be minimised with respect to all the kinematically admissible displacement vectors ($\underline{\delta}$). In order to minimise the load a set of n-1 linear, partial differential equations is solved:

$$\frac{\partial L}{\partial \delta_i} - P\frac{\partial M}{\partial \delta_i} = 0 \text{ for } i = 1,...,n-1 \tag{4.2}$$

which leads to a set of linear homogenous algebraic equations:

$$[\mathrm{H}]\underline{\Gamma} = \underline{0} \tag{4.3}$$

where:

$$[\mathrm{H}] = [\mathrm{H}(\lambda)] \text{ and } \underline{\Gamma} = (\delta_1,...,\delta_{n-1}) \tag{4.4}$$

The condition of non-triviality of the solution:

$$det[\mathrm{H}] = 0 \tag{4.5}$$

leads, finally, to the characteristic polynomial of the order n-1 for the matrix H, that can further be solved for eigenvalues λ. The eigenvector $\underline{\Gamma}$ can be interpreted directly as a mode of instability of the accelerator cold mass. The eigenvalues λ are linked to the critical buckling load by the following equation:

$$P_{cr} = \lambda k L_D^{\,2} \tag{4.6}$$

It is worth pointing out that the critical load depends directly on the stiffness of the elastic foundation k and indirectly (via the eigenvalues λ) on the ratio c/k. In other words, it is mainly the combined stiffness of the support and the cryostat (represented by the parameter k) that contributes to the general mechanical stability of the accelerator arc.

4.3 Global stability analysis - results

The above given set of equations was solved for *n-1* corresponding to the length of 4 cells (*n=8*), each of them composed of main quadrupole and main dipole. The primary global instability mode of the string composed of 4 cells is shown in Fig. 4.4. It corresponds to the bifurcation pressure roughly 21

times higher than the design pressure (2 MPa). The analysis has been carried out for the following data (Table 4.1):

Table 4.1 Data for the global stability analysis

Parameter	**Value**	**Remarks**
Dipole length	8000 [mm]	approximation
Quadrupole length	2000 [mm]	approximation
Stiffness of elastic foundation (*k*)	4 [N/mm^2]	relaxation of boundary conditions taken into account
Flexural stiffness of interconnections (*c*)	7334900 [Nmm/rad]	length of interconnections ~1000 [mm]

When computing the stiffness of elastic foundation 2 supports per dipole and 2 supports per quadrupole were accounted for. The flexural stiffness of interconnections has been computed by using the following formula:

$$c = \frac{1}{\mu}\left(\sum_{i=1}^{6} c_i + \sum_{k=1}^{4} F_k h^2\right) \tag{4.7}$$

where c_i, F_k denote the bellows flexural stiffness and the bellows axial stiffness, respectively. Here, h denotes the distance of bus-bar bellows from the vertical axis of symmetry of interconnections and *μ=2* is a relaxation factor related to the length of interconnections. It is worth pointing out that the stiffness of supports corresponds to the assumption of 0.5 mm transverse deflection under the transverse load of 10^4 [N].

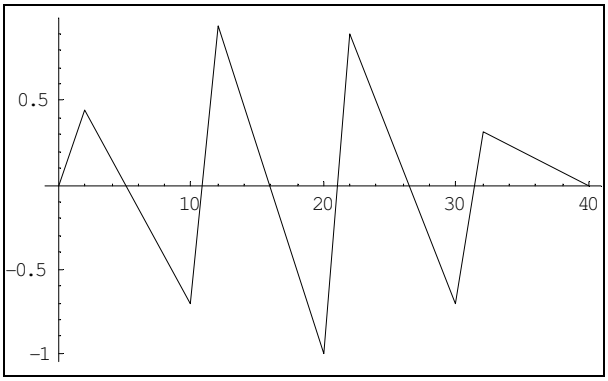

Fig. 4.4 Normalised primary instability mode for the string of 4 cells

For comparison the second normalised instability mode computed for the string of 4 cells is shown in Fig. 4.5. The subsequent instability modes correspond to higher critical pressure, therefore they are not highlighted in the present report.

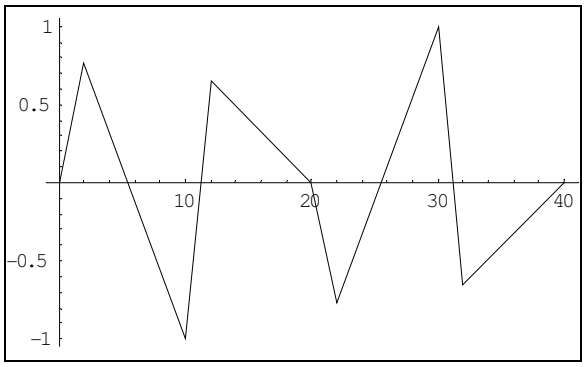

Fig. 4.5 Normalised second instability mode for the string of 4 cells

4.4 Configuration of the interconnections in the new lattice

New version of lattice implies different length of interconnections when compared to the previous version. As the slots for main quadrupoles are 3.93 m and 5.59 m long (Fig. 4.1) the length of interconnections corresponds to ~0.92 m and ~1.8 m, respectively. New configuration of magnets and interconnections including the layout of supports is shown in Fig. 4.6.

Here, a system of supports (cold feet) has been proposed, with one fixed support and one sliding support per magnet (in the vacuum vessel). The black numbers indicate dimensions, whereas, the red numbers indicate the thermal contraction of magnets in their respective vacuum vessels. Finally, the green numbers indicate the elongation of the zone of interconnections after cool-down of the accelerator. It becomes clear that the interconnections will be loaded in an asymmetric way due the fact that the fixed supports are located on one side of the magnet. The configuration of both shorter and longer interconnections is shown in Fig. 4.7.

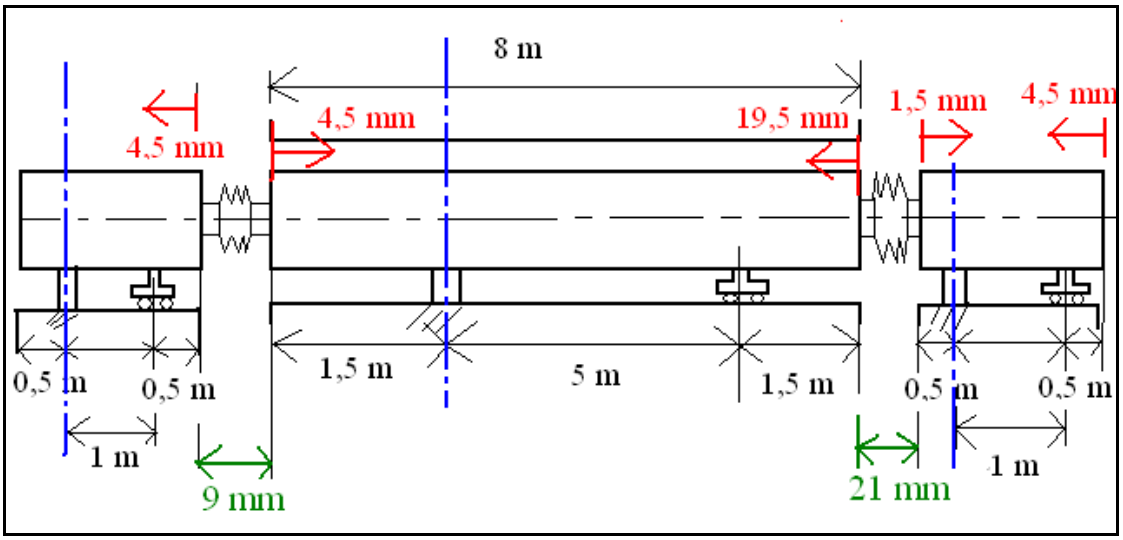

Fig. 4.6 Layout of magnet supports (cold feet) in the vacuum vessels

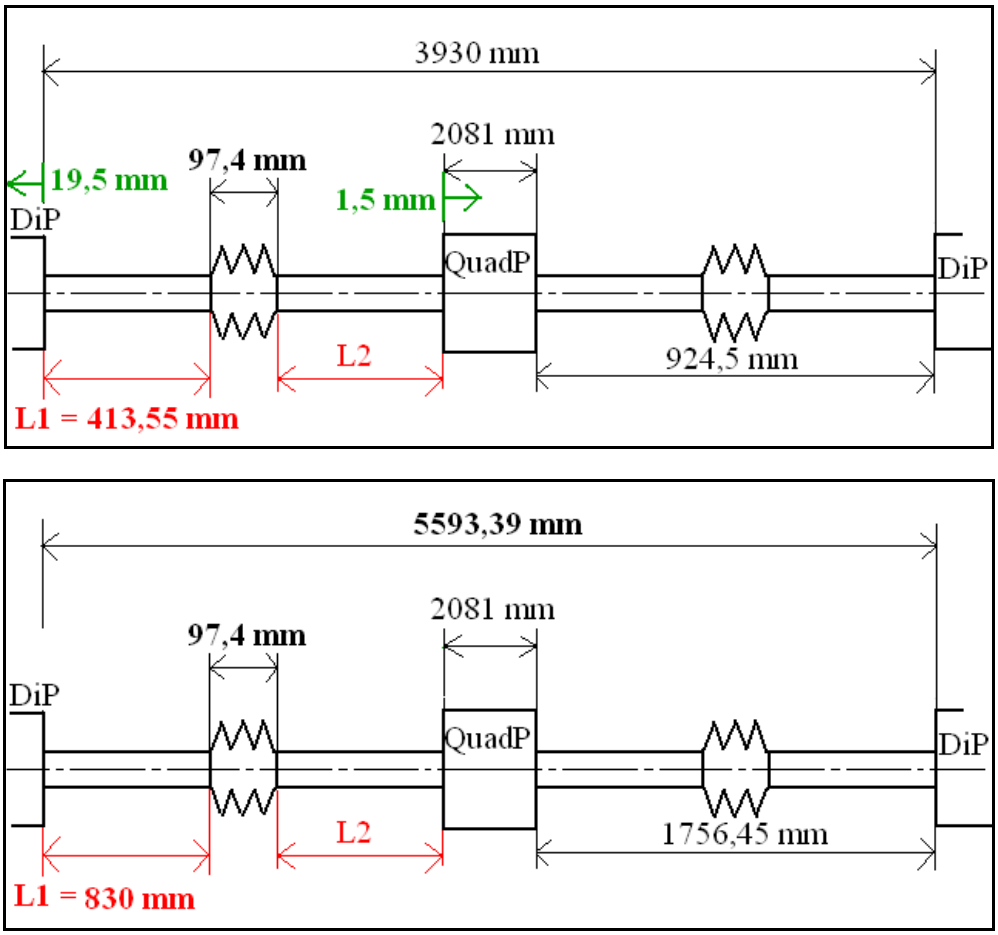

Fig. 4.7 New configuration of interconnections dipole-quadrupole-dipole

The length of the interconnections (~0.92 m and ~1.8 m) falls beyond the safe zone computed in the previous chapters (Chapter 2, Chapter 3). In particular, maximum safe distance (L_1 , L_2) between the bellows extremities and the magnet heads, obtained for the thickness of tubes of 2 mm, reached some 200 mm. Given the length of expansion joint of around 100 mm, the total safe length of single interconnect should not exceed some 500 mm. In the light of this fact, the current length of interconnections implies an additional measure of safety in order to obtain stable functioning during the cool-down, warm-up and standard operation of the accelerator. One possible way out is increase of thickness of the linking tubes. The maximum safe distance (L_1 , L_2) as a function of thickness of linking tubes is presented in Table 4.2.

Table 4.2: maximum safe distance versus thickness of linking tubes

Thickness of linking tubes [mm]	**Maximum safe distance (L_1 , L_2) [mm]**
2	220
3	255
4	289
8	~350

From this analysis it is clear that the stability measures based on thickness of linking tubes are insufficient, both in the case of shorter interconnect and in the case of longer interconnect. In addition, the influence of initial geometrical imperfections (Fig. 4.8) has been calculated and the results are presented in Fig. 4.9. The imperfection of size “e” is compatible either with mode I instability (symmetric case) or with mode II instability (asymmetric case; Fig. 4.8). It is worth pointing out that mode II imperfection is easily obtained due to the misalignment of the magnets and is particularly harmful in the case of long interconnections.

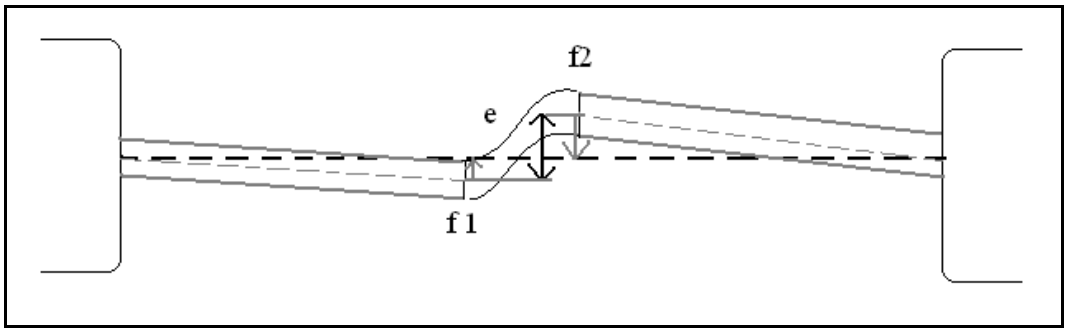

Fig. 4.8 Initial geometrical imperfections (transverse offset)

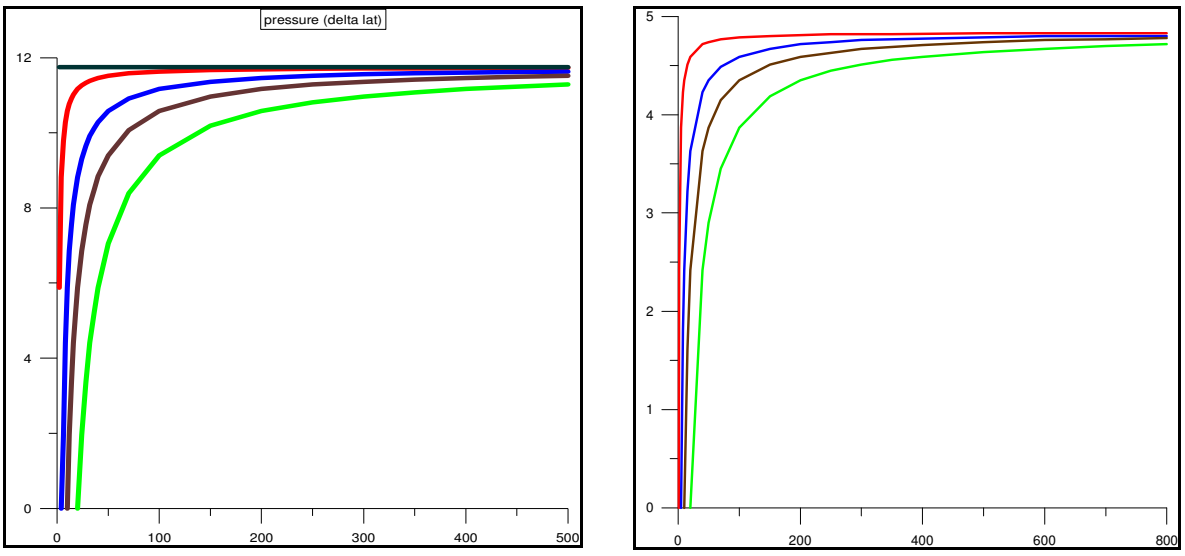

Fig. 4.9 Influence of imperfections (left: L_1=300 mm; right: L_1=700 mm)

The curves depicted in Fig. 4.9 reflect pressure as a function of transverse displacement (deflection) for a given value of initial imperfection (red: e=1 mm, blue: e=5 mm, black: e=10 mm, green: e=20 mm). For the system with imperfections an important factor is defined by the ratio between the initial offset (imperfection) and maximum allowable transverse deflection $e/\Delta_{\max}$. The load associated with the allowable deflection can be computed by using the following formula:

$$P_{all} = \left(1 - \frac{e}{\Delta_{\max}}\right) P_{bif} \tag{4.8}$$

where P_{bif} denotes the bifurcation buckling load computed for the system without initial imperfection (Chapters 2 and 3). Stability diagram computed for the ratio $e/\Delta_{\max}$ equal to 0.0; 0.25 and 0.5 is presented in Fig. 4.10. Thus, the allowable load (pressure) for $e/\Delta_{\max} = 0.25$ is equal to 0.75% of the bifurcation buckling load for the interconnect without imperfections.

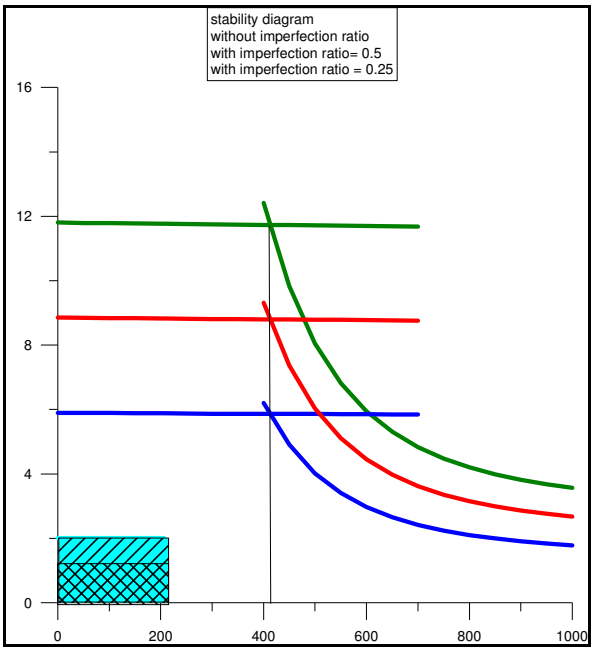

Fig. 4.10 Stability diagram corrected for the influence of imperfections

Both sensitivity analysis with respect to the thickness of linking tubes and sensitivity analysis with respect to the initial imperfections lead to the conclusion that in the case of long interconnections a special hardware conceived to improve their stability has to be implemented. A concept of such hardware is presented in Fig. 4.11. The principle is based on a coupling between all the interconnects (Fig. 4.12) provided by a circular plate carrying locks for the linking tubes, installed in the middle of each interconnection slot (preferably close to the extremities of bellows expansion joints). In the case of interconnections 1.8 m long two stabilising plates should be installed on either side of the expansion joints and should be connected to each other by means of rigid rods in order to create a stabilising cage. The concept of such cage has been illustrated in Fig. 4.13. Both hardware components are sufficient to provide enough stability to the interconnections nearly twice (0.92 m) or nearly four times (1.8 m) longer than the safe length without any hardware (0.5 m).

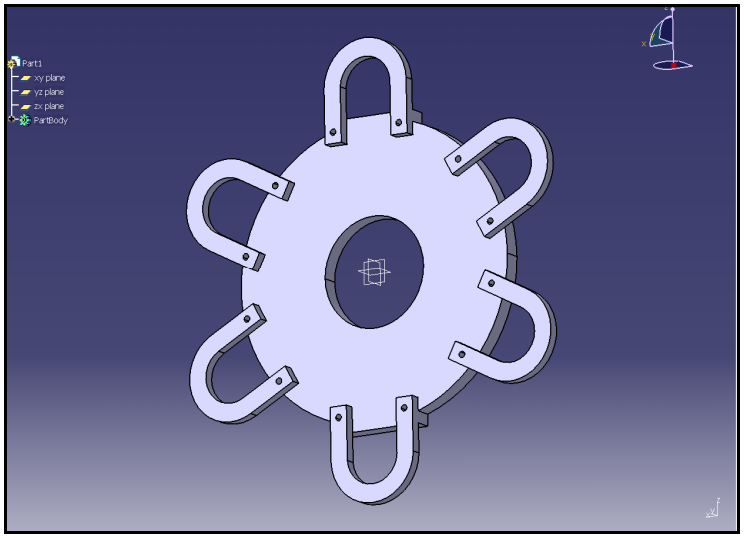

Fig. 4.11 Hardware designed to stabilise the interconnections (0.92 m long)

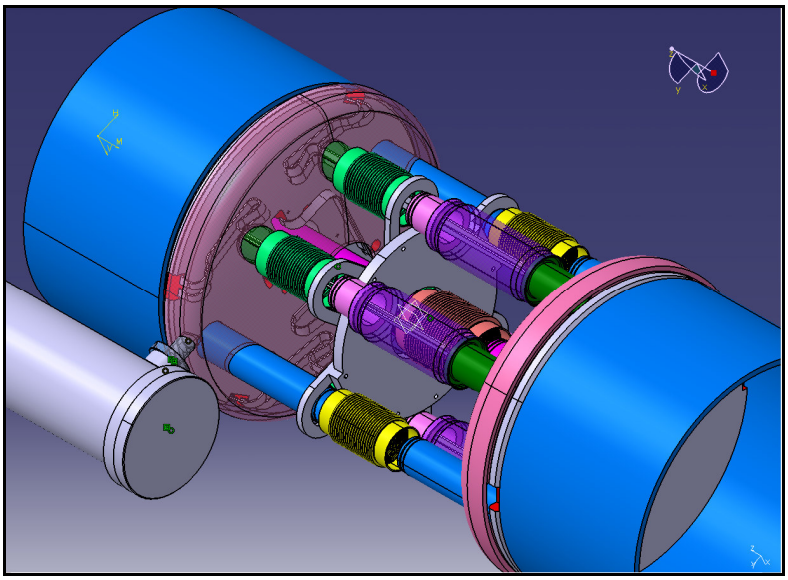

Fig. 4.12 Stabilising plate in the middle of interconnections

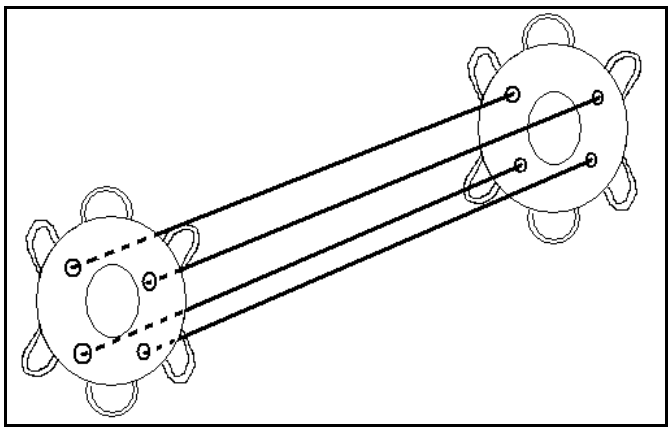

Fig. 4.13 A concept of hardware to stabilise long interconnections (1.8 m long)

4.5 Finite Element Model – analysis of transverse deformation

In order to analyse transverse motion due to the cool-down, warm-up and alignment processes of SIS300 standard cell supported by cold feet and connected by means of interconnection systems a finite element model of the cell has been created (Figs 4.14, 4.15, 4.16):

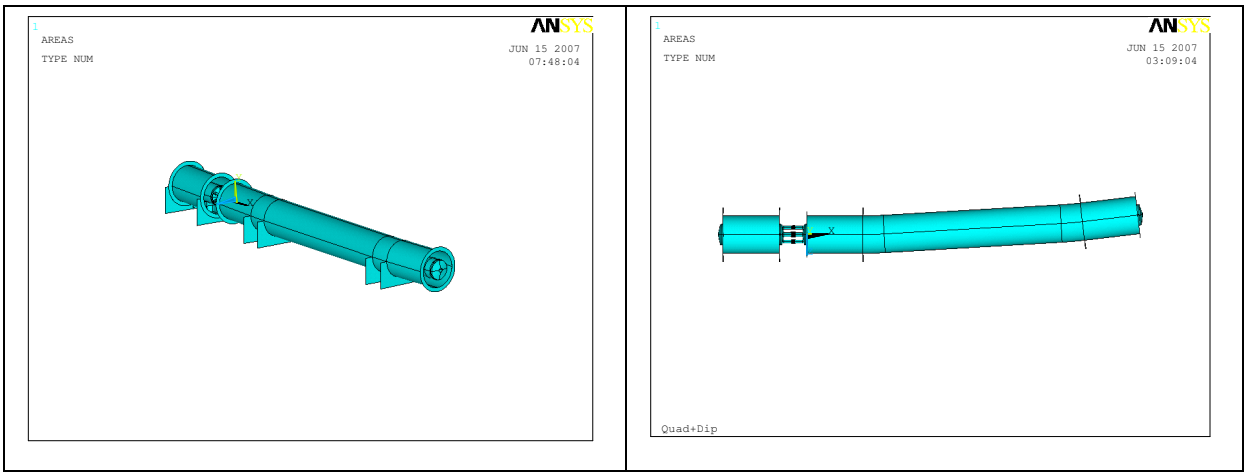

Fig. 4.14 Finite element model of SIS300 lattice (one cell)

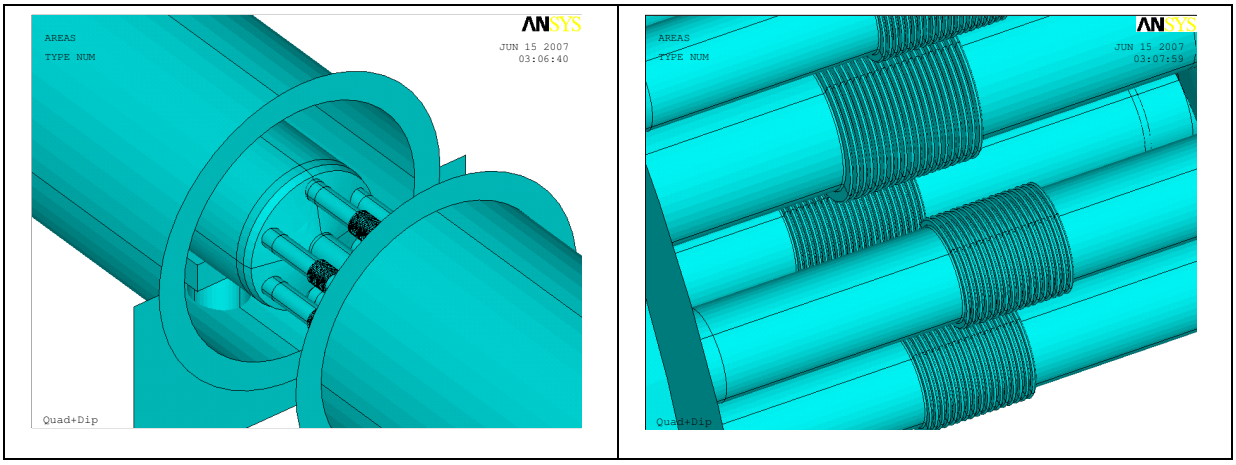

Fig. 4.15 View over the interconnections (short version)

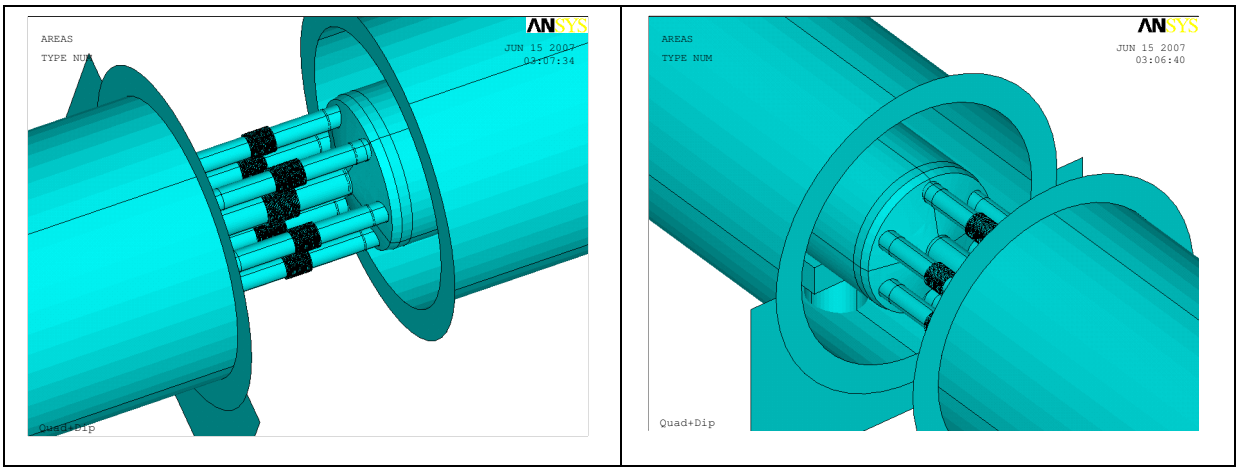

Fig. 4.16 View over the interconnections

4.6 Conclusions

a. New lattice based on FODO principle implies longer interconnections when compared to the previous lattice version. The length of 0.92 m and 1.8 m falls beyond the safe distance between the bellows extremities and the magnet heads. Therefore, in order to avoid semi-global instability (catastrophic behaviour) a specific hardware has to be installed in the middle of interconnections.

b. The magnets can be supported on 2 composite supports (cold feet), one of them fixed and the other one sliding in the longitudinal direction. The average linear stiffness of supports, represented by the elastic foundation, equal to 4 N/mm^2 is sufficient and provides the safety factor of around 20 w.r.t. the design pressure. The stiffness of supports corresponds to the assumption of 0.5 mm transverse deflection (per support) under the transverse load of 10^4 [N].

c. The MQ-MB and MB-MQ interconnections will be loaded in a different way during the cool-down and warm-up process. This is due to the asymmetric layout of fixed and sliding supports. Nevertheless, the same set of expansion joints can be applied in both types of interconnections (unification principle).

5 Layout of magnetic components and interconnections in the SIS300

5.1 New lattice of SIS300

New SIS300 FODO lattice is based on principle of periodic structure composed of alternating focusing and defocusing quadrupoles. The quadrupoles are separated by long dipole magnets in the arc and – at one location in the arc extremities – by short dipoles (Fig. 5.1, cf. P. Spiller, miniTAC Lattices, 5/06/07). For what concerns the correction scheme it is composed of dipole orbit correctors (the horizontal/vertical steerers), located next to the quadrupoles in the long slot between main dipoles and the chromaticity sextupoles located next to the quadrupoles in the short slot between the dipoles. It is worth pointing out, that an optional higher order corrector can be located in the long slot between main dipoles. For beam positioning purpose, each main quadrupole is accompanied by the suitable beam position monitor (BPM). The correction scheme is presented in Fig. 5.2 (cf. P. Spiller, miniTAC Lattices, 5/06/07).

. In order to determine spatial configuration of the lattice magnetic components the following assumptions were made:

1. the minimum length of drift space between the magnets needed for the interconnection systems is equal to 500 mm,
2. the length reserved for the correction elements in the technical description of SIS300 (FAIR Technical Report) is equal to 750 mm,
3. the space next to short dipole in the arc extremity has been filled with the so called connection cryostat containing a dummy cold mass.

In order to cope with the position of main dipoles determined by the synchrotron optics, the correctors have to be integrated in the cold mass together with main quadrupoles, thus, forming sufficiently compact units. In addition, the beam position monitors shall be located in the interconnections. They are partially embedded in the quadrupole cold mass and their total length should not exceed 400 mm (250 mm outside the cold mass). Under these assumptions, the currently designed optics can be maintained.

The general view over the position of main magnets, correction elements and BPMs is given in Fig. 5.3. The plot presents both the main arc with long dipoles and the arc extremity with short dipole. The magnetic elements are contained in the continuous cryostat composed of vacuum vessels allocated to each separate magnet and flexible connections in the form of large corrugated sleeves. Arc extremity ends with the cryostat head and suitable cold-warm transition. Because of pressure loads, last vacuum vessel and the related quadrupole have to be correctly supported in order to carry enhanced longitudinal loads.

In order to present the layout of components in detail, the arc and the arc extremity were subdivided into portions, called assemblies of type A through E.

5.2 Basic assemblies

Assembly type A (Fig. 5.4) includes longer slot between the main dipoles. It contains chromaticity sextupole combined with main quadrupole and orbit corrector (steerer). It is equipped with longer symmetric interconnections, stabilized by means of special inserts (cf. Chapter 4).

Assembly type B (Fig. 5.5) includes short slot between the main dipoles. The main quadrupole is combined with the chromaticity sextupole. The interconnections have minimum length of 515 mm.

Assembly type C (Fig. 5.6) contains combined main quadrupole and orbit corrector (steerer). The quadrupole is flanked on one side by the short interconnection to the so called connection cryostat and, on the other side, by long interconnection to main dipole. Long interconnect needs stabilization by means of special insert. At one location in the synchrotron the connection cryostat will be replaced by a suitable cryogenic module.

Assembly type D (Fig. 5.7) contains short dipole combined with the error correction multipole flanked by short interconnections to main quadrupole and to the connection cryostat, respectively.

Assembly type E (Fig. 5.8) contains orbit corrector (steerer) combined with main quadrupole and extraction sextupole. It is the last component in the continuous cryostat. The continuous cryostat is closed by dished head containing the cold-warm transition (CWT). As this is last unit in the sequence of continuously cryostated magnets, special care has to be implemented in order to correctly support this component (against pressure loads).

5.3 General common features

The following common features were assumed for all the components in the continuous cryostat:

1. each component (cold mass portion) is supported by means of 2 supports: fixed and sliding,
2. each component is thermally shielded by using a continuous actively cooled thermal shield wrapped with super-insulation (MLI blankets),
3. each component is connected with its neighbours by means of the interconnection systems,
4. the vacuum vessels are connected by using flexible (corrugated) sleeves providing continuity of insulation vacuum and necessary flexibility for alignment.

A connection between the combined quadrupole/corrector and main dipole magnet and the way of supporting the magnets in the vacuum vessel are shown in Figs 5.9 & 5.10.

5.4 Optimum layout of supports

Accepting the principle of two supports per magnet (Chapter 4) – one of them fixed and the other sliding – an optimum layout of supports in the continuous cryostat has to be determined. The criterion remains reaching a minimum of the functional of elastic energy of the system. This is fundamental for the process of initial alignment of synchrotron. The elastic energy is given by the following formula:

$$E_{el} = \frac{1}{2}\int_V \underline{\underline{\sigma}} : \underline{\underline{\varepsilon}} dV = \frac{1}{2}\int_V \left(\underline{\underline{\underline{\underline{E}}}} : \underline{\underline{\varepsilon}} \right) : \underline{\underline{\varepsilon}} dV$$

where $\underline{\underline{\varepsilon}}$ denotes the strain tensor being a function of displacement field $\underline{u}$:

$$\underline{\underline{\varepsilon}} = \underline{\underline{\varepsilon}}(\underline{u})$$

In order to find a displacement field that would correspond to point of minimum of elastic energy potential, one sets:

$$\min(E_{el}) = \min|_{\underline{u}} \left(\frac{1}{2} \int_V \left(\underline{\underline{\underline{E}}} : \underline{\underline{\varepsilon}}(\underline{u}) \right) : \underline{\underline{\varepsilon}}(\underline{u}) dV \right)$$

For uniform distribution of weight, solution to this problem is obtained via the following equation:

$$\eta^3 - 3\eta + \frac{5}{4} = 0 \quad ; \quad \eta = \frac{2a}{L}$$

where *a* denotes the distance of support from the magnet end, whereas *L* is the length of the magnet. Based on this equation an optimum value for η is obtained:

$$\eta = 0.446 \quad ; \quad a = 0.223L$$

The optimum distance of supports from the magnet ends as a function of its length is given in Table 5.1:

Table 5.1 Optimum position of supports w.r.t. magnet ends

Magnet length (*L*)	Optimum position of supports (*a*)
2.5 m	0.56 m
3.3 m	0.74
5.35 m	1.2 m
8.5 m	1.9 m

Thus, the vertical deflection of the cold mass has been minimized. Here, a simplified assumption of uniform mass distribution along the cold mass axis has been made. In case of non-uniform distribution of the mass (which is closer to reality) a suitable correction on the position of the supports can be made. Another correction important from the point of view of loss of aperture is related to the length of interconnections. In the worst case the length of interconnections is equal to 1546 mm. Given the angular deflection (slope) of the magnet extremity, transverse deflection in the middle of interconnections induced by the slope is equal to around 0.15 mm. This is negligible with respect to other misalignment errors and does not compromise the required aperture. The layout of supports for all three cases is shown in Figs 5.11 and 5.12.

5.5 Conclusions

- The feasibility study of SIS300 topology based on the current version of synchrotron optics has been carried out. As a result of the study an optimum layout of the synchrotron components has been found.

- The structure (arc and arc extremity) of the synchrotron has been subdivided into a set of assemblies (A through E). Each of them presents a view over different configuration of magnetic elements and their interconnections.
- The dipole orbit correctors (steerers), chromaticity sextupoles and BPMs were integrated together with main quadrupoles to form confined portions of the cold mass.
- Two types of interconnections were identified: short interconnects (self-stable) and long interconnects that need a dedicated stabilization hardware.
- Optimum layout of supports has been computed for all magnets and the connection cryostat, in order to minimise the flexure of magnets and not to compromise the geometric aperture.

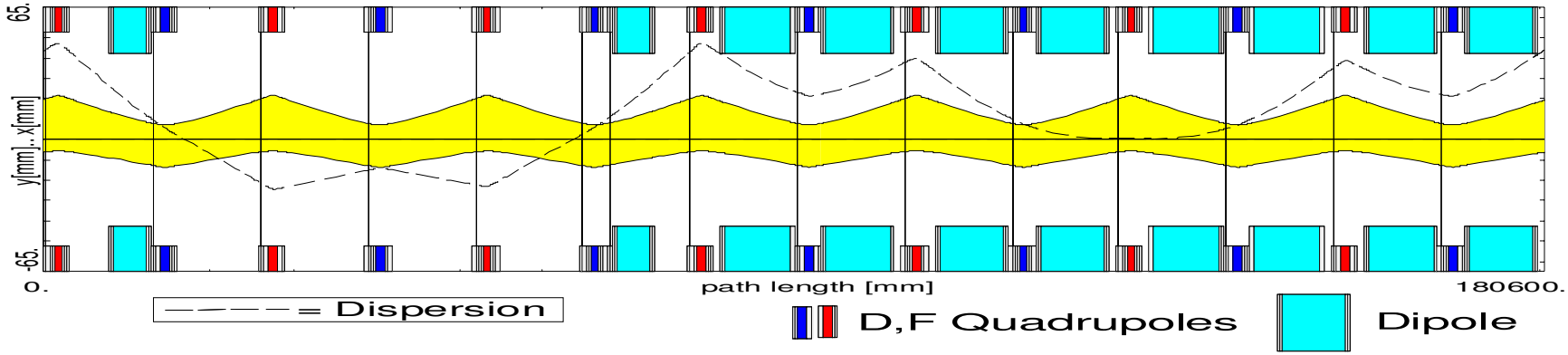

Fig. 5.1 FODO lattice for SIS300 synchrotron (source: P. Spiller, miniTAC lattices)

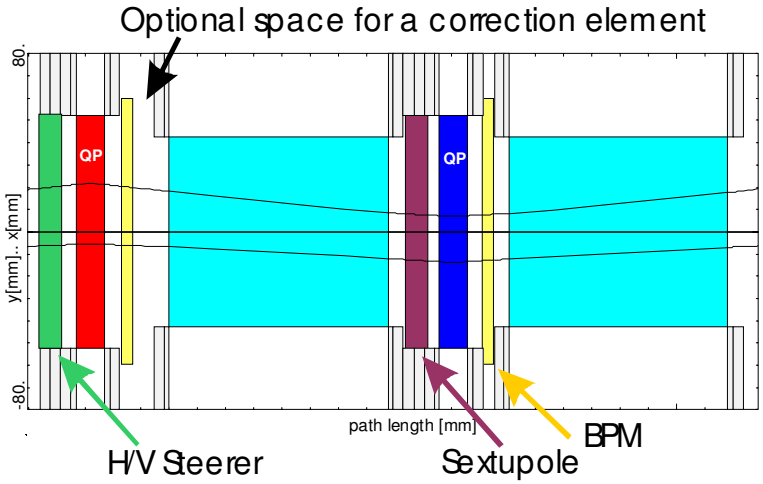

Fig. 5.2 Corrector layout for SIS300 FODO lattice (source: P. Spiller, miniTAC lattices)

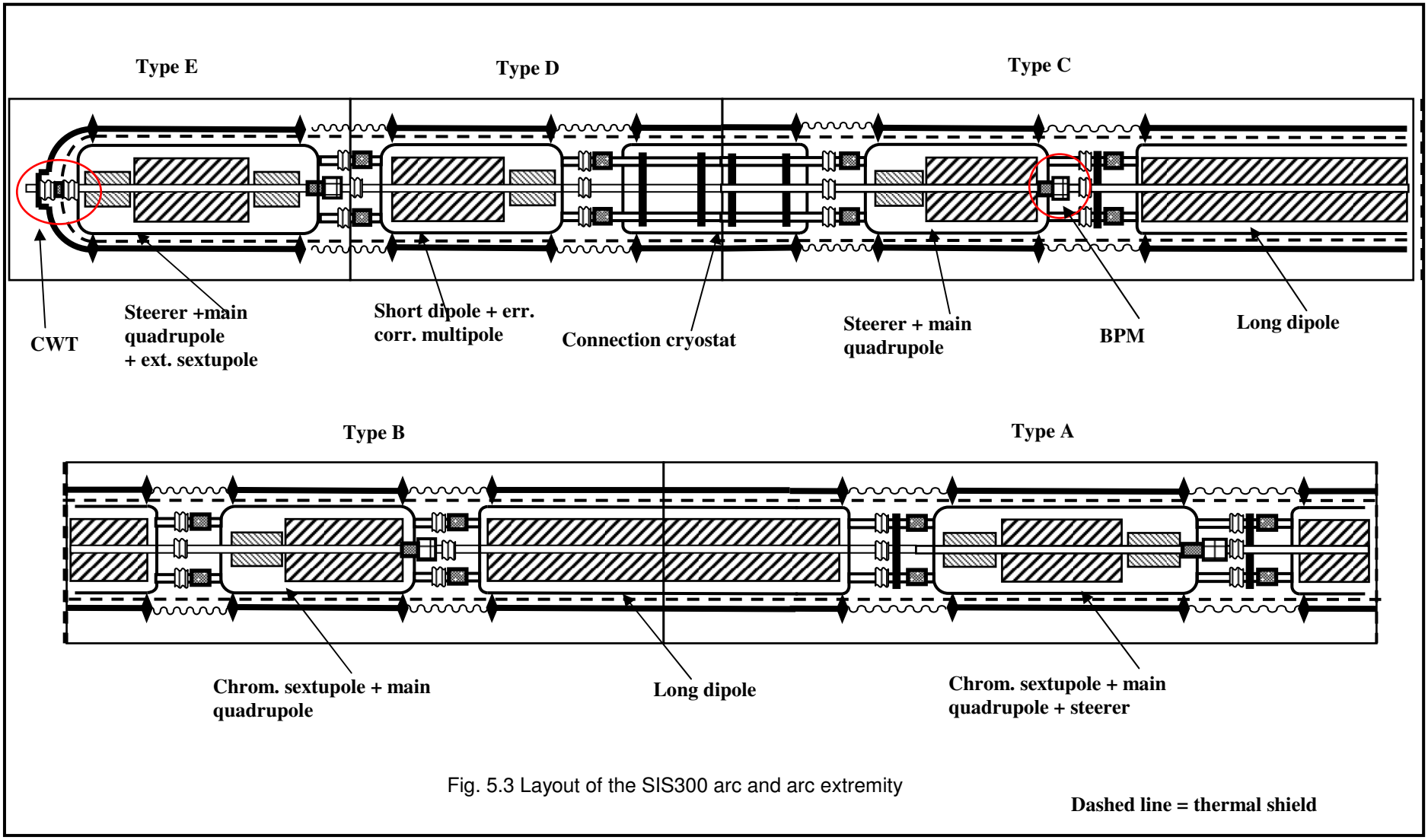

Fig. 5.3 Layout of the SIS300 arc and arc extremity

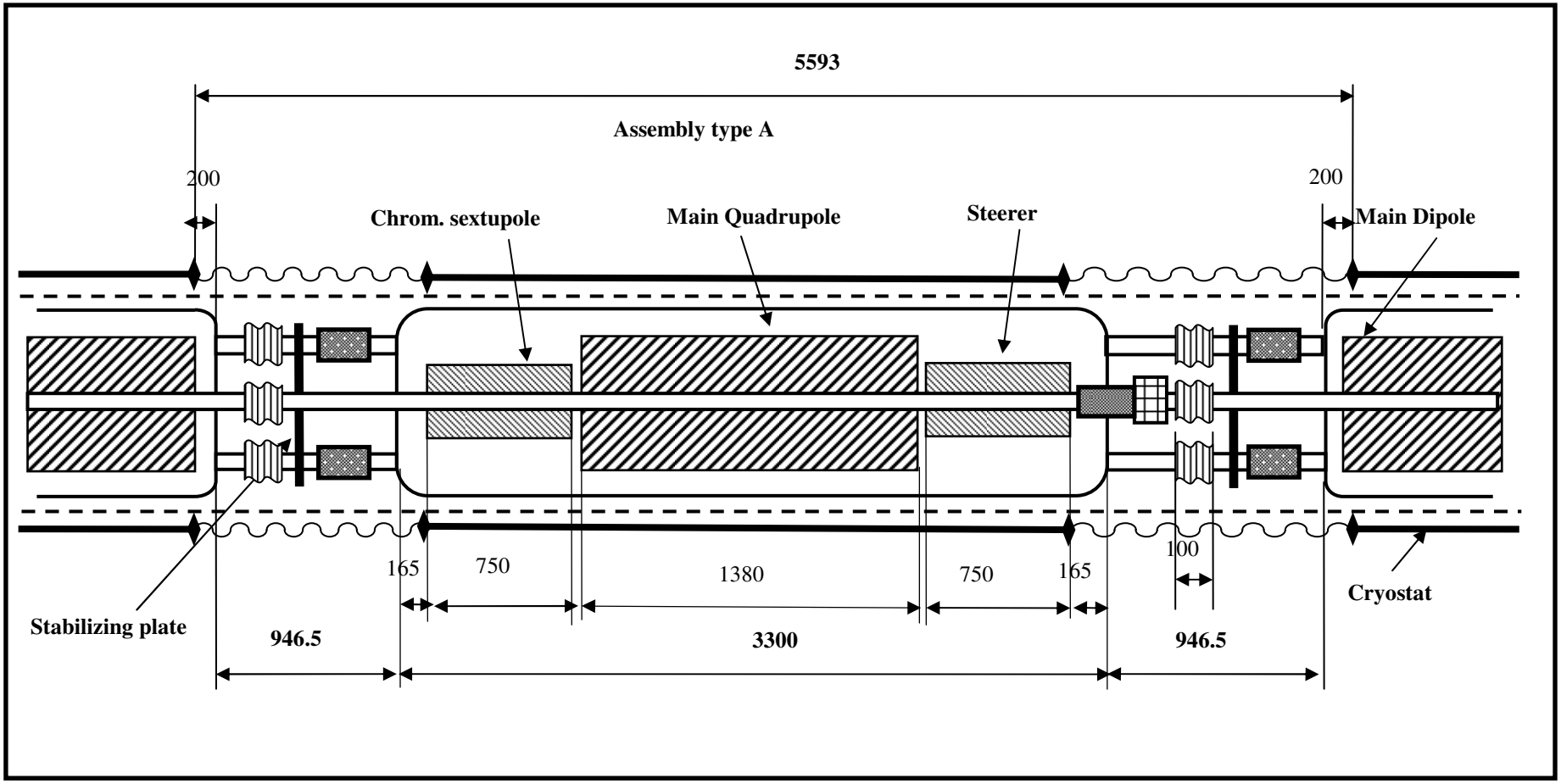

Fig. 5.4 Layout of the FODO lattice components for SIS300
Longer interconnections

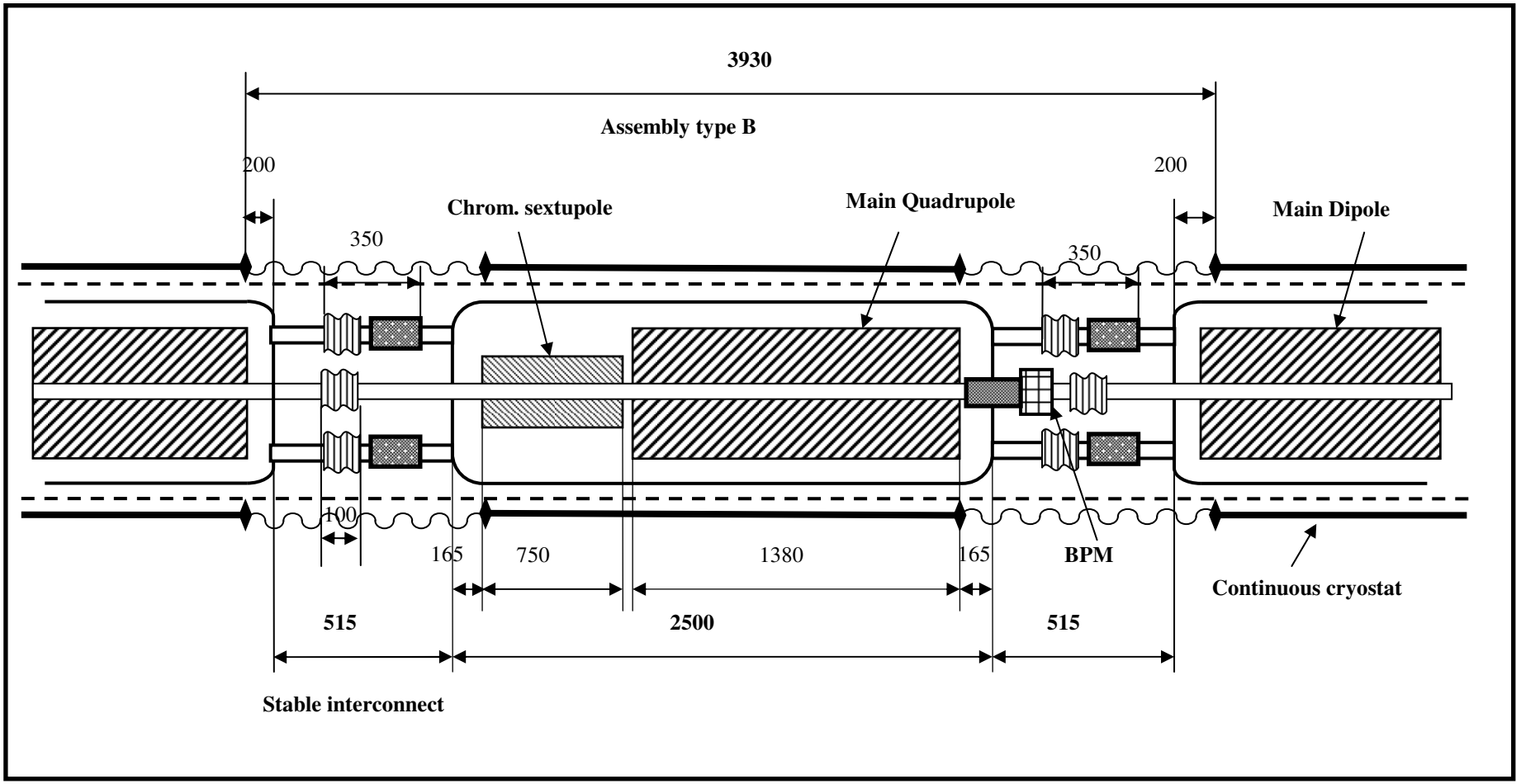

Fig. 5.5 Layout of the FODO lattice components for SIS300
Short interconnections

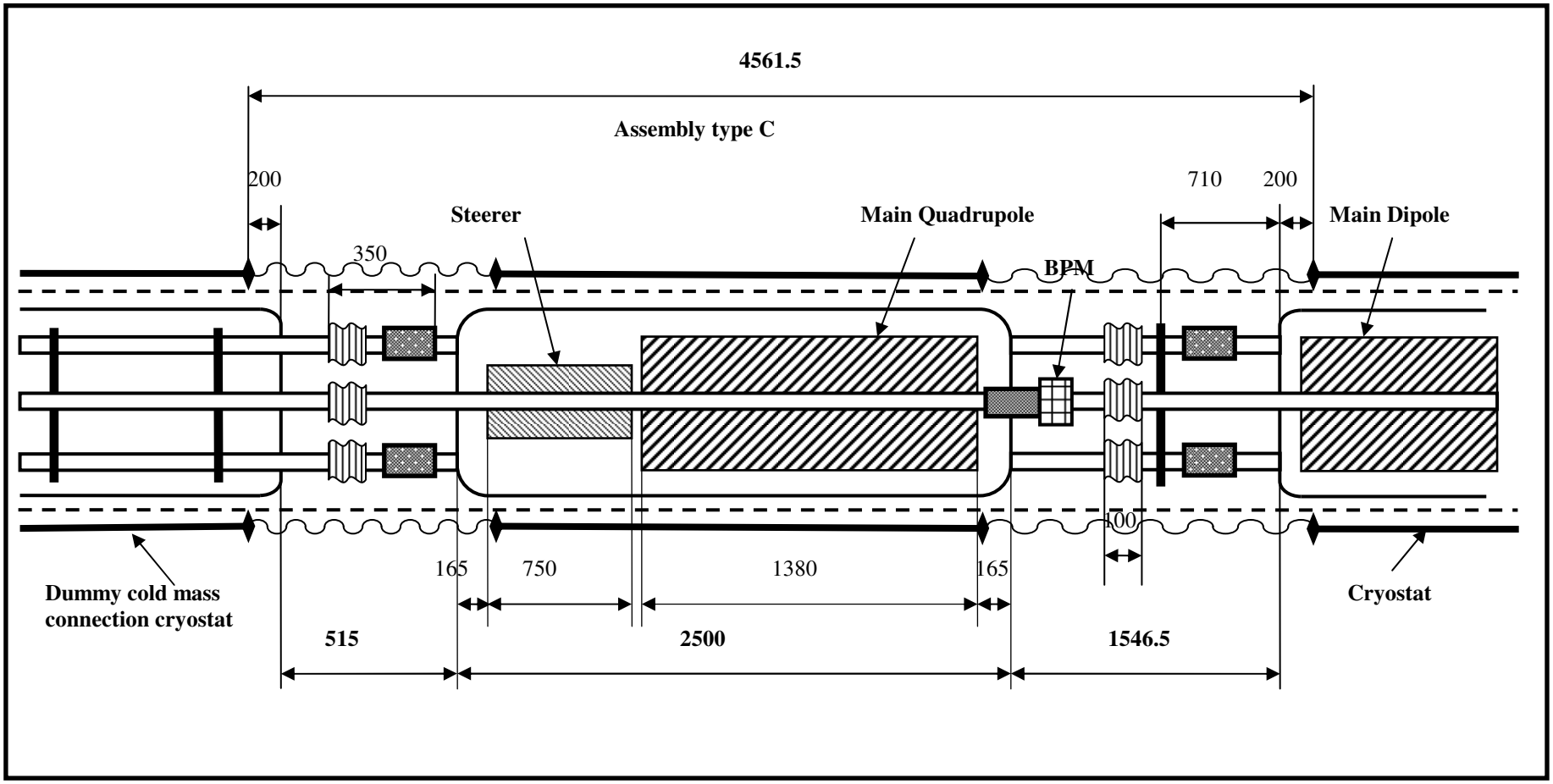

Fig. 5.6 Layout of the FODO lattice components for SIS300
Arc extremity

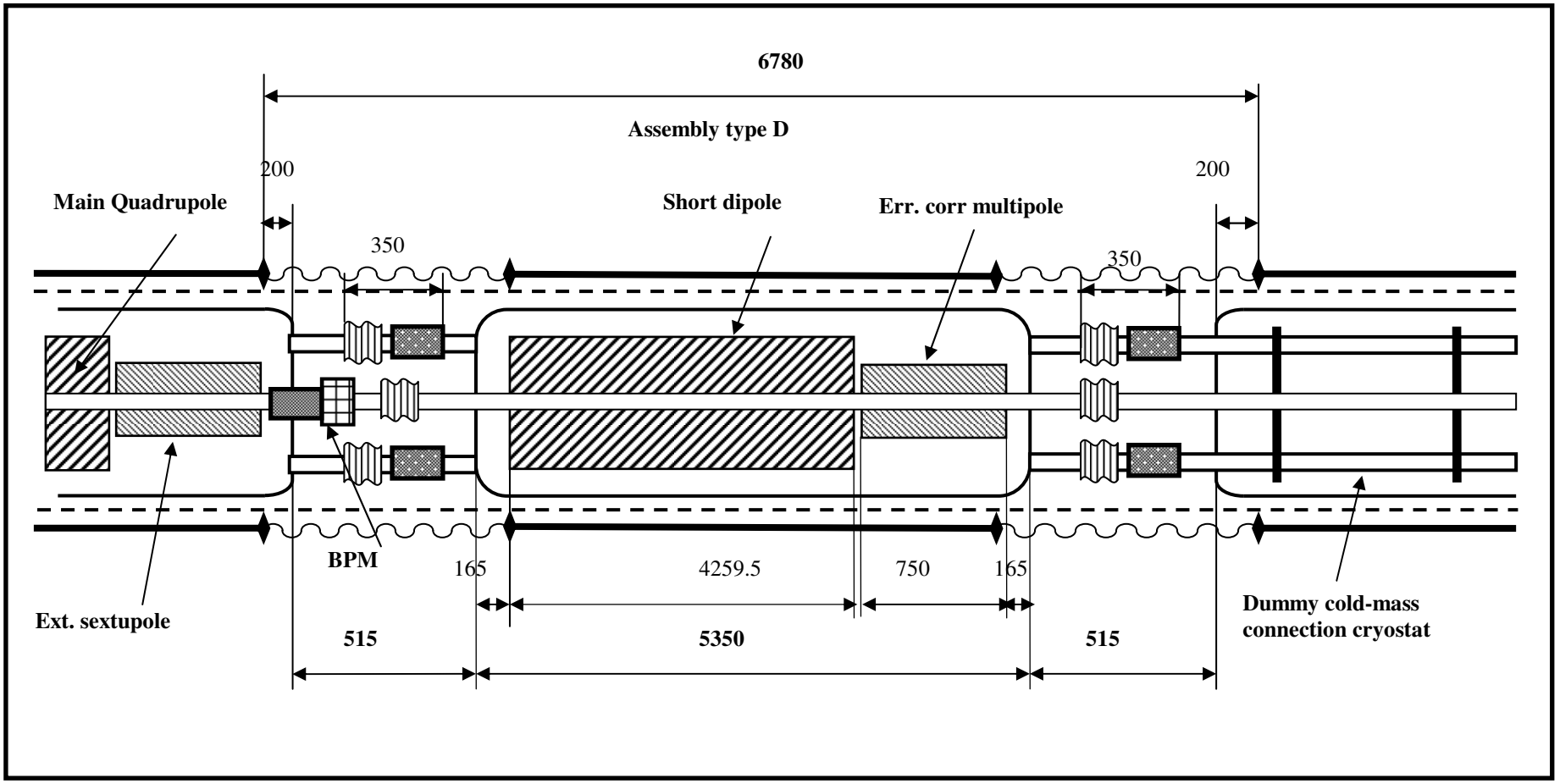

Fig. 5.7 Layout of the FODO lattice components for SIS300
Arc extremity

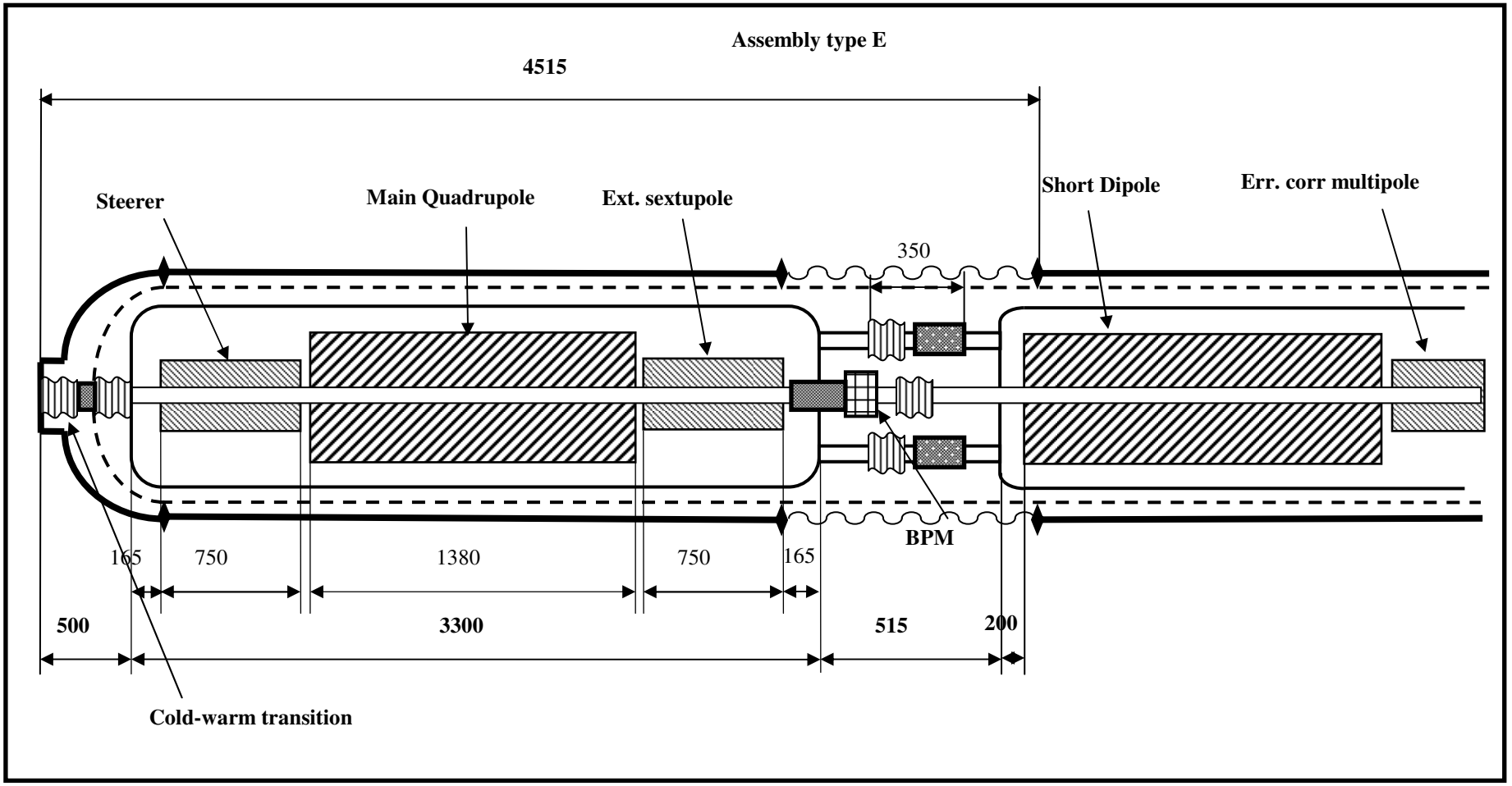

Fig. 5.8 Layout of the FODO lattice components for SIS300
End of the arc

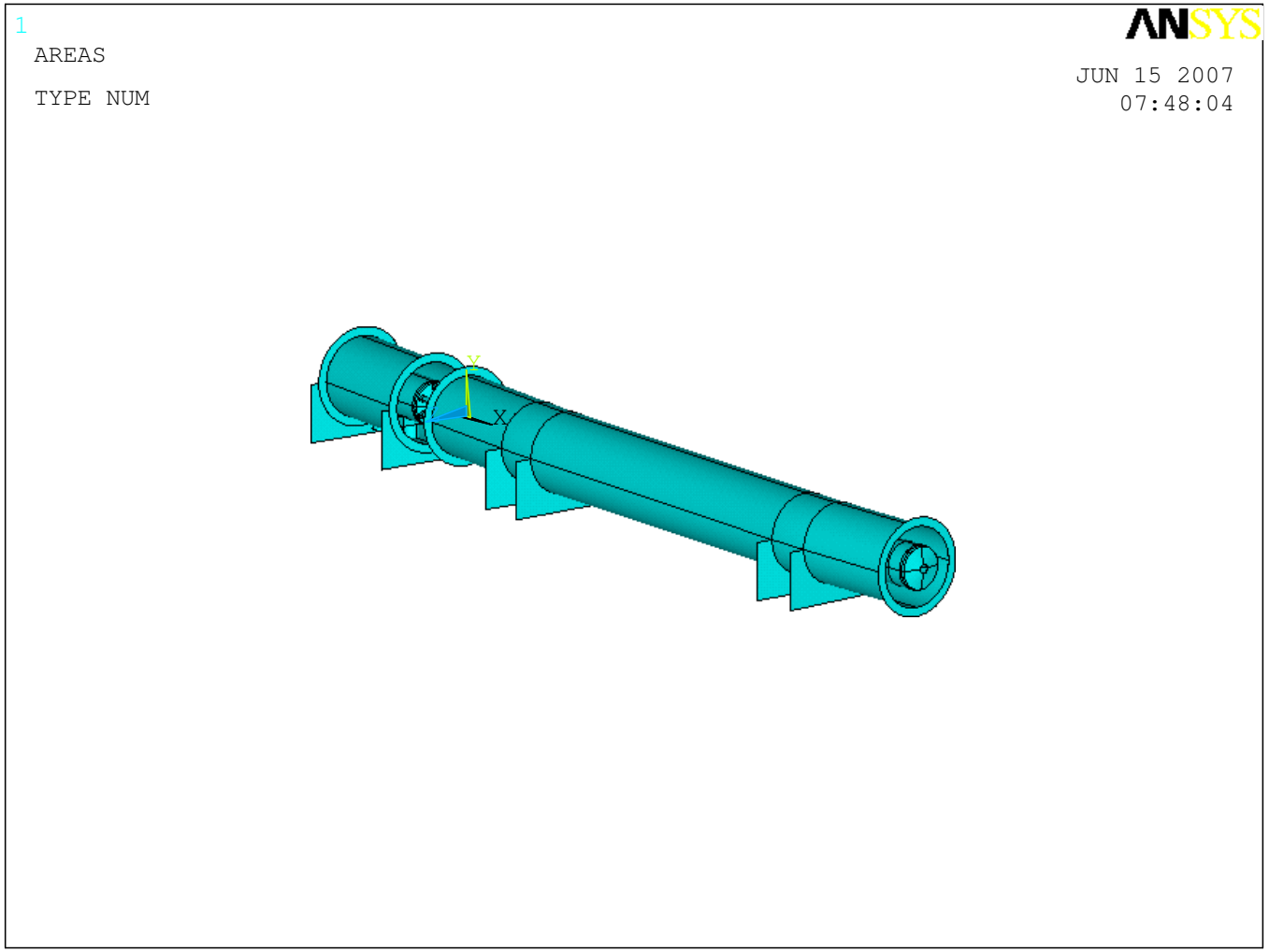

Fig. 5.9 Main quadrupole/ corrector – main dipole connection

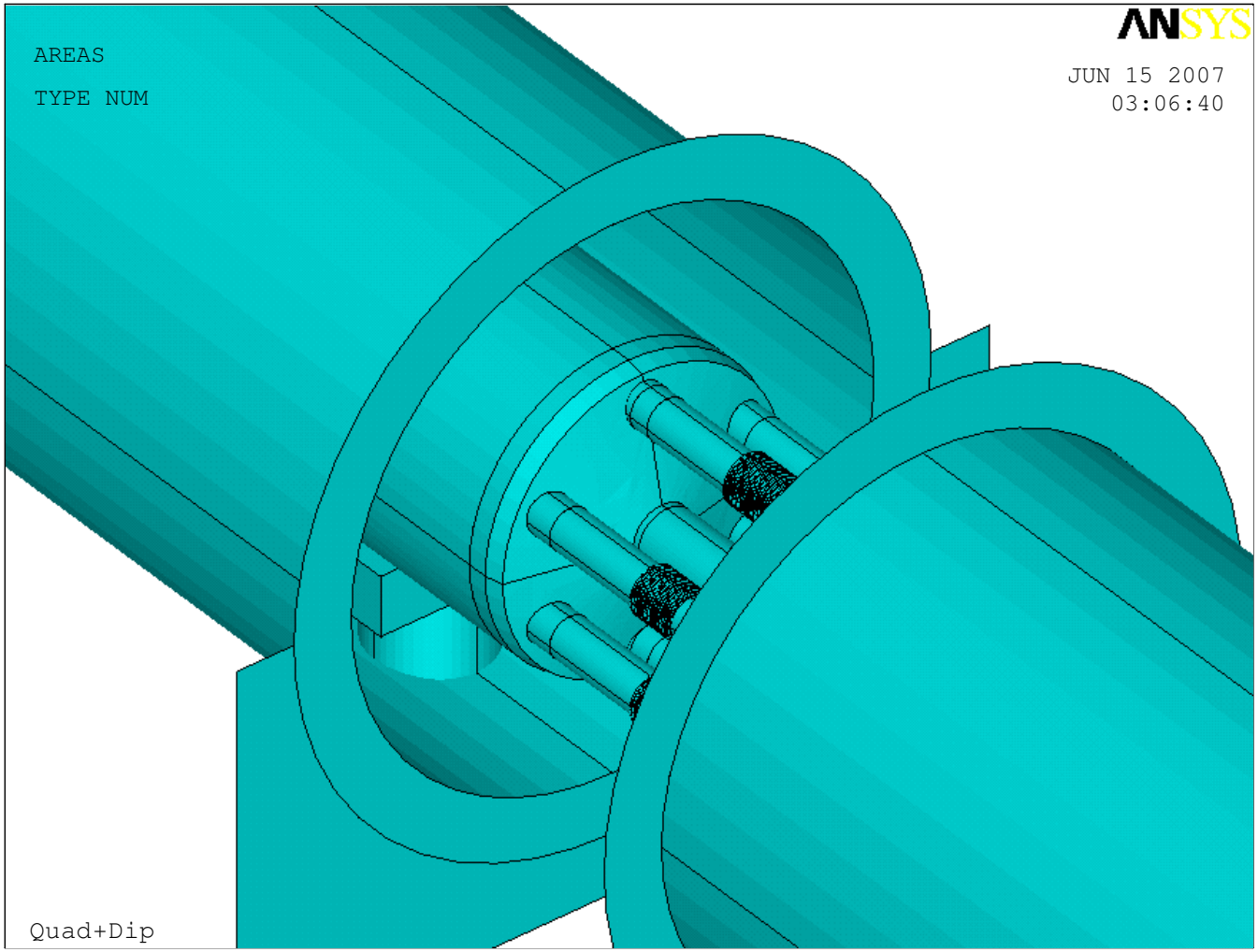

Fig. 5.10 Interconnection details

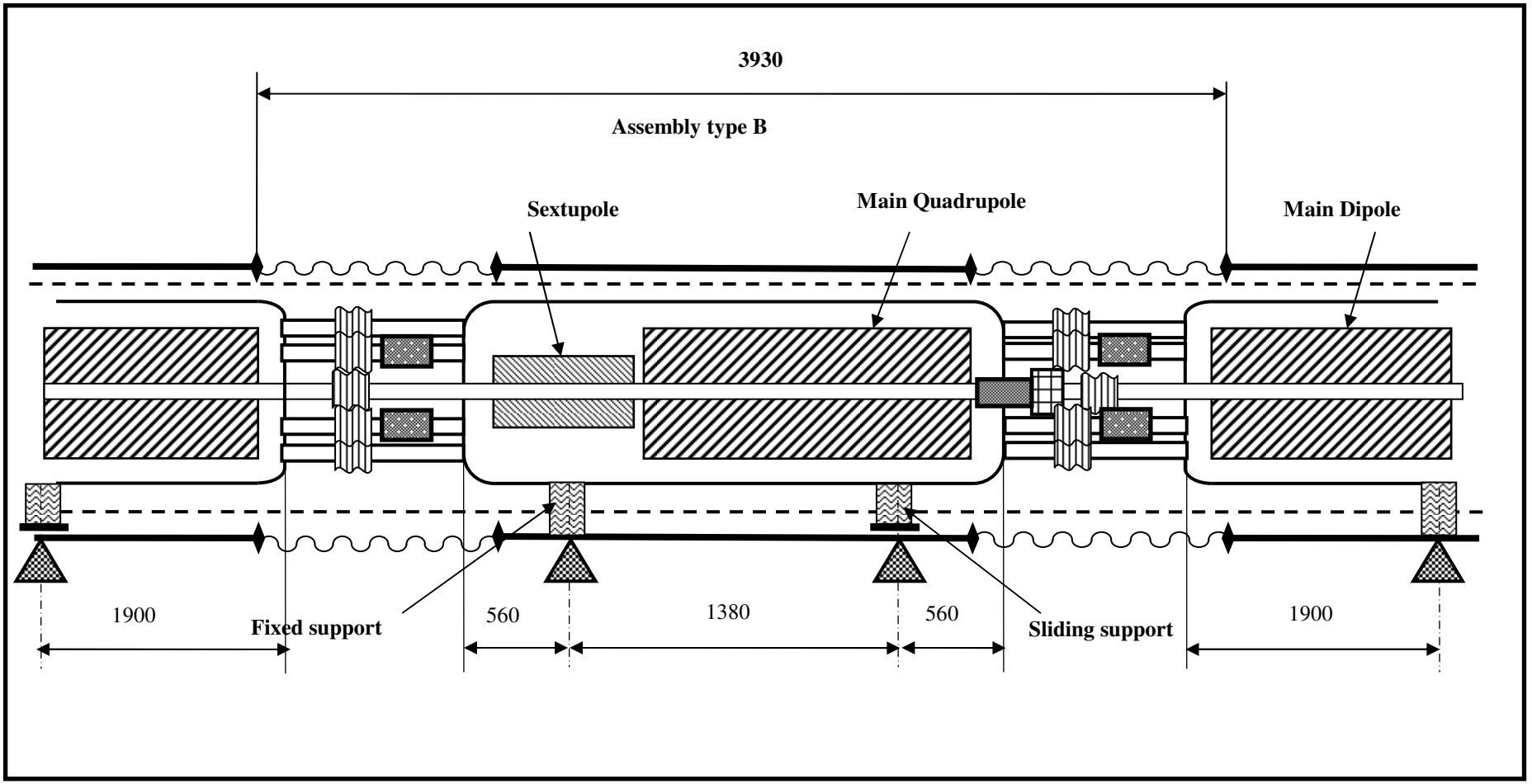

Fig. 5.11 Location of fixed and sliding supports – side view (main quadrupole & long dipole)

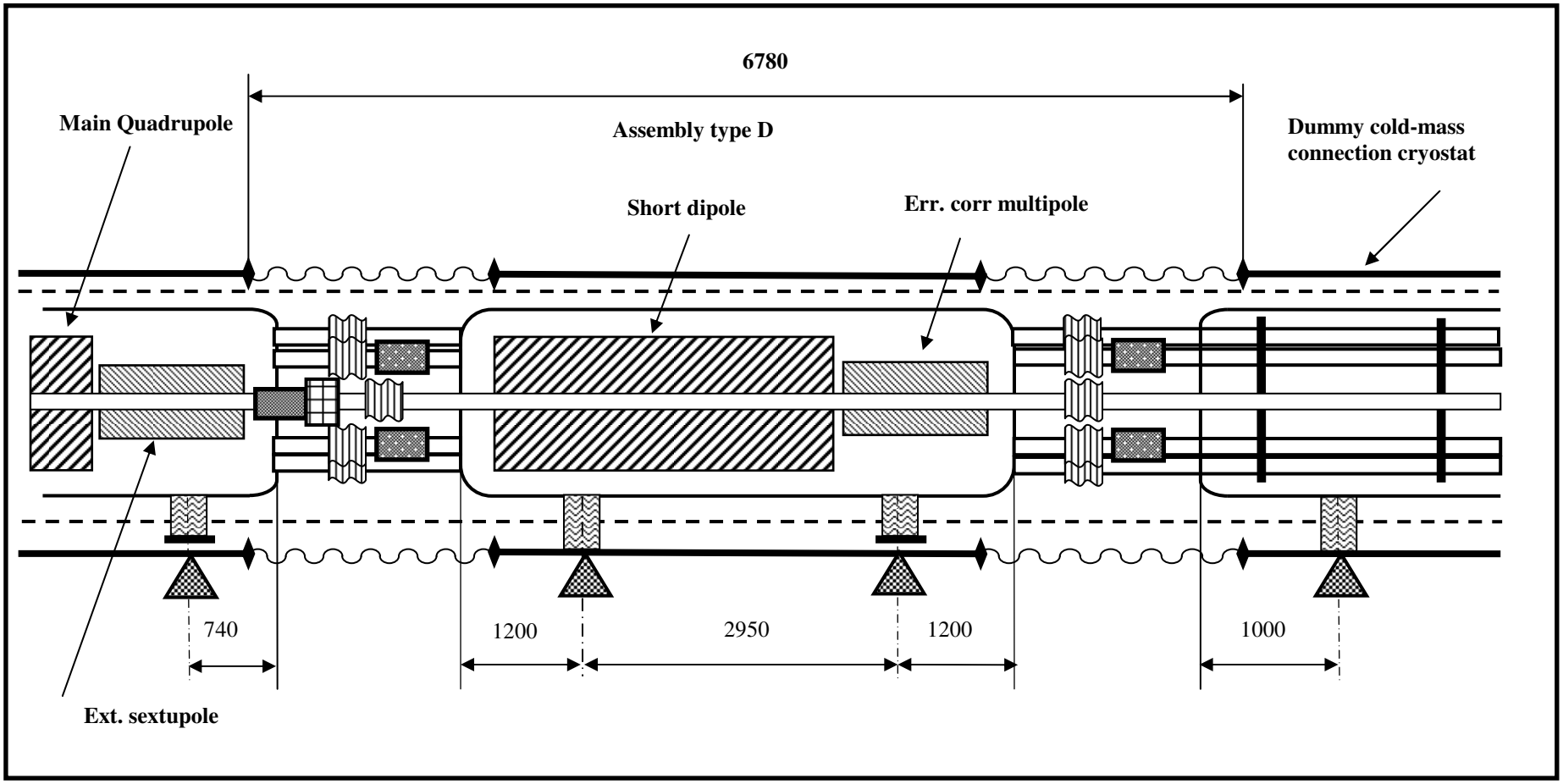

Fig. 5.12 Location of fixed and sliding supports – side view (short dipole)

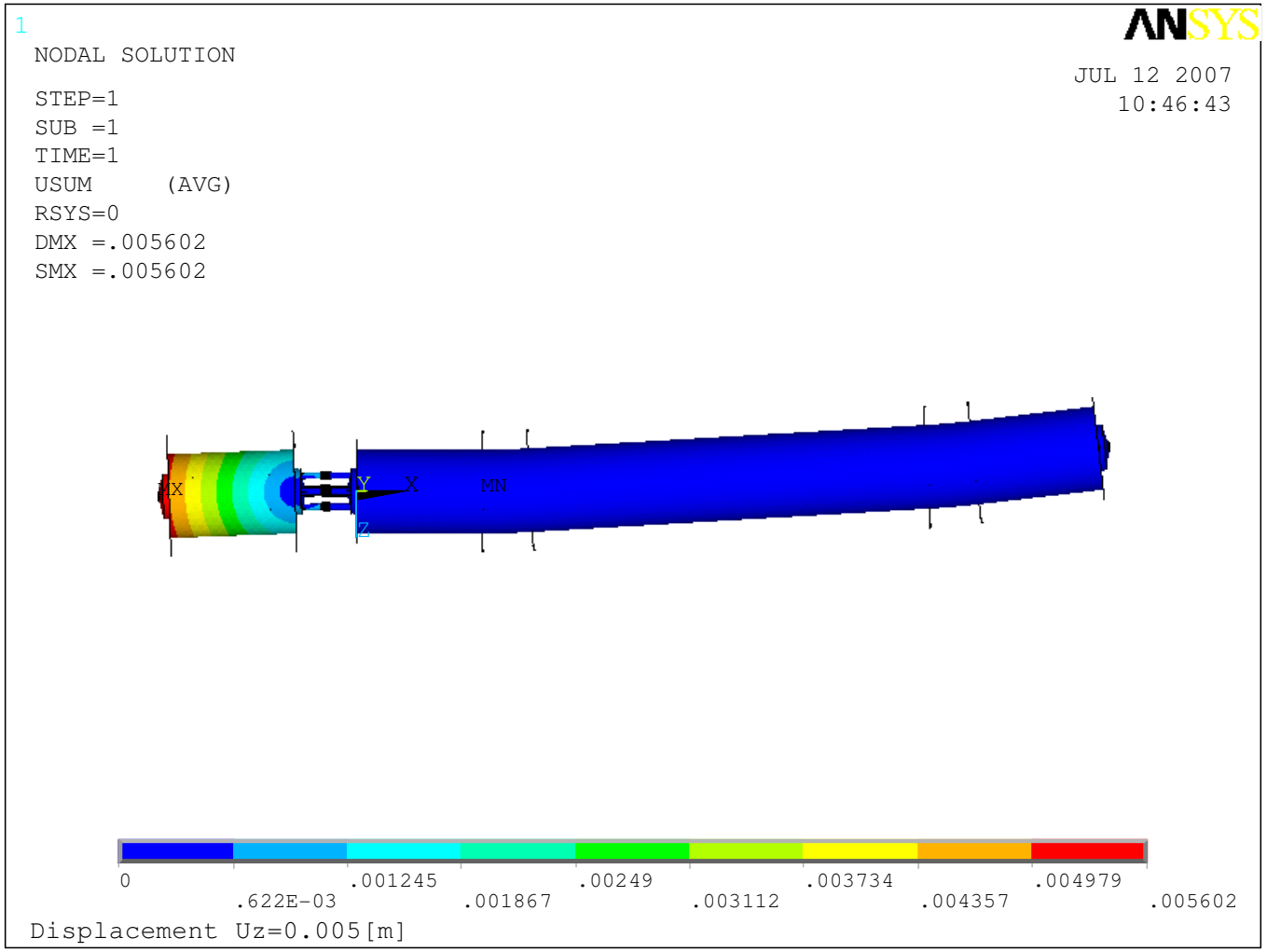

Fig. 5.13 Alignment of main quadrupole with respect to dipole (displacements)

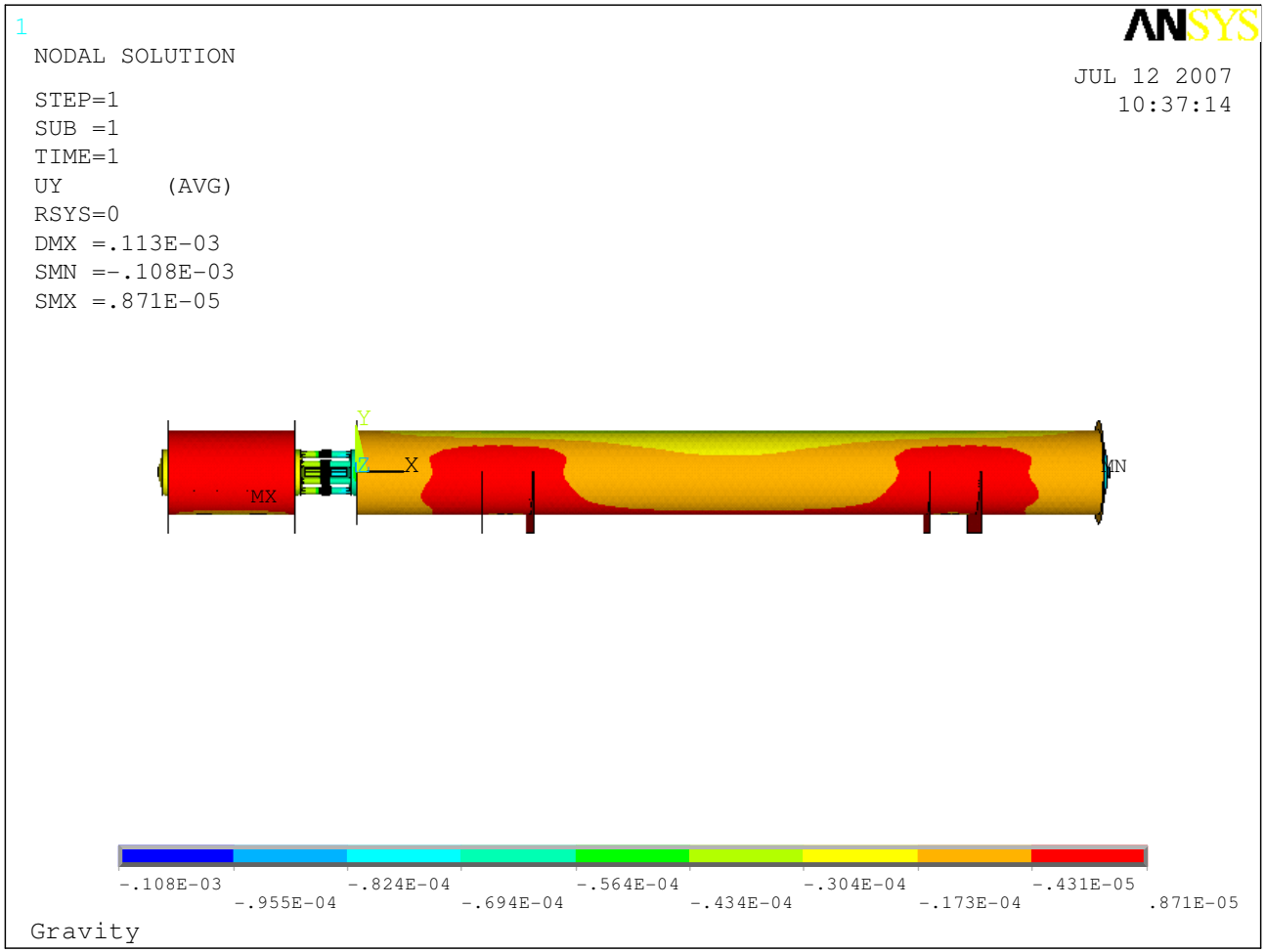

Fig. 5.14 Deflection of main components under own weight

6 FE feasibility study of SIS300 integration in the continuous cryostat

6.1 Finite element model

A feasibility study of synchrotron integration has been carried out by means of the finite element model. In order to build a model representative of the synchrotron arc assembly type "B" has been chosen (Fig. 5.11). It reflects two principal arc components: main quadrupole with the corrector (straight unit) and main dipole (curved unit). The details of the model are shown in Fig. 6.1.

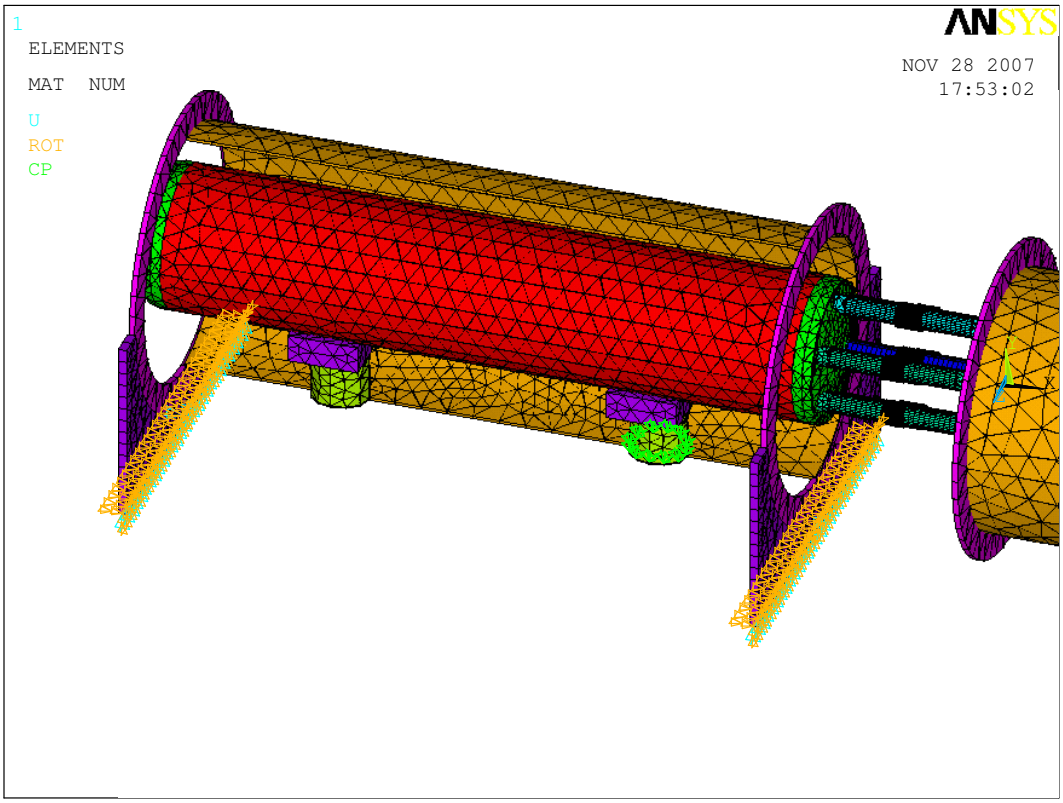

Fig. 6.1 Finite element model of main quadrupole – main dipole connection

The model comprises quadrupole and dipole vacuum vessels, quadrupole and dipole cold mass, magnet support system in the form of composite columns, quadrupole – dipole interconnections. Type LHC magnet support system has been adopted. It is based on composite thin-walled cylindrical shells supported inside the cryostat and integrated into the cold mass by means of transition parts. Each magnet is supported on two supports: one fixed and the other sliding in the longitudinal direction. Optimum location of the supports has been determined in the Section 5.4. The heads of the magnets are connected by means of the interconnection channels. Each channel is equipped with the compensation element. It is

worth pointing out that the quadrupole cold mass is straight whereas the dipole cold mass is curved which has a significant impact on the behaviour of the synchrotron under pressure loads. The details of the cold mass supporting system and interconnections are shown in Figs 6.2 and 6.3, respectively.

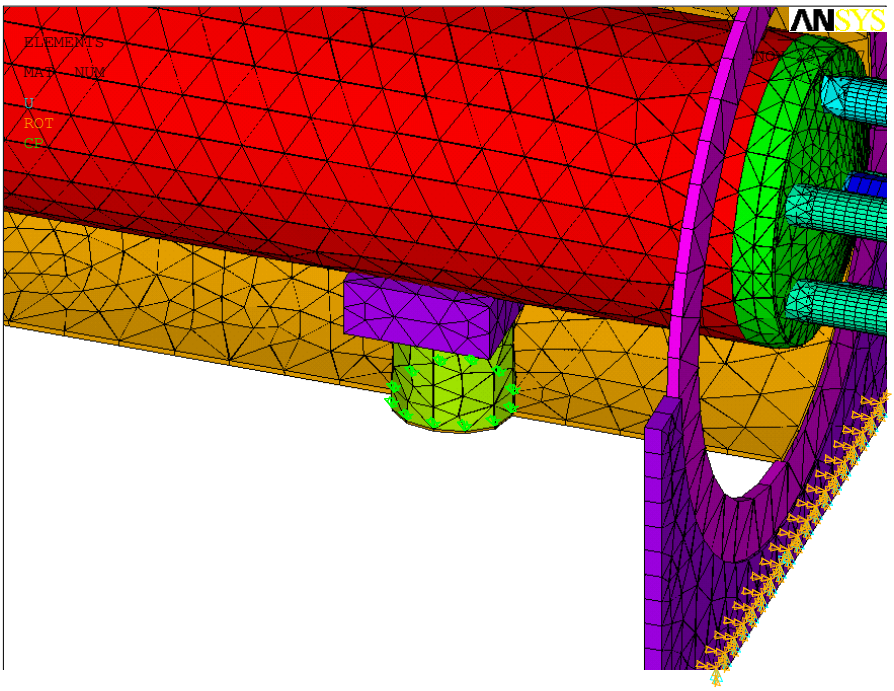

Fig. 6.2 The cold mass supporting system

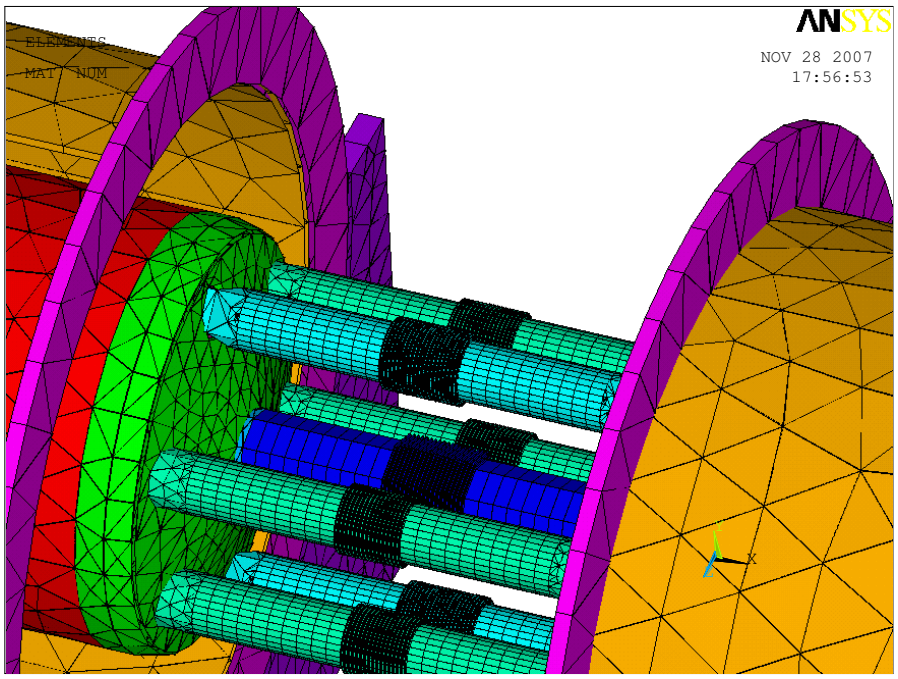

Fig. 6.3 Details of the quadrupole – dipole interconnections

The preliminary way of supporting the main quadrupole and the main dipole vacuum vessels is shown in Figs 6.4 and 6.5, respectively.

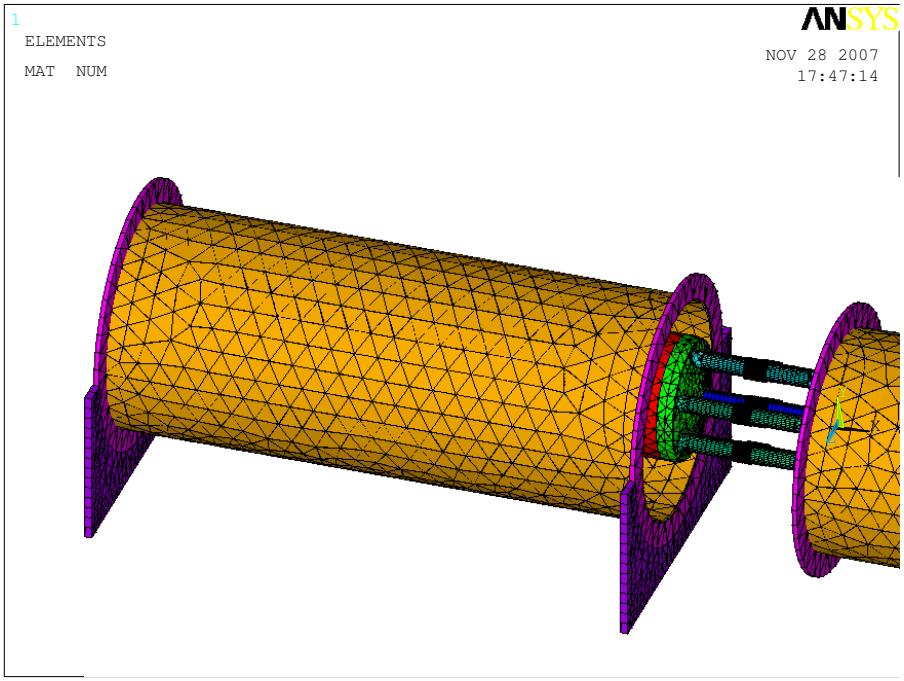

Fig. 6.4 Supporting system of the main quadrupole vacuum vessel.

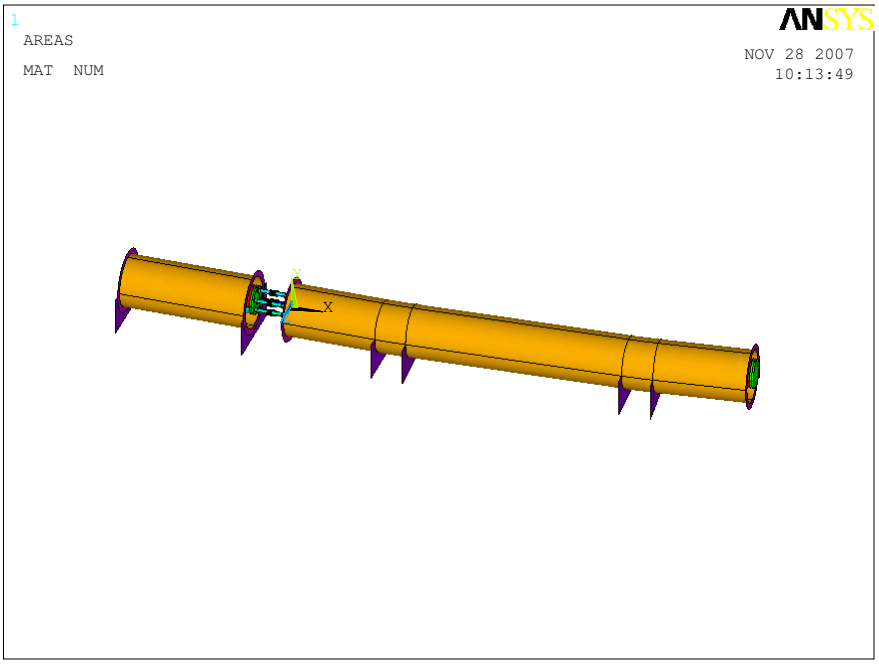

Fig. 6.5 The supports of the main dipole vacuum vessel

The finite element model has been built by using the solid and the shell elements. The analysis has been carried out entirely in the elastic domain, therefore the possible residual deformation has not been taken into account.

6.2 Boundary conditions and loads

The boundary conditions were imposed both outside and inside the vacuum vessel (Fig. 6.1):

1. supports outside the vacuum vessel – adjustable jacks
2. supports of the cold mass inside the vacuum vessel – cold feet

It has been assumed that the vacuum vessel is supported on adjustable jacks by means of the vessel reinforcements in the form of thick plates, as indicated in Fig. 6.5. Final position of the reinforcing plates remains to be determined as a function of final redistribution of the magnets weight. A desirable position of the reinforcements falls in the same planes where the magnet cold feet are located. The jacks are regarded as fixed points in the finite element model. They can be adjusted to the desired horizontal and vertical position as a function of the alignment of the synchrotron.

The cold mass (superconducting magnets) are supported on the so called cold feet, thin-walled composite cylinders constituting both a mechanical support and a thermal barrier for the heat flux from the vacuum vessel. As the vacuum vessel stays at room temperature, each cold foot forms a bridge between the ambient and the temperature of liquid helium. The cold feet have to be optimized with respect to the strength and the equivalent thermal conductivity in order to find a trade off between the supporting function (sufficient stiffness required) and the insulating function (minimum heat flux transferred from ambient to the cold mass).

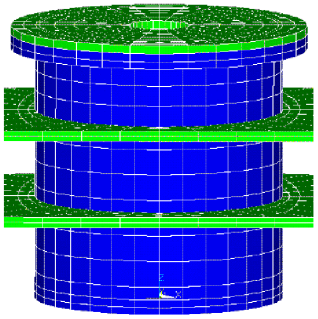

Fig. 6.6 Composite cold foot containing two thermalization plates

Typical composite structure made of epoxy resin impregnated glass fiber fabric is illustrated in Fig. 6.7.

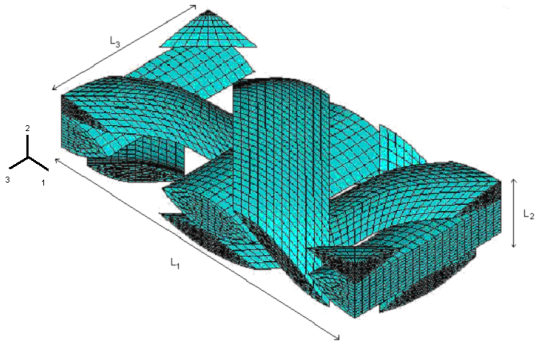

Fig. 6.7 Typical cell of epoxy resin impregnated glass fiber composite

The thermal conductivity of epoxy resin impregnated glass fiber composite has been measured at low temperatures and reliable date are available in the literature.

Each magnet is supported on 2 cold feet: one of them fixed (can not move inside the cryostat) and the other sliding (Fig. 6.2) in the longitudinal direction in order to accommodate the thermal contraction of the magnet. The sequence of fixed and sliding supports is repeated with respect to each magnet so that each interconnect is flanked by one fixed support and one sliding support. Each cold foot is equipped with upper plate that is attached to the magnet by means of specific cradle, modeled as a block of metal shown in Fig. 6.8 in light blue.

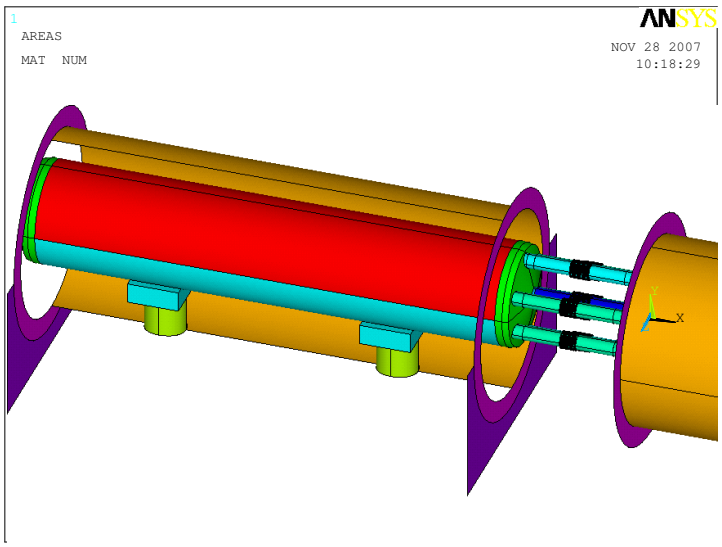

Fig. 6.8 Two composite columns supporting quadrupole magnet

During the cool down and warm up the synchrotron will be subjected to combined loads comprising:

1. the inner pressure due to helium flow,
2. own weight of the magnets,

3. misalignment across the interconnections.

Combination of all three load types may turn out critical for machine integrity and – ultimately - has to be taken into account. For cool down/ warm up of the synchrotron the inner pressure of 10 bar has been assumed, based on standard capacity of cold compressors. The own weight load takes into account average mass density of superconducting magnets. For the magnets misalignment across the interconnections 5 mm motion of one magnet with respect to another has been taken into account. The misalignment is at the origin of geometrical imperfection that may lead to instability of compensation bellows and enhanced level of local stress.

6.3 Results of finite element analysis

The model consisting of one quadrupole combined with a corrector magnet and one long curved dipole shown in Fig. 6.5 has been analyzed.

As the first load component the own weight has been taken into account. The results are shown in Figs 6.9 (side view) and 6.10 (top view).

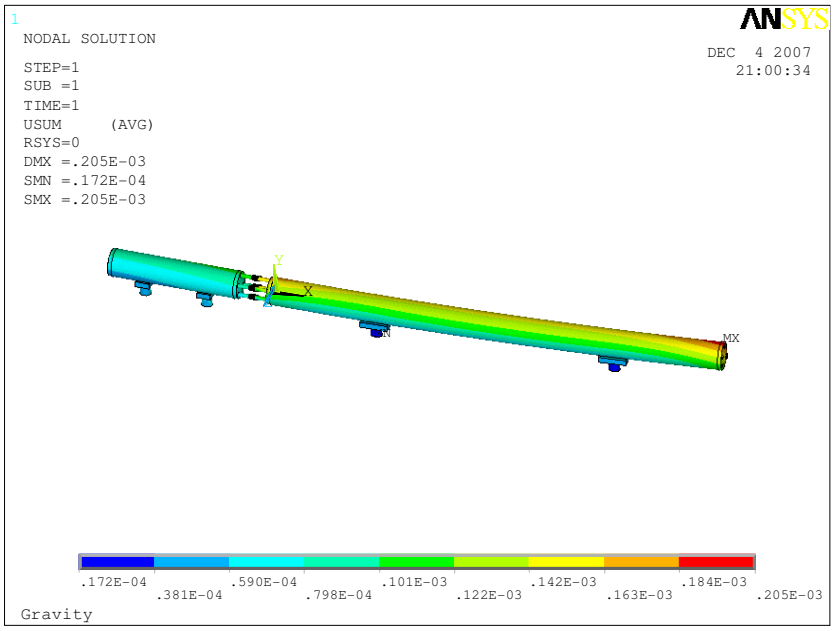

Fig. 6.9 Deflection of the cold mass due to its own weight (side view)

It is worth pointing out that maximum deflection occurs at the long magnet extremity and is of the order of 0.2 mm. The influence of magnet curvature is well visible in Fig. 6.10 via asymmetric way the long magnet deforms. This indicates combination of flexure and torsion due to the toroidal geometry of long curved magnet. Thus, both flexure and torsion will be transferred to magnet interconnections.

The results of deformation analysis under pressure load are shown in Fig. 6.11 through 6.15. The overall displacement field (all components), indicated in Fig. 6.11, shows the maximum displacement of around 2 mm. This is most probably due to non equilibrated pressure load in the axial direction, as shown in Fig. 6.12. Such displacement may occur in the arc extremity (assembly type E) containing the cold-warm transition.

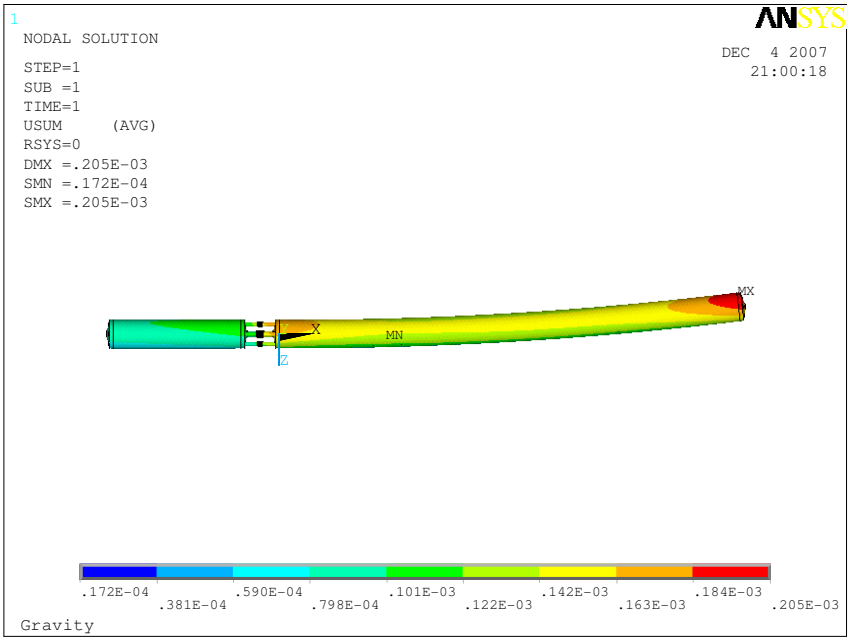

Fig. 6.10 Deflection of the cold mass due to own weight (top view)

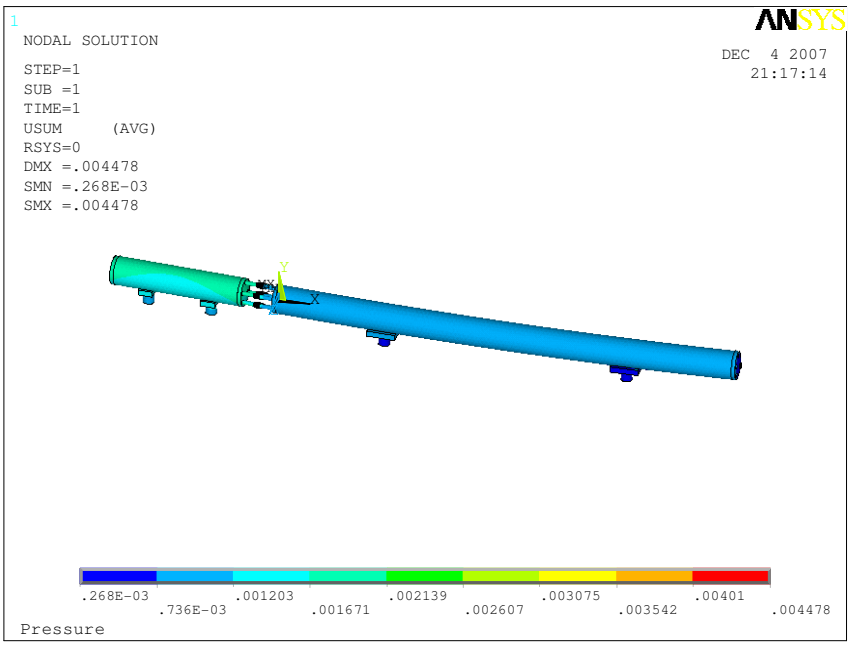

6.11 Overall displacement field due to pressure load

The components of the displacement field due to pressure are shown in Figs 6.12 through 6.14.

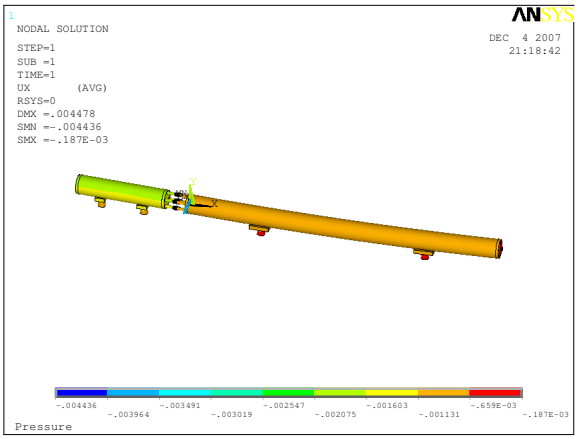

6.12 Displacement in the axial direction (x) due to pressure load

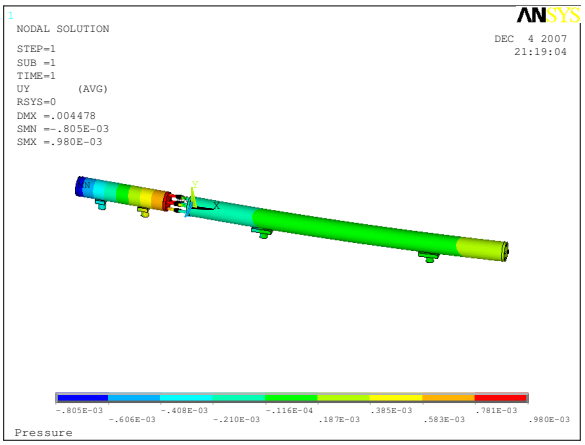

6.13 Displacement in the vertical direction (y) due to pressure load

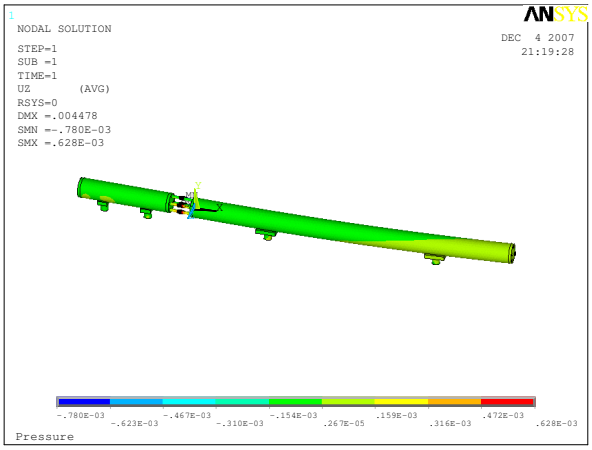

6.14 Displacement in the horizontal (z) direction due to pressure load

Finally, the motion of cold mass inside the vacuum vessel is shown in Fig. 6.15. Here, also the axial displacement by some 2 mm is well visible.

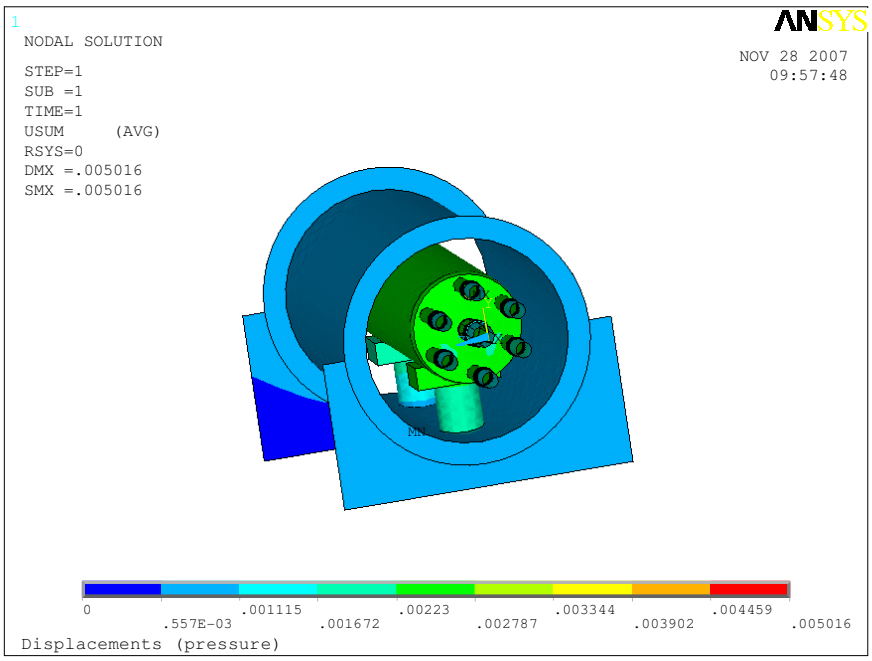

6.15 Motion of cold mass in the vacuum vessel

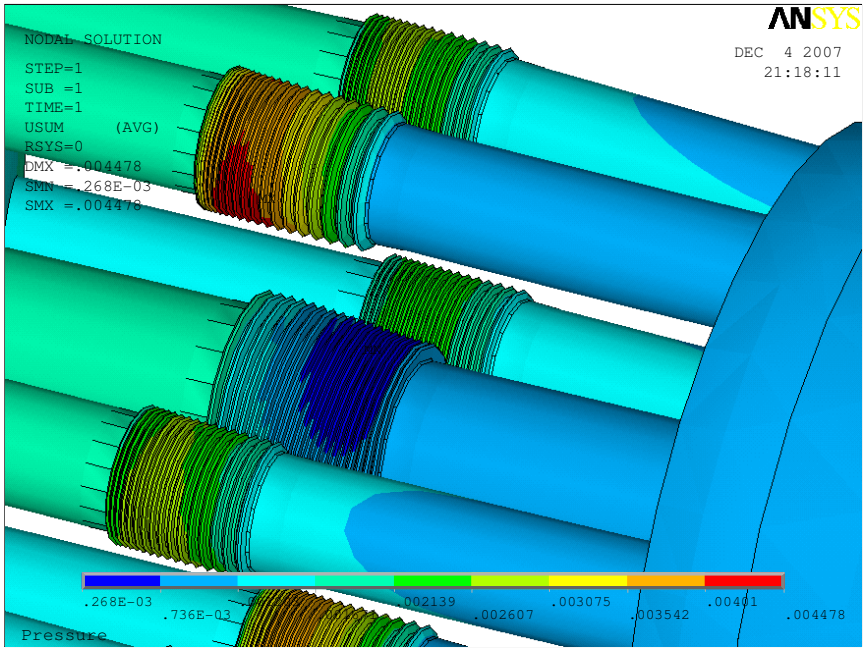

6.16 Displacements in the zone of interconnections due to pressure load

The effect of misalignment on the local stress levels and displacement fields is shown in Figs 6.17 through 6.20.

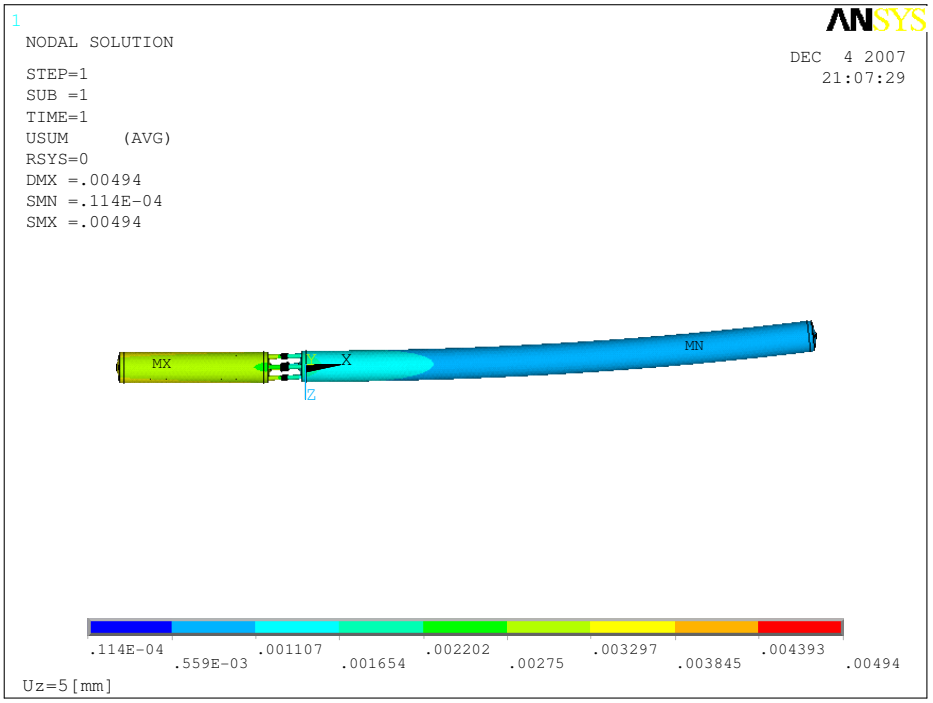

Fig. 6.17 Misalignment of 5 mm between the subsequent magnets

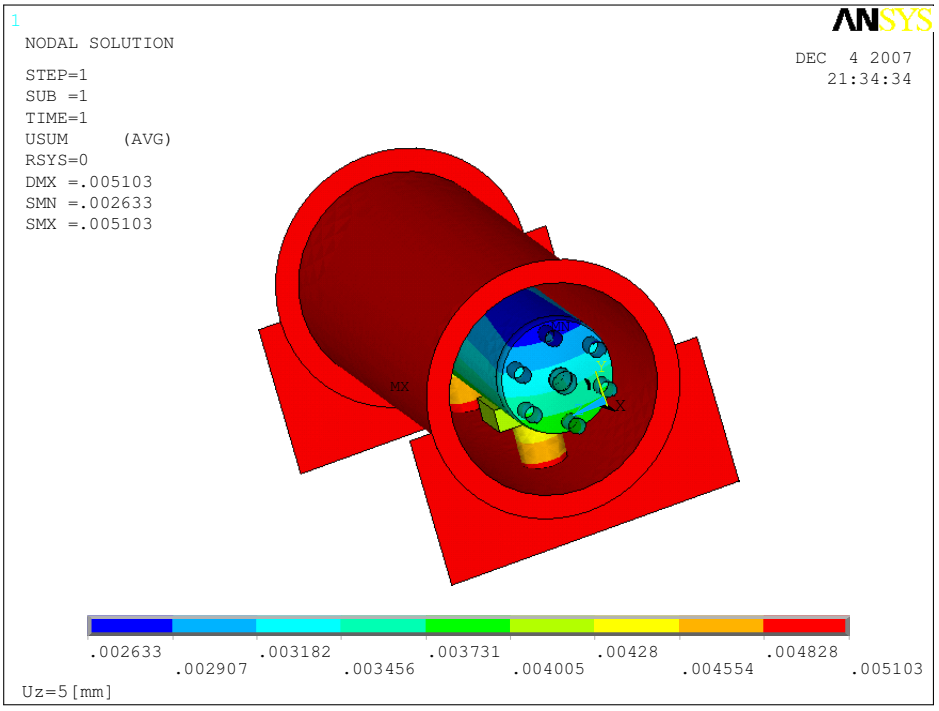

Fig. 6.18 Transverse motion of cold mass in the cryostat – deformation of cold feet

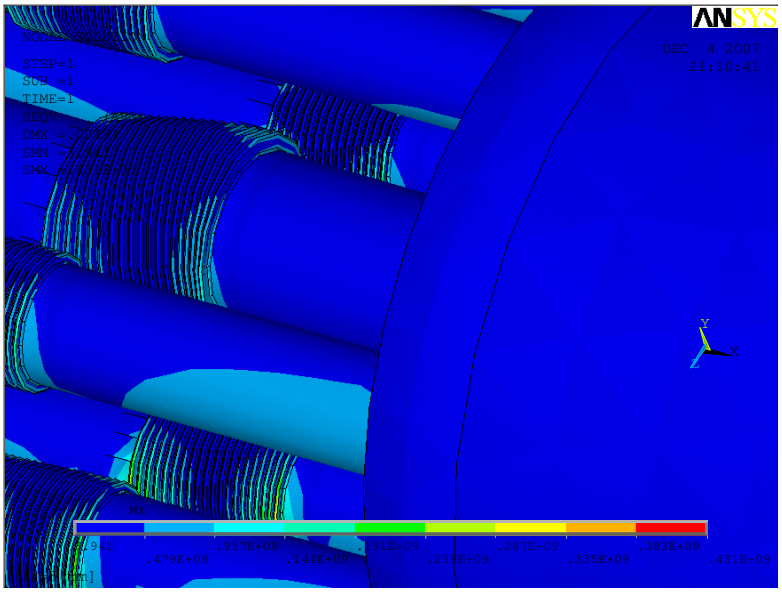

Fig. 6.19 Local levels of von Mises stress due to misalignment of magnets

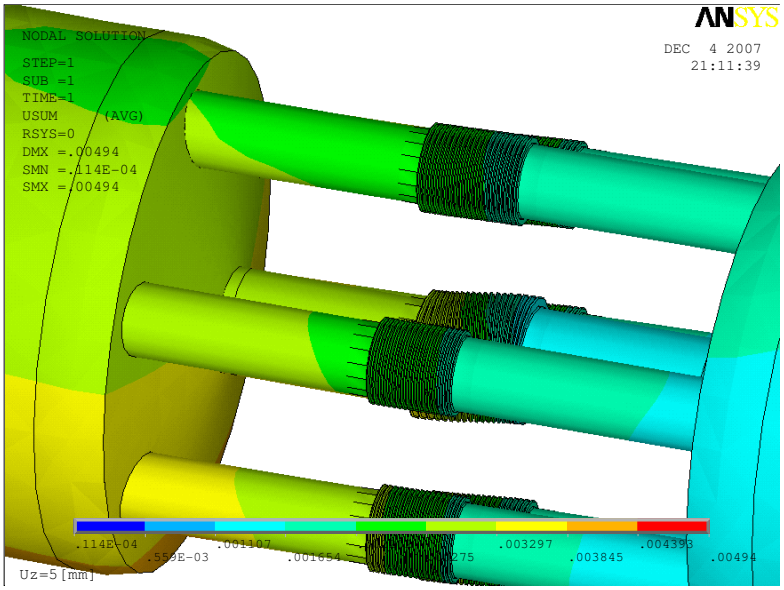

Fig. 6.20 Displacement field in the interconnection zone due to misalignment

Transverse motion of one magnet with respect to another causes a drag of its neighbour via the zone of interconnections. Motion of the cold mass in the cryostat is shown in Fig. 6.18. Due to this motion the cold feet are subjected to flexure and shear. This has to be taken into account when designing the composite structure of the cold feet. It is worth pointing out, that the quadrupole cryostat has been moved transversally by 5 mm in the z direction and the cold bore centre moves simultaneously by some 3 mm. The difference is due to the coupling across the interconnections with the neighbouring magnet. Fig. 6.19 indicates enhanced levels

of von Mises stress in the transition between the channels and the cold mass. The stress levels are mainly due to flexural effects and can be considerably reduced by increasing the wall thickness of the channels in the transition between the cold mass and the interconnections.

The complete displacement field with all three loads taken into account is shown in Figs 6.21 (plane x-y), 6.22 (plane x-z).

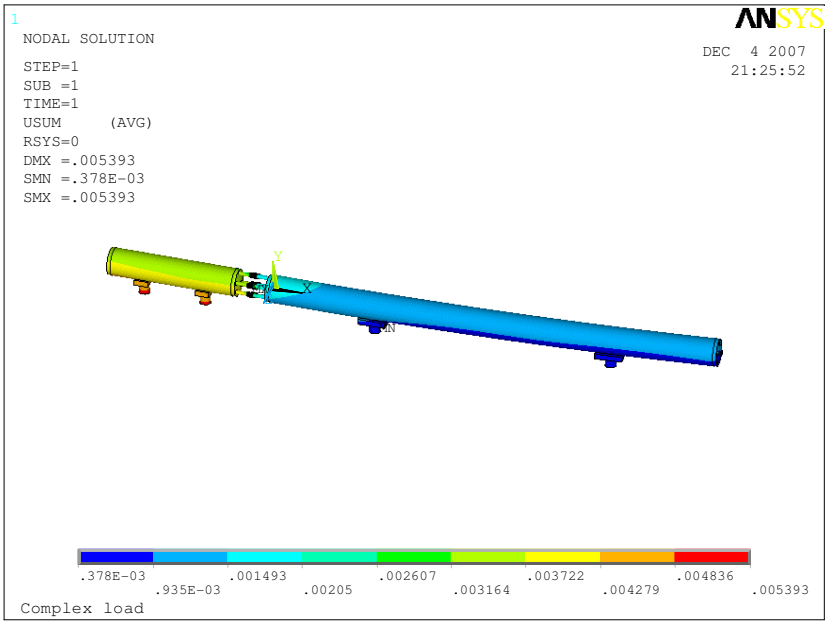

Fig. 6.21 Overall displacement field due to combined loads

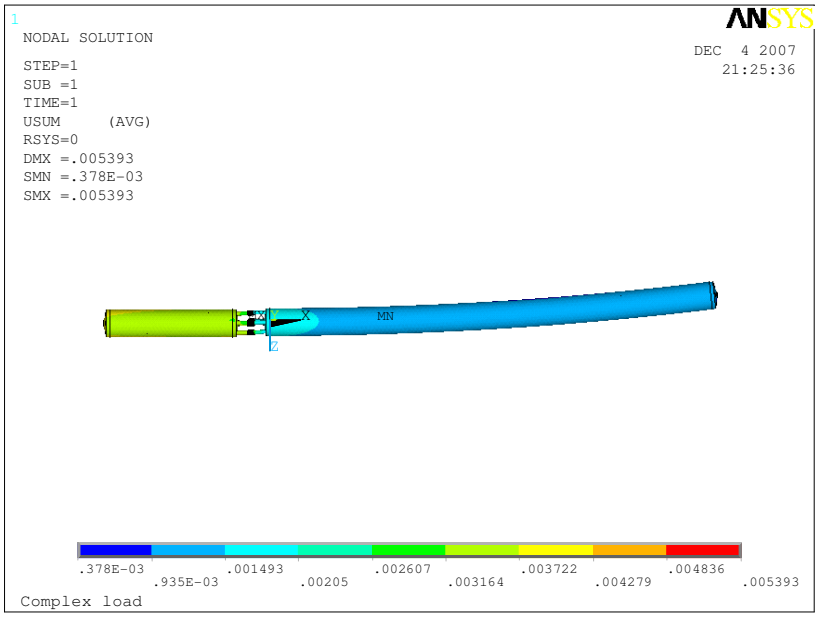

Fig. 6.22 Overall displacement field due to combined loads (plane x-z)

Finally, distortion of interconnection channels due to combined loads is shown in Fig. 6.23.

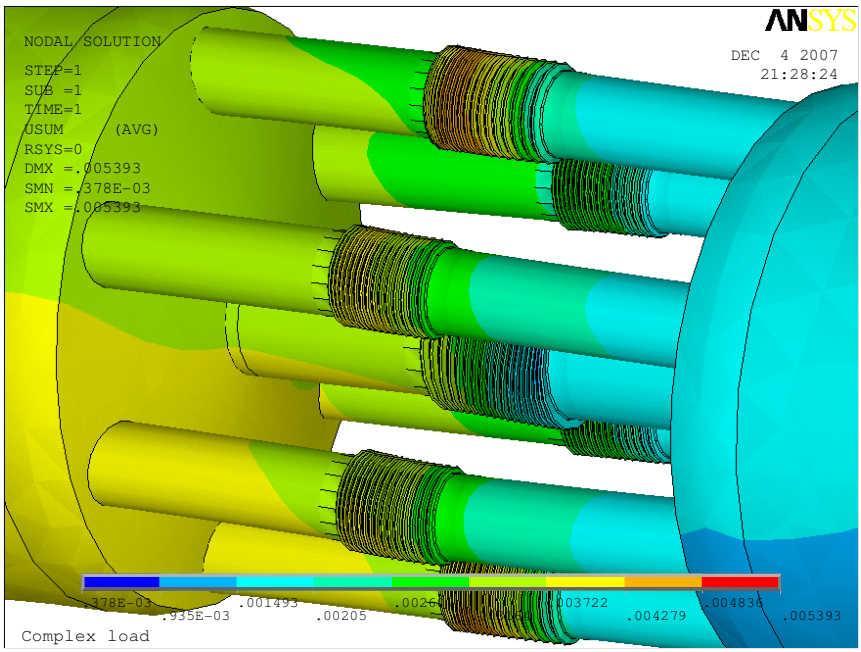

Fig. 6.23 Distortion in the zone of interconnections due to combined loads

6.4 Conclusions

1. Finite element model of arc assembly type B has been built in order to analyze the influence of combined loads on the deformation of the cold mass.
2. The boundary conditions reflecting the support of the vacuum vessel and the fixed/ sliding supports of cold mass in the vacuum vessel were modeled.
3. Three types of loads comprising: inner pressure, own weight and transverse misalignment were taken into account.
4. Small relative motion of magnets w.r.t. continuous vacuum vessel have been observed when imposing combined loads on type B assembly. This motion is due to a drag of one magnet by another across the zone of interconnections. Thanks to this effect a discontinuity of displacement in the zone of interconnections is avoided.
5. The cold feet are subjected to compression (own weight), flexure and shear (misalignment of magnets) and have to be carefully designed in order to obtain correct performance in the mechanical and thermodynamic domains.
6. High localized von Mises stresses occur in the transition between the cold mass and interconnections. The He flow channels and the bus-bar channels require reinforcement of the wall in the transition region.

7. Maximum displacements computed for type B assembly are summarized in Tables 6.1 through 6.4.

Table 6.1 Maximum displacements in the cold mass (quadrupole + dipole) due to own weight

	UX	UY	UZ	USUM
VALUE [m]	0.50823E-04	-0.17289E-03	-0.14297E-03	0.20499E-03

Table 6.2 Maximum displacements in the cold mass (quad. + dipole) due to pressure load

	UX	UY	UZ	USUM
VALUE [m]	-0.17275E-02	0.79607E-03	-0.11114E-03	0.18903E-02

Table 6.3 Maximum displacements in the cold mass due to 5 mm misalignment of cryostats

	UX	UY	UZ	USUM
VALUE [m]	0.13005E-03	0.66682E-03	0.43938E-02	0.43938E-02

Table 6.4 Maximum displacements in the cold mass due to all three loads

	UX	UY	UZ	USUM
VALUE [m]	-0.17261E-02	-0.14645E-02	0.43717E-02	0.46642E-02

7 Further work

The analysis presented in the current report has been stretched over SIS300 arc. Detailed finite element analysis has been carried out for one segment of SIS300 arc: type B assembly comprising main quadrupole and chromaticity sextupole in the form of one module and main dipole (long, curved version). Type B assembly is located in the middle of the arc and constitutes a self-equilibrated segment of the synchrotron.

Detailed finite element analysis has to be carried out for all assemblies in the arc of synchrotron, especially for the segments located close to the arc extremity. In particular, type E assembly contains a combination of main quadrupole, steerer and extraction sextupole and is located in the end of arc. This segment is subjected to non equilibrated pressure loads and much higher deformation than the other synchrotron segments, located in the middle of arc. Here, a special reinforced supporting system both for the cold mass and for the vacuum vessel has to be designed.

Special attention has to be focused on the synchrotron straight parts, where the lump groups of magnets containing main quadrupoles and steerers exist. These segments have to be very carefully analyzed in view of inner and outer pressure loads, associated with cool down and warm up (helium flow) as well as atmospheric pressure acting on the discontinuous cryostat. Also in SIS300 straights a special reinforced supporting system has to be designed.

As the SIS300 magnets will be working in the high energy mode with the ramp rate for dipoles of 1T/s and for quadrupoles of 10 T/s^2, it is of fundamental importance to take this effect into account when designing the structure of magnets and their supports. As soon as more data related to the behaviour of magnets is available, a suitable analysis will be carried out.

Another problem is related to the internal structure of main quadrupole cold mass, where the horizontal and vertical steerers as well as higher order correctors like extraction or chromaticity sextupoles are proposed to be integrated. A correct way of integration of the correctors is fundamental for their alignment with respect to main magnets and to closed orbit. The structure has to be carefully designed and verified by using the finite element model both in stretcher mode and in high energy mode.

In the present analysis integration of smaller components like beam position monitors (BPM) or cold-warm transitions (CWT) has not been taken into account. In the future analysis integration of BPMs and CWTs will be carried out, based on the existing design (BPM) or on the design proposed in this report (CWT).

Appendix_1: Optimum geometric configurations for SIS300 compensation system

APPENDIX 1A: BEAM VACUUM BELLOWS EXPANSION JOINT – OPTIMUM PARAMETERS

```
*******************************************
RESULTS OF THE OPTIMIZATION OF U-TYPE BELLOWS
    WITH RESPECT TO THE AXIAL FLEXIBILITY
*******************************************

GENERAL INPUT DATA:

INTERNAL DIAMETER=   100.0
NUMBER OF PLIES=      1
NOMINAL PRESSURE=      .10
CRITICAL PRESSURE=     .10
BELLOWS EXTENSION=     5.0
BELLOWS COMPRESSION=   5.0
MINIMUM FATIGUE LIFE= 500 CYCLES

THERMAL FACTOR=       1
************************
RESULTS OF COMPUTATIONS:
************************

NOTATION:

BLG   - BELLOWS LENGTH
NSEG  - NUMBER OF CONVOLUTIONS
FBL   - AXIAL STIFFNESS OF BELLOWS
XNF   - FATIGUE LIFE
TPL   - INITIAL THICKNESS OF PLIES
XSTR2 - MAXIMUM ADMISSIBLE COMPRESSION
XFMX  - MAXIMUM ROTATION ANGLE
OFMX  - MAXIMUM OFFSET

--------------------------
CONVOLUTION DEPTH= 10.0
--------------------------
```

BLG,	NSEG,	FBL,	XNF,	TPL,	XSTR2,	XFMX,	OFMX
55.0	10	9.8	******	.16	17.3	.0020	3.2
60.0	8	8.7	******	.14	19.3	.0018	2.8
60.0	9	9.1	******	.15	19.1	.0019	3.1
60.0	10	9.8	******	.16	18.9	.0021	3.5
60.0	11	8.9	******	.16	18.8	.0022	3.8
60.0	12	9.8	******	.17	18.6	.0024	4.2
65.0	8	9.0	******	.14	20.9	.0018	3.0
65.0	9	9.2	******	.15	20.8	.0020	3.4
65.0	10	8.2	******	.15	20.7	.0021	3.8
65.0	11	8.9	******	.16	20.5	.0022	4.2
65.0	12	8.2	******	.16	20.4	.0024	4.5
65.0	13	9.1	******	.17	20.2	.0025	4.9
70.0	8	9.5	******	.14	22.6	.0018	3.3
70.0	9	7.8	******	.14	22.5	.0020	3.7
70.0	10	8.2	******	.15	22.3	.0021	4.1
70.0	11	7.4	******	.15	22.2	.0023	4.5
70.0	12	8.2	******	.16	22.1	.0024	4.9
70.0	13	7.5	******	.16	21.9	.0025	5.3

70.0	14	8.4	******	.17	21.7	.0027	5.7
75.0	8	8.5	******	.13	24.3	.0019	3.5
75.0	9	8.2	******	.14	24.2	.0020	3.9
75.0	10	8.4	******	.15	24.0	.0021	4.4
75.0	11	7.4	******	.15	23.9	.0023	4.8
75.0	12	8.2	******	.16	23.7	.0024	5.2
75.0	13	7.5	******	.16	23.6	.0026	5.7
75.0	14	8.4	******	.17	23.4	.0027	6.1
75.0	15	7.9	******	.17	23.3	.0029	6.5
80.0	8	9.1	******	.13	26.0	.0019	3.7
80.0	9	8.6	******	.14	25.8	.0020	4.2
80.0	10	8.6	******	.15	25.7	.0022	4.7
80.0	11	7.5	******	.15	25.6	.0023	5.1
80.0	12	8.2	******	.16	25.4	.0024	5.6
80.0	13	7.5	******	.16	25.3	.0026	6.1
80.0	14	8.3	******	.17	25.1	.0027	6.5
80.0	15	7.8	******	.17	25.0	.0029	7.0
80.0	16	8.7	******	.18	24.7	.0030	7.4
85.0	8	9.8	******	.13	27.6	.0019	4.0
85.0	9	9.1	******	.14	27.5	.0021	4.5
85.0	10	8.9	******	.15	27.3	.0022	4.9
85.0	11	9.1	******	.16	27.2	.0023	5.4
85.0	12	8.2	******	.16	27.1	.0025	5.9
85.0	13	9.0	******	.17	26.9	.0026	6.4
85.0	14	8.3	******	.17	26.7	.0028	6.9
85.0	15	9.2	******	.18	26.5	.0029	7.4
85.0	16	8.7	******	.18	26.4	.0030	7.9
85.0	17	8.2	******	.18	26.3	.0032	8.4
90.0	9	9.7	******	.14	29.2	.0021	4.7
90.0	10	9.3	******	.15	29.0	.0022	5.2
90.0	11	9.4	******	.16	28.8	.0024	5.8
90.0	12	9.8	******	.17	28.6	.0025	6.3
90.0	13	9.0	******	.17	28.5	.0026	6.8
90.0	14	9.8	******	.18	28.3	.0028	7.3
90.0	15	9.2	******	.18	28.2	.0029	7.9
90.0	16	8.6	******	.18	28.1	.0031	8.4
90.0	17	9.6	******	.19	27.8	.0032	8.9
90.0	18	9.1	******	.19	27.7	.0034	9.4
95.0	10	9.7	******	.15	30.7	.0022	5.5
95.0	11	9.7	******	.16	30.5	.0024	6.1
95.0	12	10.0	******	.17	30.3	.0025	6.6
95.0	13	9.0	******	.17	30.2	.0027	7.2
95.0	14	9.8	******	.18	30.0	.0028	7.7
95.0	15	9.1	******	.18	29.9	.0029	8.3
95.0	17	9.5	******	.19	29.5	.0032	9.4
95.0	18	9.0	******	.19	29.4	.0034	9.9
100.0	14	9.8	******	.18	31.7	.0028	8.1
100.0	17	9.5	******	.19	31.2	.0033	9.9
100.0	**19**	**10.0**	**********	**.20**	**30.8**	**.0035**	**11.1**
100.0	20	9.5	******	.20	30.7	.0037	11.6

CONVOLUTION DEPTH= 10.5

BLG,	NSEG,	FBL,	XNF,	TPL,	XSTR2,	XFMX,	OFMX
60.0	7	9.3	******	.14	19.3	.0017	2.4
60.0	8	9.1	******	.15	19.2	.0019	2.8
60.0	9	9.5	******	.16	19.0	.0020	3.1
60.0	11	9.3	******	.17	18.8	.0023	3.8
65.0	7	9.9	******	.14	21.0	.0018	2.6
65.0	8	9.4	******	.15	20.9	.0019	3.0
65.0	9	9.6	******	.16	20.7	.0020	3.4
65.0	10	8.6	******	.16	20.6	.0022	3.8
65.0	11	9.2	******	.17	20.4	.0023	4.2

65.0	12	8.5	******	.17	20.3	.0025	4.5
70.0	8	8.3	******	.14	22.6	.0019	3.3
70.0	9	8.2	******	.15	22.4	.0021	3.7
70.0	10	8.6	******	.16	22.3	.0022	4.1
70.0	11	7.8	******	.16	22.2	.0024	4.5
70.0	12	8.5	******	.17	22.0	.0025	4.9
70.0	13	7.8	******	.17	21.9	.0027	5.3
75.0	8	8.8	******	.14	24.3	.0020	3.5
75.0	9	8.5	******	.15	24.1	.0021	3.9
75.0	10	7.3	******	.15	24.0	.0023	4.4
75.0	11	7.8	******	.16	23.8	.0024	4.8
75.0	12	8.5	******	.17	23.6	.0025	5.2
75.0	13	7.8	******	.17	23.5	.0027	5.7
75.0	14	7.3	******	.17	23.4	.0029	6.1
80.0	8	9.4	******	.14	25.9	.0020	3.7
80.0	9	8.9	******	.15	25.8	.0021	4.2
80.0	10	8.9	******	.16	25.6	.0023	4.7
80.0	11	7.8	******	.16	25.5	.0024	5.1
80.0	12	8.5	******	.17	25.3	.0026	5.6
80.0	13	7.8	******	.17	25.2	.0027	6.1
80.0	14	8.6	******	.18	25.0	.0029	6.5
80.0	15	8.0	******	.18	24.9	.0030	7.0
85.0	9	9.3	******	.15	27.4	.0022	4.5
85.0	10	9.1	******	.16	27.3	.0023	4.9
85.0	11	8.0	******	.16	27.2	.0025	5.4
85.0	12	8.5	******	.17	27.0	.0026	5.9
85.0	13	9.2	******	.18	26.8	.0027	6.4
85.0	14	8.6	******	.18	26.7	.0029	6.9
85.0	15	8.0	******	.18	26.5	.0031	7.4
85.0	16	8.8	******	.19	26.3	.0032	7.9
90.0	8	9.2	******	.13	29.3	.0020	4.2
90.0	9	9.9	******	.15	29.1	.0022	4.7
90.0	10	9.5	******	.16	28.9	.0023	5.2
90.0	11	9.6	******	.17	28.8	.0025	5.8
90.0	12	8.5	******	.17	28.6	.0026	6.3
90.0	13	9.2	******	.18	28.4	.0028	6.8
90.0	14	8.6	******	.18	28.3	.0029	7.3
90.0	15	9.3	******	.19	28.1	.0031	7.9
90.0	16	8.8	******	.19	28.0	.0032	8.4
90.0	17	9.7	******	.20	27.7	.0034	8.9
95.0	10	9.9	******	.16	30.6	.0024	5.5
95.0	11	9.8	******	.17	30.4	.0025	6.1
95.0	13	9.2	******	.18	30.1	.0028	7.2
95.0	14	10.0	******	.19	29.9	.0029	7.7
95.0	15	9.3	******	.19	29.8	.0031	8.3
95.0	17	9.6	******	.20	29.4	.0034	9.4
95.0	18	9.2	******	.20	29.3	.0036	9.9
100.0	9	9.5	******	.14	32.5	.0022	5.2
100.0	14	10.0	******	.19	31.6	.0030	8.1
100.0	17	9.6	******	.20	31.1	.0034	9.9

CONVOLUTION DEPTH= 11.0

BLG,	NSEG,	FBL,	XNF,	TPL,	XSTR2,	XFMX,	OFMX
60.0	7	9.7	******	.15	19.3	.0018	2.4
60.0	8	9.5	******	.16	19.1	.0020	2.8
60.0	9	9.9	******	.17	19.0	.0021	3.1
65.0	8	9.8	******	.16	20.8	.0020	3.0
65.0	9	10.0	******	.17	20.6	.0021	3.4
65.0	10	8.9	******	.17	20.5	.0023	3.8
65.0	11	9.5	******	.18	20.3	.0025	4.2
70.0	8	8.6	******	.15	22.5	.0020	3.3
70.0	9	8.6	******	.16	22.4	.0022	3.7

70.0	10	9.0	******	.17	22.2	.0023	4.1
70.0	11	8.1	******	.17	22.1	.0025	4.5
70.0	12	8.7	******	.18	21.9	.0027	4.9
75.0	8	9.1	******	.15	24.2	.0020	3.5
75.0	9	7.4	******	.15	24.1	.0022	3.9
75.0	10	7.6	******	.16	23.9	.0024	4.4
75.0	11	8.1	******	.17	23.8	.0025	4.8
75.0	12	8.8	******	.18	23.6	.0027	5.2
75.0	13	8.1	******	.18	23.4	.0028	5.7
80.0	8	9.7	******	.15	25.9	.0021	3.7
80.0	9	7.7	******	.15	25.8	.0022	4.2
80.0	10	7.8	******	.16	25.6	.0024	4.7
80.0	11	8.2	******	.17	25.4	.0025	5.1
80.0	12	8.8	******	.18	25.2	.0027	5.6
80.0	13	8.1	******	.18	25.1	.0029	6.1
80.0	14	7.5	******	.18	25.0	.0030	6.5
85.0	8	8.7	******	.14	27.6	.0021	4.0
85.0	9	8.1	******	.15	27.4	.0023	4.5
85.0	10	8.0	******	.16	27.3	.0024	4.9
85.0	11	8.2	******	.17	27.1	.0026	5.4
85.0	12	8.8	******	.18	26.9	.0027	5.9
85.0	13	8.1	******	.18	26.8	.0029	6.4
85.0	14	8.8	******	.19	26.6	.0030	6.9
85.0	15	8.2	******	.19	26.4	.0032	7.4
90.0	8	9.4	******	.14	29.3	.0021	4.2
90.0	9	8.6	******	.15	29.1	.0023	4.7
90.0	10	9.7	******	.17	28.9	.0024	5.2
90.0	11	9.8	******	.18	28.7	.0026	5.8
90.0	12	8.8	******	.18	28.6	.0028	6.3
90.0	13	9.5	******	.19	28.4	.0029	6.8
90.0	14	8.8	******	.19	28.2	.0031	7.3
90.0	15	9.5	******	.20	28.0	.0032	7.9
90.0	16	9.0	******	.20	27.9	.0034	8.4
95.0	9	9.1	******	.15	30.8	.0023	5.0
95.0	12	8.9	******	.18	30.2	.0028	6.6
95.0	13	9.5	******	.19	30.0	.0029	7.2
95.0	15	9.5	******	.20	29.7	.0033	8.3
95.0	16	8.9	******	.20	29.5	.0034	8.8
95.0	17	9.7	******	.21	29.3	.0036	9.4
100.0	9	9.6	******	.15	32.4	.0023	5.2
100.0	13	9.5	******	.19	31.7	.0030	7.6
100.0	15	9.5	******	.20	31.3	.0033	8.7
100.0	17	9.7	******	.21	31.0	.0036	9.9

CONVOLUTION DEPTH= 11.5

BLG,	NSEG,	FBL,	XNF,	TPL,	XSTR2,	XFMX,	OFMX
60.0	8	9.9	******	.17	19.1	.0021	2.8
65.0	10	9.3	******	.18	20.5	.0024	3.8
65.0	11	9.8	******	.19	20.3	.0026	4.2
70.0	8	8.9	******	.16	22.5	.0021	3.3
70.0	9	8.9	******	.17	22.3	.0023	3.7
70.0	10	9.3	******	.18	22.1	.0024	4.1
70.0	11	9.8	******	.19	21.9	.0026	4.5
70.0	12	9.0	******	.19	21.8	.0028	4.9
75.0	8	9.4	******	.16	24.1	.0021	3.5
75.0	9	7.7	******	.16	24.0	.0023	3.9
75.0	10	8.0	******	.17	23.9	.0025	4.4
75.0	11	8.5	******	.18	23.7	.0026	4.8
75.0	12	9.0	******	.19	23.5	.0028	5.2
75.0	13	8.3	******	.19	23.4	.0030	5.7
80.0	8	9.9	******	.16	25.8	.0022	3.7
80.0	9	8.0	******	.16	25.7	.0023	4.2

80.0	10	8.1	******	.17	25.5	.0025	4.7
80.0	11	8.5	******	.18	25.3	.0027	5.1
80.0	12	7.7	******	.18	25.2	.0028	5.6
80.0	13	8.3	******	.19	25.0	.0030	6.1
85.0	8	9.0	******	.15	27.5	.0022	4.0
85.0	9	8.4	******	.16	27.4	.0024	4.5
85.0	10	8.3	******	.17	27.2	.0025	4.9
85.0	11	8.5	******	.18	27.0	.0027	5.4
85.0	12	9.1	******	.19	26.8	.0029	5.9
85.0	13	8.3	******	.19	26.7	.0030	6.4
85.0	14	9.0	******	.20	26.5	.0032	6.9
90.0	8	9.6	******	.15	29.2	.0022	4.2
90.0	9	8.8	******	.16	29.0	.0024	4.7
90.0	10	8.5	******	.17	28.9	.0025	5.2
90.0	11	8.6	******	.18	28.7	.0027	5.8
90.0	12	9.1	******	.19	28.5	.0029	6.3
90.0	13	9.7	******	.20	28.3	.0030	6.8
90.0	14	9.0	******	.20	28.1	.0032	7.3
90.0	15	9.7	******	.21	27.9	.0034	7.9
95.0	9	9.3	******	.16	30.7	.0024	5.0
95.0	12	9.1	******	.19	30.1	.0029	6.6
95.0	13	9.7	******	.20	29.9	.0031	7.2
95.0	14	9.0	******	.20	29.8	.0032	7.7
95.0	15	9.6	******	.21	29.6	.0034	8.3
95.0	16	9.1	******	.21	29.4	.0036	8.8
100.0	8	9.6	******	.14	32.6	.0023	4.7
100.0	9	9.8	******	.16	32.4	.0024	5.2
100.0	13	9.7	******	.20	31.6	.0031	7.6
100.0	15	9.6	******	.21	31.2	.0034	8.7
100.0	17	9.8	******	.22	30.8	.0038	9.9

CONVOLUTION DEPTH= 12.0

BLG,	NSEG,	FBL,	XNF,	TPL,	XSTR2,	XFMX,	OFMX
65.0	10	9.6	******	.19	20.4	.0025	3.8
70.0	7	10.0	******	.16	22.6	.0020	2.9
70.0	8	9.3	******	.17	22.4	.0022	3.3
70.0	9	9.3	******	.18	22.3	.0024	3.7
70.0	10	9.6	******	.19	22.1	.0026	4.1
75.0	8	8.3	******	.16	24.1	.0022	3.5
75.0	9	8.1	******	.17	24.0	.0024	3.9
75.0	10	8.3	******	.18	23.8	.0026	4.4
75.0	11	8.7	******	.19	23.6	.0028	4.8
75.0	12	9.3	******	.20	23.4	.0029	5.2
80.0	8	8.7	******	.16	25.8	.0023	3.7
80.0	9	8.3	******	.17	25.6	.0024	4.2
80.0	10	8.4	******	.18	25.5	.0026	4.7
80.0	11	8.8	******	.19	25.3	.0028	5.1
80.0	12	8.0	******	.19	25.1	.0030	5.6
80.0	13	8.5	******	.20	24.9	.0031	6.1
85.0	8	9.3	******	.16	27.5	.0023	4.0
85.0	9	8.6	******	.17	27.3	.0025	4.5
85.0	10	8.5	******	.18	27.1	.0026	4.9
85.0	11	8.8	******	.19	26.9	.0028	5.4
85.0	12	8.0	******	.19	26.8	.0030	5.9
85.0	13	8.5	******	.20	26.6	.0032	6.4
85.0	14	9.2	******	.21	26.4	.0033	6.9
90.0	8	9.9	******	.16	29.1	.0023	4.2
90.0	9	9.0	******	.17	29.0	.0025	4.7
90.0	10	8.7	******	.18	28.8	.0027	5.2
90.0	11	8.9	******	.19	28.6	.0028	5.8
90.0	12	9.3	******	.20	28.4	.0030	6.3
90.0	13	8.6	******	.20	28.3	.0032	6.8

90.0	14	9.1	******	.21	28.0	.0034	7.3
90.0	15	8.6	******	.21	27.9	.0035	7.9
95.0	8	9.1	******	.15	30.9	.0023	4.4
95.0	9	9.5	******	.17	30.6	.0025	5.0
95.0	10	9.0	******	.18	30.5	.0027	5.5
95.0	11	9.0	******	.19	30.3	.0029	6.1
95.0	12	9.3	******	.20	30.1	.0030	6.6
95.0	13	9.9	******	.21	29.8	.0032	7.2
95.0	14	9.1	******	.21	29.7	.0034	7.7
95.0	15	9.8	******	.22	29.5	.0036	8.3
100.0	8	9.8	******	.15	32.5	.0024	4.7
100.0	10	9.4	******	.18	32.1	.0027	5.8
100.0	12	9.4	******	.20	31.7	.0031	7.0
100.0	13	9.9	******	.21	31.5	.0032	7.6
100.0	15	9.8	******	.22	31.1	.0036	8.7

CONVOLUTION DEPTH= 12.5

BLG,	NSEG,	FBL,	XNF,	TPL,	XSTR2,	XFMX,	OFMX
65.0	7	9.7	******	.17	20.9	.0021	2.6
65.0	10	9.9	******	.20	20.3	.0026	3.8
70.0	8	9.6	******	.18	22.4	.0023	3.3
70.0	9	9.6	******	.19	22.2	.0025	3.7
70.0	10	9.9	******	.20	22.0	.0027	4.1
75.0	8	8.5	******	.17	24.1	.0023	3.5
75.0	9	8.4	******	.18	23.9	.0025	3.9
75.0	10	8.6	******	.19	23.7	.0027	4.4
75.0	11	9.0	******	.20	23.5	.0029	4.8
75.0	12	9.5	******	.21	23.3	.0031	5.2
80.0	8	9.0	******	.17	25.8	.0024	3.7
80.0	9	8.6	******	.18	25.6	.0025	4.2
80.0	10	8.7	******	.19	25.4	.0027	4.7
80.0	11	9.0	******	.20	25.2	.0029	5.1
80.0	12	8.2	******	.20	25.1	.0031	5.6
85.0	8	9.5	******	.17	27.4	.0024	4.0
85.0	9	8.9	******	.18	27.3	.0026	4.5
85.0	10	8.8	******	.19	27.1	.0027	4.9
85.0	11	9.1	******	.20	26.9	.0029	5.4
85.0	12	8.3	******	.20	26.7	.0031	5.9
85.0	13	8.8	******	.21	26.5	.0033	6.4
90.0	9	9.2	******	.18	28.9	.0026	4.7
90.0	10	9.0	******	.19	28.7	.0028	5.2
90.0	11	9.1	******	.20	28.5	.0030	5.8
90.0	12	9.6	******	.21	28.3	.0031	6.3
90.0	13	8.8	******	.21	28.2	.0033	6.8
90.0	14	9.3	******	.22	27.9	.0035	7.3
95.0	8	9.3	******	.16	30.8	.0024	4.4
95.0	9	9.7	******	.18	30.6	.0026	5.0
95.0	10	9.2	******	.19	30.4	.0028	5.5
95.0	11	9.2	******	.20	30.2	.0030	6.1
95.0	12	9.6	******	.21	30.0	.0032	6.6
95.0	14	9.3	******	.22	29.6	.0035	7.7
95.0	15	9.9	******	.23	29.4	.0037	8.3
100.0	8	10.0	******	.16	32.5	.0025	4.7
100.0	10	9.5	******	.19	32.1	.0028	5.8
100.0	11	9.4	******	.20	31.9	.0030	6.4
100.0	12	9.6	******	.21	31.7	.0032	7.0
100.0	15	9.9	******	.23	31.0	.0037	8.7

CONVOLUTION DEPTH= 13.0

BLG,	NSEG,	FBL,	XNF,	TPL,	XSTR2,	XFMX,	OFMX
70.0	8	9.9	******	.19	22.3	.0024	3.3
70.0	9	9.9	******	.20	22.1	.0026	3.7
75.0	8	8.8	******	.18	24.0	.0024	3.5
75.0	9	8.7	******	.19	23.9	.0026	3.9
75.0	10	8.9	******	.20	23.7	.0028	4.4
75.0	11	9.2	******	.21	23.5	.0030	4.8
80.0	8	9.2	******	.18	25.7	.0025	3.7
80.0	9	8.9	******	.19	25.5	.0026	4.2
80.0	10	9.0	******	.20	25.3	.0028	4.7
80.0	11	9.3	******	.21	25.1	.0030	5.1
80.0	12	8.5	******	.21	25.0	.0032	5.6
85.0	8	9.8	******	.18	27.4	.0025	4.0
85.0	9	9.1	******	.19	27.2	.0027	4.5
85.0	10	9.1	******	.20	27.0	.0029	4.9
85.0	11	8.1	******	.20	26.9	.0031	5.4
85.0	12	8.5	******	.21	26.7	.0033	5.9
85.0	13	9.0	******	.22	26.4	.0034	6.4
90.0	8	9.0	******	.17	29.1	.0025	4.2
90.0	9	9.4	******	.19	28.9	.0027	4.7
90.0	10	9.2	******	.20	28.7	.0029	5.2
90.0	11	9.4	******	.21	28.5	.0031	5.8
90.0	12	8.5	******	.21	28.3	.0033	6.3
90.0	13	9.0	******	.22	28.1	.0035	6.8
95.0	8	9.5	******	.17	30.8	.0025	4.4
95.0	9	9.9	******	.19	30.5	.0027	5.0
95.0	10	9.4	******	.20	30.3	.0029	5.5
95.0	11	9.5	******	.21	30.1	.0031	6.1
95.0	12	9.8	******	.22	29.9	.0033	6.6
95.0	13	9.0	******	.22	29.8	.0035	7.2
95.0	14	9.5	******	.23	29.5	.0037	7.7
100.0	10	9.7	******	.20	32.0	.0029	5.8
100.0	11	9.6	******	.21	31.8	.0031	6.4
100.0	12	9.8	******	.22	31.6	.0033	7.0
100.0	14	9.5	******	.23	31.2	.0037	8.1
100.0	15	10.0	******	.24	30.9	.0039	8.7

CONVOLUTION DEPTH= 13.5

BLG,	NSEG,	FBL,	XNF,	TPL,	XSTR2,	XFMX,	OFMX
75.0	8	9.1	******	.19	24.0	.0025	3.5
75.0	9	9.0	******	.20	23.8	.0027	3.9
75.0	10	9.2	******	.21	23.6	.0029	4.4
75.0	11	9.5	******	.22	23.4	.0031	4.8
80.0	8	9.5	******	.19	25.7	.0026	3.7
80.0	9	9.1	******	.20	25.5	.0028	4.2
80.0	10	9.3	******	.21	25.3	.0030	4.7
80.0	11	9.5	******	.22	25.1	.0032	5.1
85.0	8	8.7	******	.18	27.4	.0026	4.0
85.0	9	8.1	******	.19	27.2	.0028	4.5
85.0	10	8.1	******	.20	27.0	.0030	4.9
85.0	11	8.4	******	.21	26.8	.0032	5.4
85.0	12	8.7	******	.22	26.6	.0034	5.9
90.0	8	9.2	******	.18	29.0	.0026	4.2
90.0	9	9.6	******	.20	28.8	.0028	4.7
90.0	10	9.4	******	.21	28.6	.0030	5.2
90.0	11	8.4	******	.21	28.5	.0032	5.8
90.0	12	8.7	******	.22	28.2	.0034	6.3
90.0	13	9.1	******	.23	28.0	.0036	6.8
95.0	8	9.7	******	.18	30.7	.0026	4.4
95.0	10	9.6	******	.21	30.3	.0030	5.5
95.0	11	9.7	******	.22	30.1	.0032	6.1

95.0	12	10.0	******	.23	29.8	.0034	6.6
95.0	13	9.2	******	.23	29.7	.0036	7.2
95.0	14	9.6	******	.24	29.4	.0038	7.7
100.0	10	9.9	******	.21	31.9	.0031	5.8
100.0	11	9.8	******	.22	31.7	.0033	6.4
100.0	14	9.6	******	.24	31.1	.0039	8.1

CONVOLUTION DEPTH= 14.0

BLG,	NSEG,	FBL,	XNF,	TPL,	XSTR2,	XFMX,	OFMX
70.0	7	9.7	******	.19	22.4	.0024	2.9
75.0	8	9.4	******	.20	23.9	.0026	3.5
75.0	9	9.3	******	.21	23.7	.0028	3.9
75.0	10	9.4	******	.22	23.5	.0030	4.4
80.0	8	8.5	******	.19	25.7	.0027	3.7
80.0	9	9.4	******	.21	25.4	.0029	4.2
80.0	10	9.5	******	.22	25.2	.0031	4.7
80.0	11	9.7	******	.23	25.0	.0033	5.1
85.0	8	8.9	******	.19	27.3	.0027	4.0
85.0	9	8.4	******	.20	27.1	.0029	4.5
85.0	10	8.4	******	.21	26.9	.0031	4.9
85.0	11	8.6	******	.22	26.7	.0033	5.4
85.0	12	8.9	******	.23	26.5	.0035	5.9
90.0	8	9.4	******	.19	29.0	.0027	4.2
90.0	9	8.6	******	.20	28.8	.0029	4.7
90.0	10	8.5	******	.21	28.6	.0031	5.2
90.0	11	8.7	******	.22	28.4	.0033	5.8
90.0	12	8.9	******	.23	28.2	.0036	6.3
95.0	9	9.0	******	.20	30.5	.0029	5.0
95.0	10	9.8	******	.22	30.2	.0032	5.5
95.0	11	9.9	******	.23	30.0	.0034	6.1
95.0	12	9.0	******	.23	29.8	.0036	6.6
95.0	13	9.3	******	.24	29.6	.0038	7.2
100.0	9	9.4	******	.20	32.1	.0030	5.2
100.0	11	10.0	******	.23	31.6	.0034	6.4
100.0	14	9.7	******	.25	31.0	.0040	8.1

CONVOLUTION DEPTH= 14.5

BLG,	NSEG,	FBL,	XNF,	TPL,	XSTR2,	XFMX,	OFMX
75.0	8	9.7	******	.21	23.9	.0027	3.5
75.0	9	9.6	******	.22	23.7	.0029	3.9
75.0	10	9.7	******	.23	23.5	.0032	4.4
80.0	8	8.8	******	.20	25.6	.0028	3.7
80.0	9	9.7	******	.22	25.3	.0030	4.2
80.0	10	9.7	******	.23	25.1	.0032	4.7
80.0	11	9.9	******	.24	24.9	.0034	5.1
85.0	8	9.1	******	.20	27.3	.0028	4.0
85.0	9	8.7	******	.21	27.1	.0030	4.5
85.0	10	8.6	******	.22	26.9	.0032	4.9
85.0	11	8.8	******	.23	26.6	.0034	5.4
90.0	8	9.6	******	.20	28.9	.0028	4.2
90.0	9	8.9	******	.21	28.7	.0030	4.7
90.0	10	8.8	******	.22	28.5	.0033	5.2
90.0	11	8.9	******	.23	28.3	.0035	5.8
90.0	12	9.1	******	.24	28.1	.0037	6.3
95.0	9	9.2	******	.21	30.4	.0031	5.0
95.0	11	8.9	******	.23	30.0	.0035	6.1
95.0	12	9.2	******	.24	29.7	.0037	6.6
95.0	13	9.5	******	.25	29.5	.0039	7.2

100.0	8	9.4	******	.19	32.3	.0029	4.7
100.0	9	9.6	******	.21	32.1	.0031	5.2
100.0	13	9.5	******	.25	31.2	.0040	7.6

CONVOLUTION DEPTH= 15.0

BLG,	NSEG,	FBL,	XNF,	TPL,	XSTR2,	XFMX,	OFMX
80.0	8	9.0	******	.21	25.5	.0029	3.7
80.0	9	10.0	******	.23	25.3	.0031	4.2
80.0	10	10.0	******	.24	25.1	.0033	4.7
85.0	8	9.4	******	.21	27.2	.0029	4.0
85.0	9	8.9	******	.22	27.0	.0031	4.5
85.0	10	8.9	******	.23	26.8	.0033	4.9
85.0	11	9.0	******	.24	26.6	.0036	5.4
90.0	8	9.8	******	.21	28.9	.0029	4.2
90.0	9	9.1	******	.22	28.7	.0031	4.7
90.0	10	9.0	******	.23	28.5	.0034	5.2
90.0	11	9.1	******	.24	28.2	.0036	5.8
90.0	12	9.3	******	.25	28.0	.0038	6.3
95.0	8	9.2	******	.20	30.6	.0029	4.4
95.0	9	9.4	******	.22	30.3	.0032	5.0
95.0	10	9.1	******	.23	30.1	.0034	5.5
95.0	11	9.1	******	.24	29.9	.0036	6.1
95.0	12	9.3	******	.25	29.7	.0039	6.6
100.0	8	9.7	******	.20	32.3	.0030	4.7
100.0	9	9.7	******	.22	32.0	.0032	5.2
100.0	12	9.4	******	.25	31.3	.0039	7.0
100.0	13	9.6	******	.26	31.1	.0041	7.6

CONVOLUTION DEPTH= 15.5

BLG,	NSEG,	FBL,	XNF,	TPL,	XSTR2,	XFMX,	OFMX
75.0	7	9.7	******	.21	24.0	.0027	3.1
80.0	8	9.3	******	.22	25.5	.0030	3.7
85.0	8	9.6	******	.22	27.2	.0030	4.0
85.0	9	9.2	******	.23	27.0	.0032	4.5
85.0	10	9.1	******	.24	26.7	.0035	4.9
90.0	8	8.9	******	.21	28.9	.0030	4.2
90.0	9	9.3	******	.23	28.6	.0033	4.7
90.0	10	9.2	******	.24	28.4	.0035	5.2
90.0	11	9.3	******	.25	28.2	.0037	5.8
95.0	8	9.3	******	.21	30.5	.0031	4.4
95.0	9	9.6	******	.23	30.3	.0033	5.0
95.0	10	9.3	******	.24	30.1	.0035	5.5
95.0	11	9.3	******	.25	29.8	.0038	6.1
95.0	12	9.5	******	.26	29.6	.0040	6.6
100.0	8	9.9	******	.21	32.2	.0031	4.7
100.0	9	9.9	******	.23	32.0	.0033	5.2
100.0	10	9.5	******	.24	31.7	.0036	5.8
100.0	11	9.4	******	.25	31.5	.0038	6.4
100.0	12	9.5	******	.26	31.3	.0040	7.0

CONVOLUTION DEPTH= 16.0

BLG,	NSEG,	FBL,	XNF,	TPL,	XSTR2,	XFMX,	OFMX
80.0	8	9.6	******	.23	25.4	.0031	3.7
85.0	8	8.7	******	.22	27.2	.0031	4.0

85.0	9	9.4	******	.24	26.9	.0033	4.5
85.0	10	9.3	******	.25	26.7	.0036	4.9
90.0	8	9.1	******	.22	28.8	.0031	4.2
90.0	9	8.5	******	.23	28.6	.0034	4.7
90.0	10	9.4	******	.25	28.3	.0036	5.2
90.0	11	9.5	******	.26	28.1	.0039	5.8
95.0	8	9.5	******	.22	30.5	.0032	4.4
95.0	9	9.8	******	.24	30.2	.0034	5.0
95.0	10	9.5	******	.25	30.0	.0037	5.5
95.0	11	9.5	******	.26	29.8	.0039	6.1
100.0	10	9.6	******	.25	31.7	.0037	5.8
100.0	11	9.6	******	.26	31.4	.0039	6.4
100.0	12	9.7	******	.27	31.2	.0042	7.0

CONVOLUTION DEPTH= 16.5

BLG,	NSEG,	FBL,	XNF,	TPL,	XSTR2,	XFMX,	OFMX
80.0	8	9.9	******	.24	25.4	.0032	3.7
85.0	8	9.0	******	.23	27.1	.0032	4.0
85.0	9	9.6	******	.25	26.8	.0035	4.5
85.0	10	9.5	******	.26	26.6	.0037	4.9
90.0	8	9.3	******	.23	28.8	.0032	4.2
90.0	9	8.8	******	.24	28.6	.0035	4.7
90.0	10	9.6	******	.26	28.3	.0038	5.2
95.0	8	9.7	******	.23	30.4	.0033	4.4
95.0	9	8.9	******	.24	30.2	.0035	5.0
95.0	10	9.7	******	.26	29.9	.0038	5.5
95.0	11	9.7	******	.27	29.7	.0040	6.1
100.0	10	9.8	******	.26	31.6	.0038	5.8
100.0	11	9.7	******	.27	31.4	.0041	6.4
100.0	12	9.8	******	.28	31.1	.0043	7.0

CONVOLUTION DEPTH= 17.0

BLG,	NSEG,	FBL,	XNF,	TPL,	XSTR2,	XFMX,	OFMX
85.0	8	9.2	******	.24	27.1	.0033	4.0
85.0	9	9.9	******	.26	26.8	.0036	4.5
90.0	8	9.5	******	.24	28.7	.0033	4.2
90.0	9	9.0	******	.25	28.5	.0036	4.7
90.0	10	9.8	******	.27	28.2	.0039	5.2
95.0	8	9.8	******	.24	30.4	.0034	4.4
95.0	9	9.1	******	.25	30.2	.0036	5.0
95.0	10	9.9	******	.27	29.9	.0039	5.5
95.0	11	9.9	******	.28	29.6	.0042	6.1
100.0	11	9.9	******	.28	31.3	.0042	6.4

CONVOLUTION DEPTH= 17.5

BLG,	NSEG,	FBL,	XNF,	TPL,	XSTR2,	XFMX,	OFMX
85.0	8	9.5	******	.25	27.0	.0034	4.0
90.0	8	8.7	******	.24	28.7	.0035	4.2
90.0	10	10.0	******	.28	28.1	.0040	5.2
95.0	8	9.0	******	.24	30.4	.0035	4.4
95.0	9	9.3	******	.26	30.1	.0038	5.0
95.0	10	9.1	******	.27	29.9	.0040	5.5
100.0	8	9.4	******	.24	32.1	.0035	4.7
100.0	9	9.5	******	.26	31.8	.0038	5.2

CONVOLUTION DEPTH= 18.0

BLG,	NSEG,	FBL,	XNF,	TPL,	XSTR2,	XFMX,	OFMX
90.0	8	8.9	******	.25	28.7	.0036	4.2
95.0	8	9.2	******	.25	30.3	.0036	4.4
95.0	9	9.5	******	.27	30.0	.0039	5.0
95.0	10	9.2	******	.28	29.8	.0042	5.5
100.0	8	9.6	******	.25	32.0	.0036	4.7
100.0	9	9.7	******	.27	31.7	.0039	5.2

CONVOLUTION DEPTH= 18.5

BLG,	NSEG,	FBL,	XNF,	TPL,	XSTR2,	XFMX,	OFMX
95.0	8	9.4	******	.26	30.3	.0037	4.4
95.0	9	9.7	******	.28	30.0	.0040	5.0
95.0	10	9.4	******	.29	29.7	.0043	5.5
100.0	8	9.7	******	.26	31.9	.0037	4.7
100.0	9	9.9	******	.28	31.7	.0040	5.2
100.0	10	9.5	******	.29	31.4	.0043	5.8

CONVOLUTION DEPTH= 19.0

BLG,	NSEG,	FBL,	XNF,	TPL,	XSTR2,	XFMX,	OFMX
95.0	8	9.6	******	.27	30.2	.0038	4.4
95.0	9	9.9	******	.29	29.9	.0041	5.0
100.0	8	9.9	******	.27	31.9	.0039	4.7
100.0	10	9.7	******	.30	31.3	.0045	5.8

CONVOLUTION DEPTH= 19.5

BLG,	NSEG,	FBL,	XNF,	TPL,	XSTR2,	XFMX,	OFMX
95.0	8	9.8	******	.28	30.2	.0039	4.4
100.0	10	9.8	******	.31	31.3	.0046	5.8

CONVOLUTION DEPTH= 20.0

BLG,	NSEG,	FBL,	XNF,	TPL,	XSTR2,	XFMX,	OFMX
95.0	8	10.0	******	.29	30.1	.0041	4.4
100.0	9	9.5	******	.30	31.5	.0044	5.2
100.0	10	10.0	******	.32	31.2	.0048	5.8

APPENDIX 1B: BUS BAR BELLOWS EXPANSION JOINT – OPTIMUM PARAMETERS

```
*******************************************
RESULTS OF THE OPTIMIZATION OF U-TYPE BELLOWS
    WITH RESPECT TO THE AXIAL FLEXIBILITY
*******************************************

GENERAL INPUT DATA:

INTERNAL DIAMETER=    70.0
NUMBER OF PLIES=      4
NOMINAL PRESSURE=     2.00
CRITICAL PRESSURE=    2.00
BELLOWS EXTENSION=     5.0
BELLOWS COMPRESSION=   5.0
MINIMUM FATIGUE LIFE= 500 CYCLES

THERMAL FACTOR=       1
************************
RESULTS OF COMPUTATIONS:
************************

NOTATION:

BLG   - BELLOWS LENGTH
NSEG  - NUMBER OF CONVOLUTIONS
FBL   - AXIAL STIFFNESS OF BELLOWS
XNF   - FATIGUE LIFE
TPL   - INITIAL THICKNESS OF PLIES
XSTR2 - MAXIMUM ADMISSIBLE COMPRESSION
XFMX  - MAXIMUM ROTATION ANGLE
OFMX  - MAXIMUM OFFSET

--------------------------
CONVOLUTION DEPTH=  5.0
--------------------------

BLG,   NSEG,   FBL,   XNF,   TPL,   XSTR2,   XFMX,   OFMX
-------------------------------------------------------------
 65.0   19   149.8  1675.7    .18   12.5    .0024    7.2
 65.0   20   144.3  1875.8    .18   12.1    .0025    7.6

--------------------------
CONVOLUTION DEPTH=  5.5
--------------------------

BLG,   NSEG,   FBL,   XNF,   TPL,   XSTR2,   XFMX,   OFMX
-------------------------------------------------------------
 80.0   14   144.6  4358.9    .18   19.9    .0022    6.5
 80.0   27   149.9  8275.5    .22   10.8    .0035   12.6

--------------------------
CONVOLUTION DEPTH=  6.0
--------------------------

BLG,   NSEG,   FBL,   XNF,   TPL,   XSTR2,   XFMX,   OFMX
-------------------------------------------------------------
 80.0   14   153.6  4734.0    .20   19.2    .0024    6.5
 80.0   16   155.0  4837.8    .21   17.7    .0026    7.4
 80.0   19   156.8  5855.6    .22   15.5    .0029    8.8
 80.0   20   151.0  6573.9    .22   14.9    .0030    9.3
 80.0   23   154.2  7846.5    .23   12.6    .0033   10.7
 80.0   26   156.6  9570.3    .24   10.0    .0037   12.1
```

```
--------------------------
CONVOLUTION DEPTH=  6.5
--------------------------

BLG,   NSEG,   FBL,   XNF,   TPL,   XSTR2,   XFMX,   OFMX
-----------------------------------------------------------
 80.0   17   156.3  6344.3    .23   16.2    .0029    7.9
 80.0   20   157.2  7816.5    .24   13.9    .0032    9.3
 80.0   21   151.2  8791.3    .24   13.2    .0034    9.8
 80.0   23   157.0  9735.3    .25   11.3    .0036   10.7
 80.0   24   151.1  ******    .25   10.7    .0037   11.2

--------------------------
CONVOLUTION DEPTH=  7.0
--------------------------

BLG,   NSEG,   FBL,   XNF,   TPL,   XSTR2,   XFMX,   OFMX
-----------------------------------------------------------
 80.0   19   169.2  8164.2    .26   13.5    .0033    8.8
 80.0   20   161.9  9249.5    .26   12.8    .0035    9.3
 80.0   22   165.9  ******    .27   10.8    .0037   10.2

--------------------------
CONVOLUTION DEPTH=  7.5
--------------------------

BLG,   NSEG,   FBL,   XNF,   TPL,   XSTR2,   XFMX,   OFMX
-----------------------------------------------------------
 80.0   19   173.1  9574.6    .28   12.5    .0036    8.8
 80.0   21   175.3  ******    .29   10.4    .0038    9.8
 95.0   20   178.3  ******    .29   16.2    .0038   11.1
 95.0   25   179.1  ******    .31   11.0    .0045   13.8

--------------------------
CONVOLUTION DEPTH=  8.0
--------------------------

BLG,   NSEG,   FBL,   XNF,   TPL,   XSTR2,   XFMX,   OFMX
-----------------------------------------------------------
 95.0   18   178.9  ******    .30   17.3    .0037    9.9

--------------------------
CONVOLUTION DEPTH=  8.5
--------------------------

BLG,   NSEG,   FBL,   XNF,   TPL,   XSTR2,   XFMX,   OFMX
-----------------------------------------------------------
 95.0   12   180.4  ******    .28   22.7    .0030    6.6
 95.0   13   182.4  ******    .29   21.6    .0032    7.2
 95.0   14   185.5  ******    .30   20.5    .0033    7.7
 95.0   16   182.4  ******    .31   18.4    .0036    8.8
 95.0   18   183.5  ******    .32   16.3    .0040    9.9
 95.0   20   184.0  ******    .33   14.1    .0043   11.1
 95.0   22   184.5  ******    .34   11.7    .0046   12.2

--------------------------
CONVOLUTION DEPTH=  9.0
--------------------------

BLG,   NSEG,   FBL,   XNF,   TPL,   XSTR2,   XFMX,   OFMX
-----------------------------------------------------------
 95.0   19   178.5  ******    .34   14.4    .0044   10.5
 95.0   21   177.9  ******    .35   12.1    .0047   11.6

--------------------------
```

CONVOLUTION DEPTH= 9.5

BLG,	NSEG,	FBL,	XNF,	TPL,	XSTR2,	XFMX,	OFMX
95.0	18	189.8	******	.36	14.4	.0044	9.9
95.0	20	187.4	******	.37	11.9	.0048	11.1

CONVOLUTION DEPTH= 10.0

BLG,	NSEG,	FBL,	XNF,	TPL,	XSTR2,	XFMX,	OFMX
95.0	19	197.6	******	.39	11.9	.0048	10.5

CONVOLUTION DEPTH= 10.5

BLG,	NSEG,	FBL,	XNF,	TPL,	XSTR2,	XFMX,	OFMX
110.0	16	209.5	******	.40	19.6	.0045	10.2

CONVOLUTION DEPTH= 11.0

BLG,	NSEG,	FBL,	XNF,	TPL,	XSTR2,	XFMX,	OFMX
110.0	12	209.7	******	.38	24.5	.0039	7.7
110.0	13	206.8	******	.39	23.1	.0041	8.3
110.0	14	206.6	******	.40	21.7	.0043	9.0

CONVOLUTION DEPTH= 11.5

BLG,	NSEG,	FBL,	XNF,	TPL,	XSTR2,	XFMX,	OFMX
110.0	12	213.6	******	.40	23.9	.0041	7.7

CONVOLUTION DEPTH= 12.0

BLG,	NSEG,	FBL,	XNF,	TPL,	XSTR2,	XFMX,	OFMX
110.0	10	240.4	******	.40	26.0	.0038	6.4
125.0	10	246.9	******	.39	31.3	.0039	7.3

CONVOLUTION DEPTH= 12.5

BLG,	NSEG,	FBL,	XNF,	TPL,	XSTR2,	XFMX,	OFMX

NO SOLUTION

CONVOLUTION DEPTH= 13.0

BLG,	NSEG,	FBL,	XNF,	TPL,	XSTR2,	XFMX,	OFMX

NO SOLUTION

```
-------------------------
CONVOLUTION DEPTH= 13.5
-------------------------

BLG,   NSEG,   FBL,   XNF,   TPL,   XSTR2,   XFMX,   OFMX
-----------------------------------------------------------
NO SOLUTION

-------------------------
CONVOLUTION DEPTH= 14.0
-------------------------

BLG,   NSEG,   FBL,   XNF,   TPL,   XSTR2,   XFMX,   OFMX
-----------------------------------------------------------
NO SOLUTION

-------------------------
CONVOLUTION DEPTH= 14.5
-------------------------

BLG,   NSEG,   FBL,   XNF,   TPL,   XSTR2,   XFMX,   OFMX
-----------------------------------------------------------
NO SOLUTION

-------------------------
CONVOLUTION DEPTH= 15.0
-------------------------

BLG,   NSEG,   FBL,   XNF,   TPL,   XSTR2,   XFMX,   OFMX
-----------------------------------------------------------
NO SOLUTION
```

APPENDIX 1C: HE FLOW BELLOWS EXPANSION JOINT – OPTIMUM PARAMETERS

```
*****************************************
RESULTS OF THE OPTIMIZATION OF U-TYPE BELLOWS
    WITH RESPECT TO THE AXIAL FLEXIBILITY
*****************************************

GENERAL INPUT DATA:

INTERNAL DIAMETER=    70.0
NUMBER OF PLIES=      3
NOMINAL PRESSURE=     2.00
CRITICAL PRESSURE=    2.00
BELLOWS EXTENSION=     5.0
BELLOWS COMPRESSION=   5.0
MINIMUM FATIGUE LIFE= 500 CYCLES

THERMAL FACTOR=       1
**********************
RESULTS OF COMPUTATIONS:
**********************

NOTATION:

BLG   - BELLOWS LENGTH
NSEG  - NUMBER OF CONVOLUTIONS
FBL   - AXIAL STIFFNESS OF BELLOWS
XNF   - FATIGUE LIFE
TPL   - INITIAL THICKNESS OF PLIES
XSTR2 - MAXIMUM ADMISSIBLE COMPRESSION
XFMX  - MAXIMUM ROTATION ANGLE
OFMX  - MAXIMUM OFFSET

--------------------------
CONVOLUTION DEPTH=  5.0
--------------------------

BLG,   NSEG,   FBL,   XNF,   TPL,   XSTR2,   XFMX,   OFMX
-----------------------------------------------------------
 80.0   16   143.8  2220.8    .19   20.6    .0022    7.4
 80.0   19   144.9  2568.0    .20   19.1    .0025    8.8

--------------------------
CONVOLUTION DEPTH=  5.5
--------------------------

BLG,   NSEG,   FBL,   XNF,   TPL,   XSTR2,   XFMX,   OFMX
-----------------------------------------------------------
 80.0   15   157.0  2372.0    .21   20.4    .0023    7.0
 80.0   18   154.5  2843.3    .22   18.7    .0026    8.4
 80.0   21   158.0  3342.0    .23   17.0    .0029    9.8
 80.0   22   152.8  3708.9    .23   16.5    .0030   10.2
 80.0   25   155.8  4449.8    .24   14.7    .0033   11.6
 80.0   26   150.5  4959.6    .24   14.2    .0034   12.1
 80.0   28   159.2  5285.7    .25   12.7    .0036   13.0
 80.0   29   154.5  5859.2    .25   12.2    .0037   13.5

--------------------------
CONVOLUTION DEPTH=  6.0
--------------------------

BLG,   NSEG,   FBL,   XNF,   TPL,   XSTR2,   XFMX,   OFMX
-----------------------------------------------------------
```

```
 80.0   24   160.0  5184.8    .26   14.2    .0035   11.2
 80.0   25   154.3  5817.8    .26   13.7    .0036   11.6

-------------------------
CONVOLUTION DEPTH=  6.5
-------------------------

BLG,   NSEG,   FBL,   XNF,   TPL,   XSTR2,   XFMX,   OFMX
-----------------------------------------------------------
 80.0   23   164.7  5881.5    .28   13.8    .0037   10.7

-------------------------
CONVOLUTION DEPTH=  7.0
-------------------------

BLG,   NSEG,   FBL,   XNF,   TPL,   XSTR2,   XFMX,   OFMX
-----------------------------------------------------------
 95.0   13   172.1  8047.6    .26   24.9    .0027    7.2
 95.0   20   178.8  ******    .30   19.7    .0036   11.1

-------------------------
CONVOLUTION DEPTH=  7.5
-------------------------

BLG,   NSEG,   FBL,   XNF,   TPL,   XSTR2,   XFMX,   OFMX
-----------------------------------------------------------
 95.0   20   179.4  ******    .32   18.9    .0039   11.1

-------------------------
CONVOLUTION DEPTH=  8.0
-------------------------

BLG,   NSEG,   FBL,   XNF,   TPL,   XSTR2,   XFMX,   OFMX
-----------------------------------------------------------
 95.0   22   179.9  ******    .35   16.3    .0044   12.2

-------------------------
CONVOLUTION DEPTH=  8.5
-------------------------

BLG,   NSEG,   FBL,   XNF,   TPL,   XSTR2,   XFMX,   OFMX
-----------------------------------------------------------
 95.0   20   194.1  ******    .37   16.9    .0044   11.1
 95.0   22   192.6  ******    .38   14.9    .0047   12.2

-------------------------
CONVOLUTION DEPTH=  9.0
-------------------------

BLG,   NSEG,   FBL,   XNF,   TPL,   XSTR2,   XFMX,   OFMX
-----------------------------------------------------------
 95.0   21   198.3  ******    .40   14.9    .0048   11.6

-------------------------
CONVOLUTION DEPTH=  9.5
-------------------------

BLG,   NSEG,   FBL,   XNF,   TPL,   XSTR2,   XFMX,   OFMX
-----------------------------------------------------------
110.0   16   207.0  ******    .40   23.9    .0042   10.2

-------------------------
CONVOLUTION DEPTH= 10.0
-------------------------

BLG,   NSEG,   FBL,   XNF,   TPL,   XSTR2,   XFMX,   OFMX
```

```
-------------------------------------------------------------
110.0   13   217.9  ******    .40   26.3    .0039    8.3

--------------------------
CONVOLUTION DEPTH= 10.5
--------------------------

BLG,   NSEG,   FBL,   XNF,   TPL,   XSTR2,   XFMX,   OFMX
-------------------------------------------------------------
110.0   11   229.9  ******    .40   27.9    .0036    7.0

--------------------------
CONVOLUTION DEPTH= 11.0
--------------------------

BLG,   NSEG,   FBL,   XNF,   TPL,   XSTR2,   XFMX,   OFMX
-------------------------------------------------------------
NO SOLUTION

--------------------------
CONVOLUTION DEPTH= 11.5
--------------------------

BLG,   NSEG,   FBL,   XNF,   TPL,   XSTR2,   XFMX,   OFMX
-------------------------------------------------------------
NO SOLUTION

--------------------------
CONVOLUTION DEPTH= 12.0
--------------------------

BLG,   NSEG,   FBL,   XNF,   TPL,   XSTR2,   XFMX,   OFMX
-------------------------------------------------------------
NO SOLUTION

--------------------------
CONVOLUTION DEPTH= 12.5
--------------------------

BLG,   NSEG,   FBL,   XNF,   TPL,   XSTR2,   XFMX,   OFMX
-------------------------------------------------------------
NO SOLUTION

--------------------------
CONVOLUTION DEPTH= 13.0
--------------------------

BLG,   NSEG,   FBL,   XNF,   TPL,   XSTR2,   XFMX,   OFMX
-------------------------------------------------------------
NO SOLUTION

--------------------------
CONVOLUTION DEPTH= 13.5
--------------------------

BLG,   NSEG,   FBL,   XNF,   TPL,   XSTR2,   XFMX,   OFMX
-------------------------------------------------------------
NO SOLUTION

--------------------------
CONVOLUTION DEPTH= 14.0
--------------------------

BLG,   NSEG,   FBL,   XNF,   TPL,   XSTR2,   XFMX,   OFMX
-------------------------------------------------------------
NO SOLUTION
```

```
--------------------------
CONVOLUTION DEPTH= 14.5
--------------------------

BLG,   NSEG,   FBL,   XNF,   TPL,   XSTR2,   XFMX,   OFMX
-------------------------------------------------------------
NO SOLUTION

--------------------------
CONVOLUTION DEPTH= 15.0
--------------------------

BLG,   NSEG,   FBL,   XNF,   TPL,   XSTR2,   XFMX,   OFMX
-------------------------------------------------------------
NO SOLUTION
```

Appendix_2: Analysis of plastic strain fields in bellows convolutions

INTRODUCTION

Preliminary analysis of plastic strain fields evolution under cyclic loads has been carried out by using bi-linear model of stainless steel 316L and the following data:

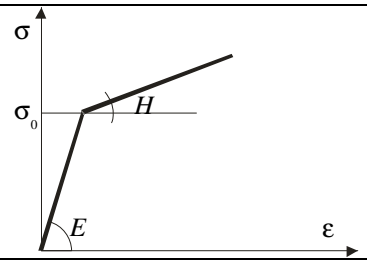

Young's modulus	E=190 GPa
Hardening modulus	H=480 MPa
yield stress	σ_0=450 MPa
Poisson' coefficient	ν=0.3

Fig. A2.1: Bilinear model of stainless steel 316L

Dimensions of the analyzed bellows are as follows (Table A2.1):

	[mm]	beam	bus-bar	He-flow
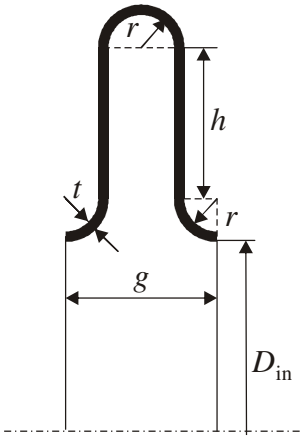	D_{in}	100	70	70
	t	0.2	0.2	0.2
	r	1.315	1.25	1.19
	g	5.26	5.0	4.76
	h	7.37	3.5	4.62

Table A2.1: Characteristic dimensions of beam, bus-bar and He-flow bellows

For numerical analysis three bellows convolutions were taken into account (Fig. A2.2). The displacement boundary conditions are applied to simulate the extension/compression effect. These values as well as the values of the applied internal pressure are presented in Table A2.2

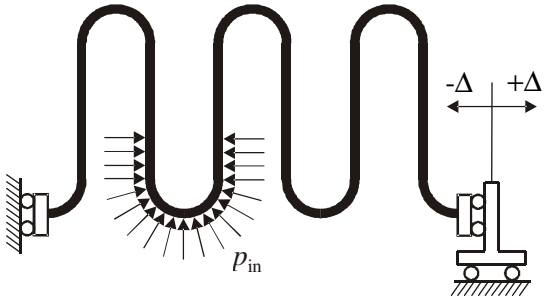

Fig. A2.2: Model for numerical calculations

	beam	bus-bar	He-flow
+Δ / -Δ [mm]	0.79	0.94	0.75
p_{in} [bar]	1	20	20

Table A2.2: Loading parameters for the expansion bellows

NUMERICAL RESULTS.

The **beam vacuum bellows** works in the nearly elastic regime and the plastic effects are not observed (under the above assumptions).

Bus-bar bellows:

The evolution of plastic strains stabilizes after 7 cycles. Maximum plastic strain intensity is observed at root point on the outer surface of the shell and is equal to 0.0299. At the inner surface of the root point the strain intensity is equal to 0.0210.
At the crest point the strain intensities are equal to 0.0132 and 0.0095 on the inner and the outer surface, respectively.

He-flow bellows:

The evolution of plastic strains stabilizes after 3 cycles. Maximum plastic strain intensity is observed at the root point on the outer surface of the shell and is equal to 0.0377. At the root point of the inner surface the strain intensity is equal to 0.0193.
At the crest point the plastic strain intensities are equal to 0.00280 and 0.00128 on the inner and the outer surface, respectively.

The evolution of the plastic strain intensities is presented in Figures A2.3 and A2.4

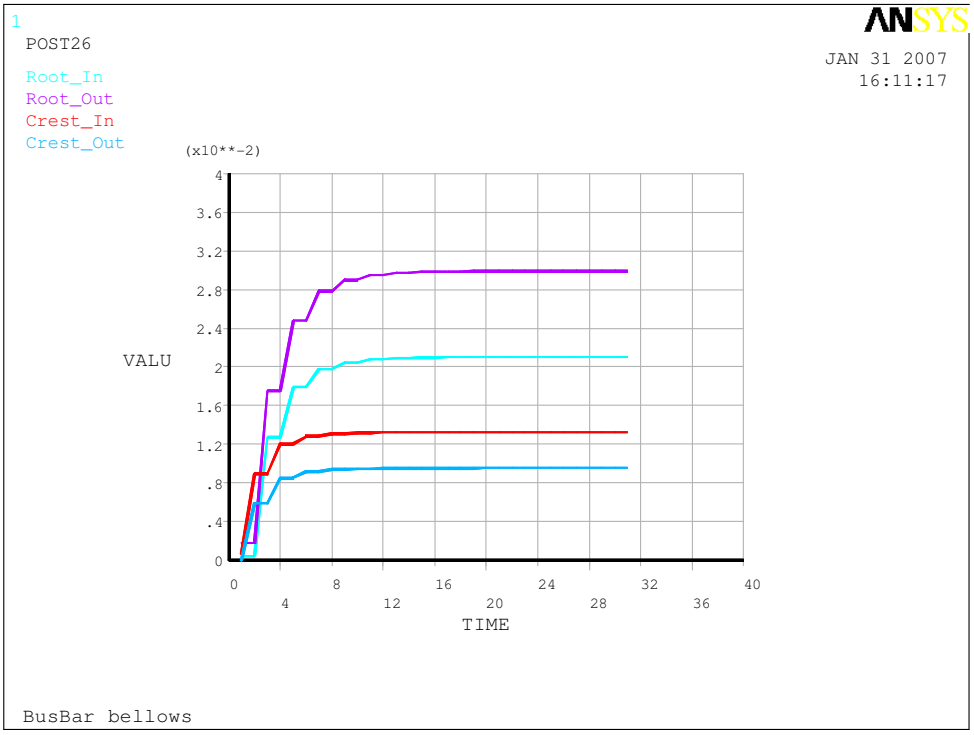

Fig. A2.3: Plastic strain intensity evolution in the bus-bar bellows

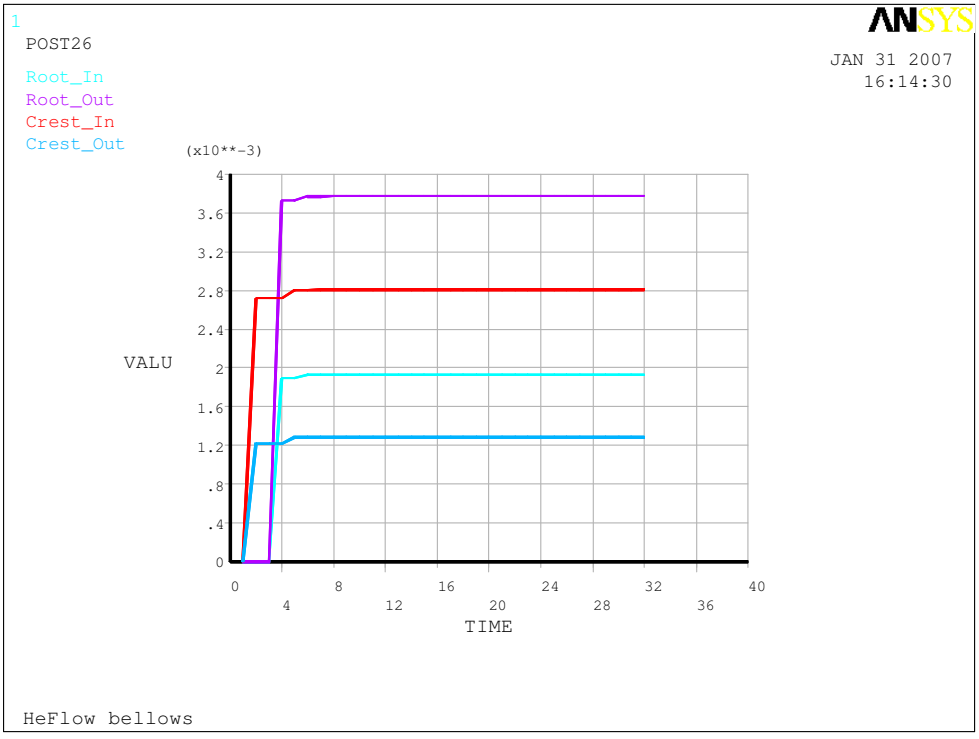

Fig. A2.4: Plastic strain intensity evolution in the He-flow bellows

Appendix_3 Analysis of thermal performance of cold-warm transition (CWT)

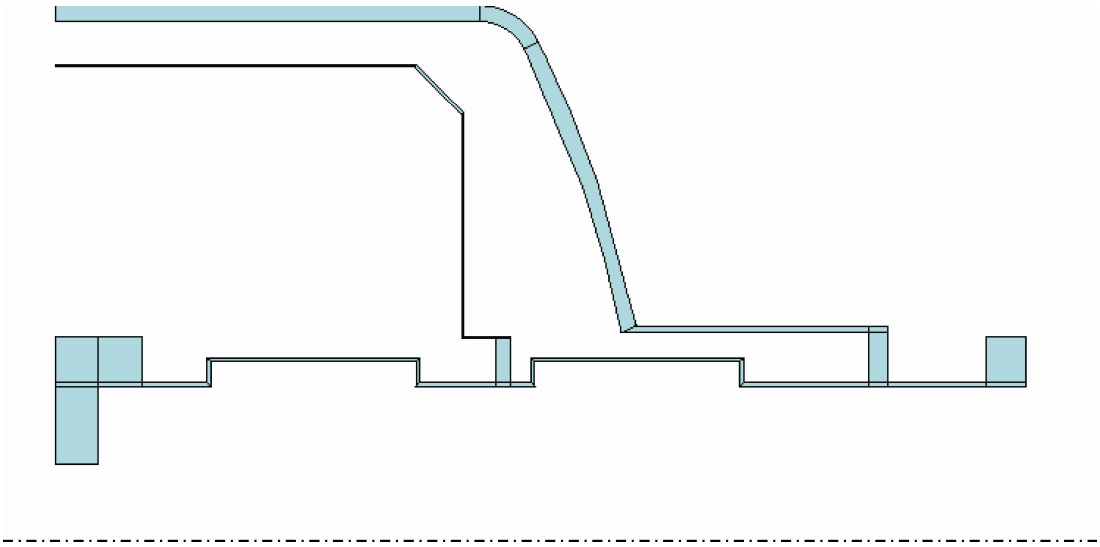

Fig. A3.1: Model of the cold-warm transition (CWT) for SIS300

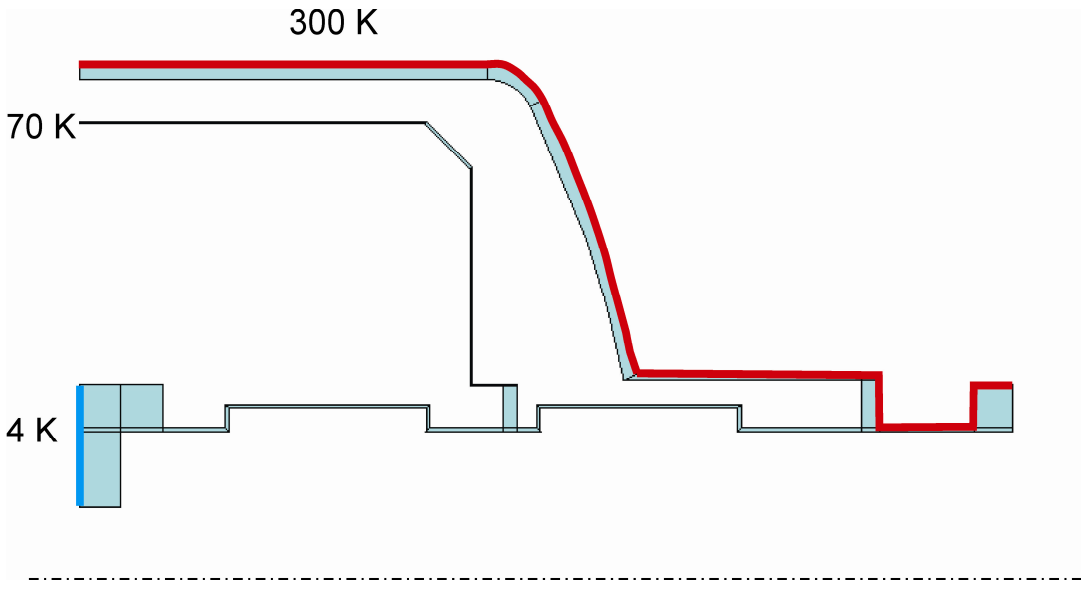

Fig. A3.2: Boundary conditions (I) for SIS300 CWT (temperatures)

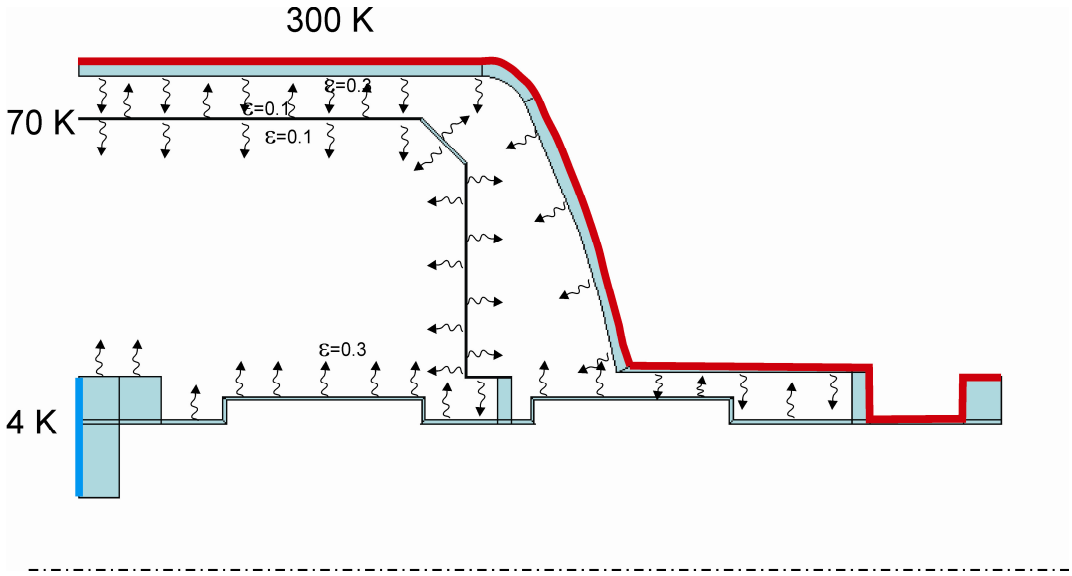

Fig. A3.3: Boundary conditions (II) for SIS300 CWT (fluxes)

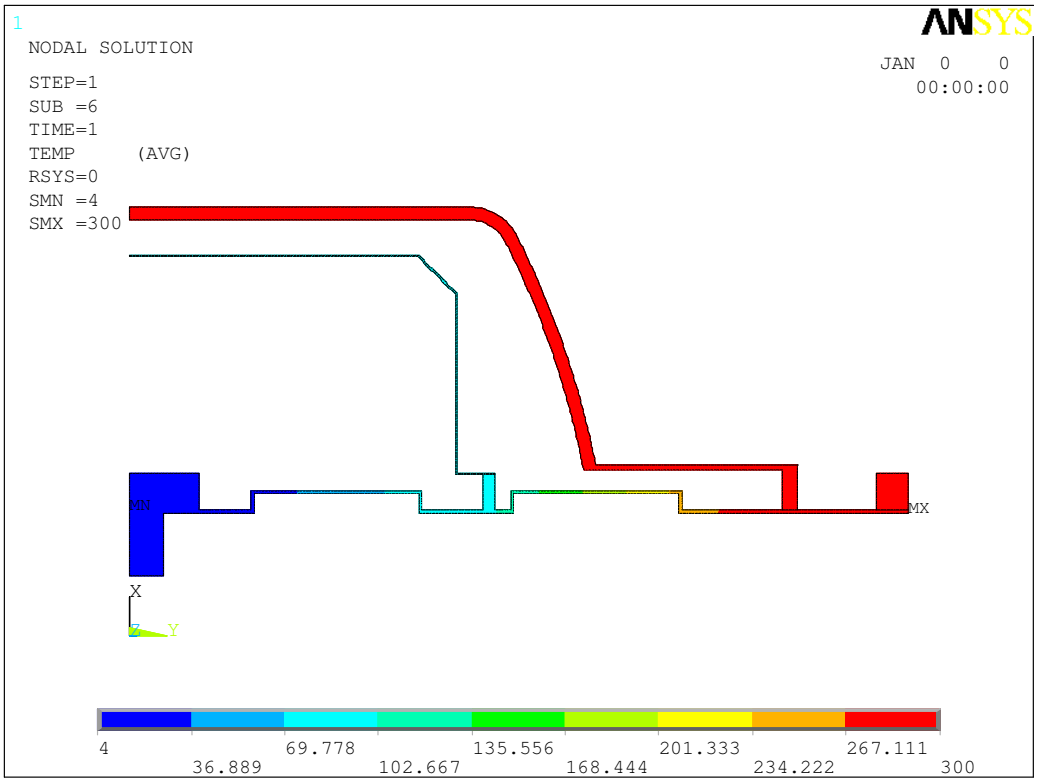

Fig. A3.4: Temperature distribution in the SIS300 CWT